Revised Manuscript with Changes Marked
Click here to access/download;Revised Manuscript with Changes Marked;main manuscript.pdf
Click here to view linked References

A Robust Bi-Level Optimization Framework for Participation of Multi-Energy Service Providers in Integrated Power and Natural Gas Markets

Nima Nasiri[a], Amin Mansour Saatloo[b], Mohammad Amin Mirzaei[b], Sajad Najafi Ravadanegh[a], Kazem Zare[b], Behnam Mohammadi-ivatloo[b], Mousa Marzband[c,d]

[a]*Electrical Engineering Department of Azarbaijan Shahid Madani University, Tabriz, Iran*
[b]*Faculty of Electrical and Computer Engineering, University of Tabriz, Tabriz, Iran*
[c]*Northumbria University, Electrical Power and Control Systems Research Group, Ellison Place NE1 8ST, Newcastle upon Tyne, United Kingdom*
[d]*Center of research excellence in renewable energy and power systems, King Abdulaziz University, Jeddah, Saudi Arabia*

Abstract

This paper presents a bi-level scheduling model for a new energy system under the concept of multi-energy service providers (MESPs) to participate in the integrated power and natural gas market (IPNGM). While the presented bi-level model takes full consideration of the unit commitment constraints of the power network and line pack constraints of the gas network into consideration at the lower level, the MESPs minimize the cost of purchasing power and natural gas by operating energy storage systems as well as the demand response program (DRP) as flexible technologies at the upper level. In order to solve the bi-level problem, an iterative-based two-step algorithm is developed. Moreover, since the MESPs cannot accurately predict other participants in the IPNGM, especially renewable energy sources (RESs), the power price determined by IPNGM is considered an uncertain parameter, and a robust optimization (RO) method is employed to capture this uncertainty. The proposal is formulated as a mixed-integer linear programming (MILP) and carried out on the IEEE 6-bus power system integrated with the 6-node natural gas network and considering one MES using the CPLEX solver in the general algebraic modeling system (GAMS) environment. Further, to show the model flexibility, simulation

Email address: s.najafi@azaruniv.ac.ir Corresponding author (Sajad Najafi Ravadanegh)

results are extended to the IEEE 118-bus power system integrated with the 10-node natural gas network by considering six MESs. The obtained results verified the effectiveness of the model by reducing the cost of the purchased power and natural gas up to 4.39% by employing flexible energy sources.

Keywords: Market-clearing, multi-energy systems, integrated electricity and natural gas networks, energy storage systems, demand response program, line pack system, robust optimization.

Nomenclature

Acronyms

CHP	Combined heat and power
IPNGM	Integrated power and natural gas market
IPNGMO	Integrated power and natural gas market operator
MESP	Multi energy service provider
MES	Multi energy system
LMEP	Local marginal electric price
LMGP	Local marginal gas price
GAMS	General algebraic modeling system
MILP	Mixed integer linear programing
IENGN	Integrated electricity and natural gas networks
GFPP	Gas fired power plant
NGFPP	Non-gas fired power plant
DRP	Demand response program
TSS	Thermal storage system

ESS	Electrical storage system
EB	Eectrical boiler
Index and sets	
i,b	Indices of power units, power system buses
n,sp,u	Indices of natural gas nods, natural gas producer, fixed pressure points
w,t,h	Indices of wind turbine, time period, multi energy system
l,Tr,z	Set of natural gas local demand, power transmission lines , natural gas network pipeline
CU,GU	Set of NGFPP, GFPP
A_b^i	Location of power units i at power system bus b
A_b^h	Location of MES h at power system bus b
A_b^w	Location of wind turbine w at power system bus b
A_n^{sp}	Location of natural gas producer sp at node n
A_n^h	Location of MES h at natural gas node n
Parameters	
γ_{sp}^{Gas}	Offer prices of natural gas producers sp ($/KCh)
P_i^{Min}, P_i^{Max}	Minimum / maximum power generation capacity of unit i (MW)
C_i^{SU}, C_i^{SD}	Startup / shutdown of NGFPP costs ($/MWh)
C_i^{GSU}, C_i^{GSD}	Start-up / shut-down of GFPPs fuel consumption (MWh)
T_i^U, T_i^D	Minimum on / off time of generation units (h)
R_i^{up}, R_i^{dn}	Ramp up/down of generation units (MW)
$\nu_{sp}^{Max}, \nu_{sp}^{Min}$	Maximum / minimum capacity of natural gas producers (Kcf)
Pr_n^{Max}, Pr_n^{Min}	Maximum / minimum pressure in natural gas network nodes (Bar)
η_{hc}, η_{hd}	Charging / discharging coefficient of the heating storage system
CHP_h^{Max}	Maximum capacity generation of the CHP unit (MW)
EB_h^{Max}	Maximum capacity heat production of the EB (MW)
HC_h^{Max}/HD_h^{Max}	Maximum charge/discharge capacity of the TSS (MW)
SC_h^{Max}/SD_h^{Max}	Maximum charge/discharge capacity of the ESS (MW)

HS_h^{Max}/ES_h^{Max}	Maximum capacity storage of the heat/electrical storage systems (MW)
y_h^K	Electric power generated from K points of CHP unit in MES h (MW)
$PR_{n,u}/PR_{m,u}$	Fixed pressure values u in the nodes of pipelines (n, m) of the NG network (Bar)
$P_w^{Wind,Max}$	Maximum output power of wind turbine (MW)
$\beta_{h,t}^{LMEP}/\gamma_{s,t}^{LMGP}$	Local marginal Electricity price/ local marginal gas price ($/MWh)
CHP_h^{Max}	Maximum natural gas input of CHP in MES h
EB_h^{Max}	Maximum input power of electric boiler in MES h
HC_h^{Max}/HD_h^{Max}	Maximum charging and discharging capacity at the heating storage system in MES h
SC_h^{Max}/SD_h^{Max}	Maximum charging and discharging capacity at the electricity storage system in MES h
ES_h^{Max}	Maximum electricity energy stored at power storage in MES h
HS_h^{Max}	Maximum heating stored in heat storage in MES h
SC_h^{Max}/SD_h^{Max}	Maximum charging and discharging capacity at the ESS in MES h
HS_h^{Max}	Maximum heating stored in TSS in MES h
$HL_{h,t}^h/EL_{h,t}^e/GL_{h,t}^g$	Heat, electric, gas demand of MES h in the period t (MW)
$L_{l,t}$	Local and industrial natural gas demand l in natural gas network at time period t (Kcf)
T_i^{Ue}, T_i^{De}	Minimum up and down time for startup and shutdown of generation unit I (h)
LPF^{Shup}, LPF^{Shdo}	Shifting-up and shifting-down load factor in DRP

Variables

$P_{i,t}$	Output power of generation unit i in time period t (MW)
$P_{w,t}^{Wind}$	Output power of wind turbine w in time period t (MW)
$F_{b,j,t}$	Electric power flow in power transmission lines (b,j) at period t (MW)
$\delta_{b,t}$	Voltage angle of power system bus b in period t (Rad)
$\lambda_{b,t}^e$	Dual variable of power system bus b in period t ($/MWh)
$\lambda_{n,t}^G$	Dual variable of natural gas network node n in period t ($/Kcfh)
$ES_{h,t}/HS_{h,t}$	The amount of electric/heat energy stored in electric and thermal storage systems at time t (MW)

$v_{sp,t}$	Gas produced from natural gas well sp in period t (Kcf)
$Pr_{n,t}$	Pressure at the nth node of the natural gas network in period t (Bar)
$\Delta HS_{h,t}, \Delta ES_{h,t}$	Changes of heating and electric stored in heat and electric storage in MES h at period t
$h_{n,m,t}$	Average mass of natural gas (line pack) in pipelines (n, m) in time period t (Kcf)
$q^{in}_{n,m,t}/q^{out}_{n,m,t}$	The amount of natural gas inlet / outlet flow in pipelines (n, m) in time period t (Kcf)
$f^{Elec,in}_{h,t}, f^{Gas,in}_{h,t}$	Electric power and natural gas inputs of MES h in the period t (MW)
$f^{Elec,out}_{h,t}, f^{Gas,out}_{h,t}$	Electric, natural gas output power of MES h in the period t (MW)
$f^{Heat,out}_{h,t}$	Heating output power of MES h in the period t (MW)
$f^{1}_{h,t}, ..., f^{15}_{h,t}$	Energy flow variables in MES h at time period t (MW)
$EL^{e}_{h,t}, EL^{g}_{h,t}$	Electric, natural gas demands of MES h in the period t (MW)
$\alpha^{K}_{h,t}$	Coefficient of CHP generation in point k of MES h at time period t
$FC_{i,t}$	Operation cost of generation unit i at time period t
$D^{Shup}_{h,t}, D^{Shdo}_{h,t}$	Shifting-up and shifting-down loads in MES h at period t
Binary Variables	
$I_{i,t}$	Commitment states of generation unit i in time period t
$y_{i,t}/z_{i,t}$	Startup and shutdown states of generation unit i in time period t
$HY_{h,t}$	Charge and discharge state of TSS in MES h at period t
$EY_{h,t}$	Charge and discharge state of ESS in MES h at period t
$y_{n,m,t}$	Binary variable to specify the direction of natural gas flow in the pipeline (n,m) at time t
$DR^{shup}_{h,t}, DR^{shdo}_{h,t}$	States of shifting-up and shifting-down loads in DRP at period t

1. Introduction

1.1. Motivation

In the modern power system, energy and load service providers aggregate end-users' power demand and participate in the wholesale power market, which is run by an independent system operator (ISO) [1]. Once the wholesale power market has been cleared, energy service providers deliver the price and power to the end-

users [2]. They may plan to minimize the cost or maximize the profit dependently. Nevertheless, the advent of multi-energy technologies such as combined heat and power (CHP) units, electrical boilers, various energy storage systems including electrical storage systems (ESS), thermal storage systems (TSS), gas storage systems (GSS) and etc. lead to an extensive interaction among multiple energy carriers in the transmission and distribution levels [3]. Thus, techno-economic interactions of the existence of multiple energy carriers, which were designed exclusively for the electricity markets, cannot respond to the requirements. Hence, researchers are looking for new and efficient mechanisms for techno-economic interactions of the multiple energy carriers. Motivated by the above discussion, this work aims to introduce a new scheduling model to involve demand-side multi-energy carrier technologies of the distribution level in the integrated power and natural gas markets (IPNGM). To do so, this work's main innovation comes in twofold. The first novelty is introducing a bilevel model to enable demand-side multi-energy technologies to participate in the wholesale electricity market by integrating them with a new energy system so-called multi-energy service provider (MESP). In the proposed bilevel model, the MESP modeling takes place in the upper level, where it participates in the IPNGM by operating its multi-energy technologies. In the lower level, where the second main novelty of this work lies, the integrated power and natural gas networks are modeled by considering unit commitment constraints for the power network and line pack constraints for the natural gas network. In the previous works, these constraints, especially unit commitment constraints of the power network, have been ignored since they make the lower problem complicated and the bilevel problem cannot be recast as a simple single-level one using KKT conditions. However, this works advances the state-of-the-art in bilevel modeling of the IPNGM by full consideration of power network constraints at the lower level and proposes a two-step algorithm to solve the bilevel problem. Moreover, this works investigates the impact of flexible technologies including electrical and thermal storage systems as well as demand response program on the IPNGM. Further, to capture the uncertainty concerns power market, a robust approach is proposed in this work to make the scheduling robust against the worst-case uncertainty realization.

1.2. Literature review

MESPs have a considerable role in different sections of the smart grids such as residential sector energy management [4], wind generation uncertainty management [5], energy storage systems and virtual power plants (VPPs) optimal management [6], ventilation systems controlling [7], and integrated DRP [8]. In addition, MESPs have a role in the energy trading procedure with the wholesale and retail energy markets. So far, many types of research have been dedicated to evaluate the energy trading mechanisms of MESPs with the wholesale and retail energy markets.

Two-stage stochastic programming for MESPs' participation in the day-ahead and real-time markets has been presented in [9]. A bidding strategy for a demand service provider has been introduced in [10], where the objective is to maximize the service provider's profit using the coupon-based DRP with a high injection of wind energy. Two bi-level approaches based on uncertainty management for the participation of distribution system service providers in the wholesale power market have been proposed in [11], in which the upper-level deals with the operation of the service provider and the lower level clears the wholesale market. Moreover, a distribution system service provider can participate in both wholesale and retail markets in [12]. To investigate the optimal decision-making aspects of a distribution system service provider in trading with microgrids (MGs) and the wholesale market simultaneously, a bilevel optimization approach has been proposed in [13]. In another study, an iterative-based two-stage framework for distribution system service provider participation in the day-ahead wholesale market with the aim of demand prediction for the distribution system has been introduced in [14], in which DRP and distribution system reliability are also considered. For participation of the distributed energy resources (DERs) aggregator in the real-time electricity market, a bilevel framework has been designed in [15], in which DERs aggregator problem is solved in the upper level, and real-time market clearing is conducted in the lower level. A bilevel problem to model a tri-layer market structure has been introduced in [16], where the upper level maximizes energy service providers' profit, and the lower level clears the market and maximizes the end-users profit. In a similar context, in [17], a tri-layer market structure has been proposed, which at

the first layer wholesale power market maximizes social welfare and at the second and third layers, respectively, demand response aggregator and energy consumers maximize their profits. In [18], a study toward electrical multi-layer market participants has been conducted, in which wholesale electricity market participants like electrical energy producers and RESs were modeled at the first layer, and responsive consumers like electrical fleets and DRP participants were modeled at the second layer. In [19], an optimization approach is presented for designing a hybrid solar/battery/diesel generator system considering the environmental effects in one of the regions of China. A photovoltaic/wind turbine/fuel cell hybrid renewable energy system in [20] is proposed to provide electricity for a Turkey region, considering reliability requirements. The Dragon fly algorithm is used in the presented approach to solving the proposed problem.

Recently, a new range of research has studied the techno-economic interactions of MESPs and other multi-energy entities with the multi-energy wholesale and retail markets. For instance, several similar pieces of research for energy trading of MESPs in the day-ahead and real-time markets have been done in [21, 22]. A hybrid stochastic/robust approach for the multi-energy retailer has been proposed in [23], in which the aims of the optimization problem are maximizing electricity, local heat, and natural gas consumers' social welfare and profit of the IPNGM. A multi-energy bidding strategy was integrated with DRP for energy trading of MESPs with IPNGM in [24] to maximize the MESPs' profit. In another study in [25], a tri-layer day-ahead multi-energy market structure for MESPs' simultaneous trading with the multi-energy wholesale and retail markets has been presented. A risk-based stochastic bilevel problem for the decision-making of MESPs to participate in the pool electricity and natural gas markets in the presence of rival MESPs has been proposed in [26]. In [27], to optimal operation of an MG in the day-ahead and real-time markets, a hybrid stochastic/IGDT scheduling model has been introduced. In order to industrial MGs' participation in the wholesale markets, a tri-level optimization framework has been presented in [28], in which at the first level, MGs try to minimize their purchased electricity costs and at the second and third levels of wholesale market-clearing and CHP units settling was performed, respectively.

In [29], an optimal scheduling model based on stochastic optimization is presented to evaluate the implementation effect of the DRP in the energy hub system considering the electricity and natural gas network constraints. This approach utilizes a water wave optimization algorithm to solve the proposed problem. An optimal approach has been investigated in [30] for the design of combined cooling, heating, and power systems in a water sports complex to reduce losses and environmental pollution.

To evaluate the trading mechanism of multi-energy players and multiple energy carriers, a bilevel model has been introduced in [31], where MESPs aggregate bids/offers of the multi-energy players and participate in the wholesale market to maximize their profits. In [32], a price-making mechanism by MESPs was presented using a bilevel model based on the Stackelberg game, in which the electricity price settlement was conducted at the upper level, and integration of the DRP was performed at the second layer. A multi-energy provider entity has been simulated in [33], which behaves as an aggregator of DERs among the wholesale market and local energy systems. Study [34] presents a bi-level scheduling model to evaluate the strategic behavior of an energy aggregator entity in the wholesale electricity market in the presence of other rivals. To study the strategic behavior of the multi-energy provider entities and power distribution system, a multi-follower bilevel optimization approach has been proposed in [35]. A mathematical programming of equilibrium constraint (MPEC) for investigating the strategic behavior of a profit-based multi-energy service provider entity in the electricity and heat markets has been proposed in [36], where the entity sends the price bids and values to the upstream markets at the upper level and market clearing was performed at the lower level. In [37], to study the strategic behavior of the MESPs in the presence of rival MESPs for participation in the day-ahead multi-energy markets, a price-making bidding strategy has been proposed. In [38], a bilevel model between a multi-energy retailer and multi-energy consumers of MESPs has been presented, in which maximizing the retailer profit and minimizing the purchased energy cost of consumers are the upper level and lower level of the problem, respectively.

Several iterative-based solution algorithms for bi- or multi-level problems have

been effectively introduced by researchers. For instance, an iterative-based bilevel planning algorithm for solving the IENGN with the consideration of wind energy intermittency has been proposed in [39]. An iterative-based two-stage stochastic framework for MESPs participation in IPNGM has been presented in [40]. In [41], a distributed algorithm based on benders decomposition to preserve the privacy of participants has been proposed to solve the optimal dispatch of the integrated electrical distribution and natural gas systems. In [42], a decomposition algorithm to achieve the best result of the recognition of electrical distribution and natural gas markets balancing with the line pack system and GSS considerations have been proposed. A distributed algorithm with DRP implementation has been presented in [43] to demonstrate a MESPs entity interaction with the electricity and natural gas corporations. In [44], a two-step sequential stochastic market clearing approach for demand response provider and ISO has been introduced.

1.3. Research gaps and contributions

To the best of the authors' knowledge, there is no focus on the robust scheduling of MESPs for participating in IPNGM in order to achieve optimal dispatch of power and natural gas for MESs under an iterative-based two-step framework. According to the reviewed literature, there exist some research gaps as follows:

1. Some literature, e.g., [4–20], have focused on the behavior of electrical energy service providers and the wholesale power market. However, the proliferation of technologies such as CHP units, electrical boilers, multi-energy storage systems and etc. require new models and management entities to interact with multiple energy carriers at the distribution and transmission levels.Hence, the mentioned research, which was designed for studying the only power market, should be restructured.
2. Many of the works like [27, 28, 30, 34–36] discussed MESPs' interactions with the wholesale power market, in which limitations of only the power network were considered, and natural gas constraints were ignored. Considering natural gas energy as one of the most important inputs of the multi-energy carrier systems, ignoring the natural gas network constraints causes unreal results.

3. In some other research such as [25, 41], the main goal is investigating the technical operation and economic interactions of MESs with multiple energy networks. However, the impact of an iterative-based two-step algorithm was not evaluated. Given the decisions of MESPs and the operator of the IPNGM have impacts on each other, so, the iterative-based two-step algorithm assists the manager of the entities to accurately evaluate the variations owing to the decisions and behaviors of the operators.

Table 1: Comparative evaluations between this study and other publications

Ref	Name of service	MESP			IPGM (Network constraints)		Linepack	Algorithm	Uncertainty
		DRP	ESS	HSS	Power	Gas			
[10]	Load serving entities	✓	×	×	✓	×	×	KKT	Stochastic
[11]	Distribution company	✓	×	×	✓	×	×	KKT	IGDT
[14]	Energy service providers	✓	×	×	✓	×	×	Two step	Robust
[15]	Renewable energy aggregator	×	✓	×	✓	×	×	KKT	Stochastic
[16]	Load serving entities	✓	×	×	✓	×	×	KKT	×
[17]	Demand response aggregator	✓	×	×	✓	×	×	KKT	×
[18]	PEV aggregators and retailers	✓	×	×	✓	×	×	KKT	Stochastic
[21]	Energy hub operators	×	✓	✓	×	×	×	×	Stochastic
[23]	Multi-energy retailer	✓	✓	✓	×	×	×	×	robust-stochastic
[24]	Multi-energy load serving entity	✓	✓	×	×	×	×	×	×
[25]	Load serving entity	✓	✓	×	×	×	×	×	CVaR
[26]	Hub manager	×	✓	×	×	×	×	KKT	CVaR
[32]	multi-energy provider	✓	×	×	×	×	×	×	×
[40]	Energy hub operator	×	✓	✓	✓	✓	✓	Two stage	Stochastic
Proposed paper	Multi energy service provider	✓	✓	✓	✓	✓	✓	Two step	Robust

To cover these research gaps and Table 1, in this paper, a bi-level approach is introduced to evaluate the MESPs impacts on the IPNGM. At the upper level, MESPs is obliged to participate in the IPNGM and dispatch the power and natural gas to MESs. The objective of the MESPs is to determine the optimal demand for flexible energy sources to minimize the total costs of the multiple energy carriers. At the lower level, the operator of the IPNGM collects bids/offers and maximizes social welfare. To simulate the IPNGM, a unit commitment problem constrained to IENGN in the presence of the flexible line pack system is used. To evaluate the counter effect of flexible energy sources and price bids introduced by IPNGM, an iterative-based two-step framework is proposed, where the first step is to determine the local marginal prices of power and natural gas via solving the unit commitment problem. Thereupon, MESPs in the presence of flexible energy sources and via introduced prices by IPNGM perform optimal scheduling at the second step. To consider the unexpected behavior of the other market participants and the stochastic nature of the RESs in the IPNGM, the introduced price by the IPNGM is considered an uncertain parameter, and the RO method is taken into account to tackle this issue. The main contribution of this paper is listed below:

1. A bi-level scheduling mechanism is proposed to evaluate the impacts of the IPNGM constrained to the IENGN on the optimal scheduling of MESPs in the presence of a flexible line pack system of the natural gas network.
2. An iterative-based two-step framework is introduced to solve the robust bi-level approach and to investigate the effect of the flexible energy sources on prices set by the IPNGM.
3. The impacts of flexible electrical and thermal storage systems employed by MESPs are investigated on the IPNGM behavior and optimal dispatch of the electrical energy sources.
4. The effect of optimal DRP implementation by MESPs on IENGN constraints is studied.

The rest of the paper is organized as follows: The next section presents the mathematical model of the introduced scheduling problem. The third section presents the iterative-based two-step algorithm and mechanism of the market-clearing. Nu-

merical results and case studies are provided in section four. Finally, the last section concludes the paper.

2. Upper level: mathematical modeling of the MESPs

In the proposed problem, MESPs aim to minimize the cost of purchased power and natural gas from IPNGM. In the objective function of Eq. (1), the first and second terms are associated with purchased power and natural gas from IPNGM, respectively.

$$\min \left\{ \sum_{t} \sum_{h} (\beta_{h,t}^{LMEP} \cdot f_{h,t}^{Elec,in} + \gamma_{h,t}^{LMGP} \cdot f_{h,t}^{Gas,in}) \right\} \tag{1}$$

2.1. MES constraints

Figure 1 shows the MES proposed in this paper. The proposed MES is equipped with a CHP unit, electric boiler, heating and electrical storage systems. In addition, it has two inputs of electricity and natural gas and three outputs of electricity, heating and natural gas. According to Figure 1, the formulation of the MES is as follows.

The positive variables in Eq. (2) represent purchased power and natural gas by MESPs from IPNGM, respectively. The proposed MESs is a directional graph with one-way energy flow at each branch. Therefore, in Eq. (3), variables are positive. Equations (4)- (7) are assigned to the CHP unit operation constraints. It should be noted that the CHP unit is modeled using the post-pressure method. Equation (8) shows the electrical boiler input limitation. Equations (9)- (11) illustrate electrical, natural gas, and thermal energy balancing of MESs, respectively. Equations (12)-(13) are related to the input and output of TSS. Further, they demonstrate that charging and discharging modes cannot be applied simultaneously. Equation (14) represents the amount of stored energy in the TSS, which is limited by Eq. (15), as well as for ESS through Eqs. (16)-(19). The initial and final SoC of ESS and TSS should be equal, as described in Eq. (20). The DRP of multi-carrier energy systems is represented via Eqs. (21)-(24), in which Eq. (21) represents that upward shift and downward shift of end-users load must be equal. Moreover, Eqs. (22)- (23) show

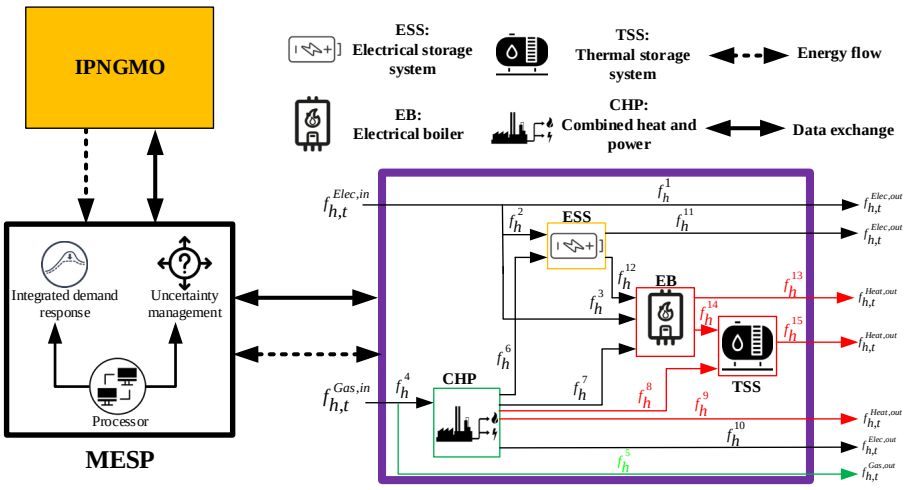

Figure 1: The proposed MESP

the amount of load that can be shifted, which is considered 15% of the total load of MES. Moreover, to prevent simultaneous upward and downward shifts, Eqs. (26)-(34) model the relationship between the input and output of equipment in MESs.

$$f_{h,t}^{Elc,in}, f_{h,t}^{Gas} \geqslant 0 \quad \forall h, \forall t \tag{2}$$

$$f_{h,t}^{1}, f_{h,t}^{2}, \ldots, f_{h,t}^{15} \geqslant 0 \quad \forall h, \forall t \tag{3}$$

$$f_{h,t}^{4} \leqslant CHP_{h}^{MAX} \quad \forall h, \forall t \tag{4}$$

$$f_{h,t}^{7} + f_{h,t}^{10} = \sum_{K} \alpha_{h,t}^{K} y_{h}^{K} \quad \forall h, \forall t \tag{5}$$

$$0 \leqslant \alpha_{h,t}^{K} \leqslant 1 \quad \forall h, \forall t, \forall k \tag{6}$$

$$\sum_{K} \alpha_{h,t}^{K} = 1 \quad \forall h, \forall t \tag{7}$$

$$f_{h,t}^{3} + f_{h,t}^{7} + f_{h,t}^{12} \leqslant EB_{h}^{Max} \quad \forall h, \forall t \tag{8}$$

$$f_{h,t}^{Elc,out} = EL_{h,t}^{e} \quad \forall h, \forall t \tag{9}$$

$$f_{h,t}^{Gas,out} = GL_{h,t}^{g} \quad \forall h, \forall t \tag{10}$$

$$f_{h,t}^{Heat,out} = HL_{h,t}^{h} \quad \forall h, \forall t \tag{11}$$

$$f_{h,t}^{8} + f_{h,t}^{14} \leqslant HY_{h,t} HC_{h}^{Max} \quad \forall h, \forall t \tag{12}$$

$$f_{h,t}^{15} \leqslant (1 - HY_{h,t}) HD_h^{Max} \quad \forall h, \forall t \tag{13}$$

$$HS_{h,t} = HS_{h,t-1} + \Delta HS_{h,t-1} \quad \forall h, \forall t \tag{14}$$

$$0 \leqslant HS_{h,t} \leqslant HS_h^{Max} \quad \forall h, \forall t \tag{15}$$

$$f_{h,t}^{2} + f_{h,t}^{6} \leqslant EY_{h,t} SC_h^{Max} \quad \forall h, \forall t \tag{16}$$

$$f_{h,t}^{11} + f_{h,t}^{12} \leqslant (1 - EY_{h,t}) SD_h^{Max} \quad \forall h, \forall t \tag{17}$$

$$ES_{h,t} = ES_{h,t-1} + \Delta ES_{h,t-1} \quad \forall h, \forall t \tag{18}$$

$$0 \leqslant ES_{h,t} \leqslant ES_h^{Max} \quad \forall h, \forall t \tag{19}$$

$$ES_{h,ini} = ES_{h,end}, HS_{h,ini} = HS_{h,end} \forall h, \forall t \tag{20}$$

$$\sum_t D_{h,t}^{Shup} = \sum_t D_{h,t}^{Shdo} \quad \forall h \tag{21}$$

$$0 \leqslant D_{h,t}^{shup} \leqslant EL_{h,t}^{e} LPF^{Shup} DR_{h,t}^{shup} \quad \forall h, \forall t \tag{22}$$

$$0 \leqslant D_{h,t}^{shdo} \leqslant EL_{h,t}^{e} LPF^{Shdo} DR_{h,t}^{shdo} \quad \forall h, \forall t \tag{23}$$

$$0 \leqslant DR_{h,t}^{shdo} + DR_{h,t}^{shup} \leqslant 1 \quad \forall h, \forall t \tag{24}$$

$$f_{h,t}^{Elec,out} = f_{h,t}^{1} + f_{h,t}^{10} + f_{h,t}^{11} + D_{h,t}^{Shedo} - D_{h,t}^{Shup} \quad \forall h, \forall t \tag{25}$$

$$f_{h,t}^{Gas,out} = f_{h,t}^{5} \quad \forall h, \forall t \tag{26}$$

$$f_{h,t}^{Heat,out} = f_{h,t}^{9} + f_{h,t}^{13} + f_{h,t}^{15} \quad \forall h, \forall t \tag{27}$$

$$f_{h,t}^{Elec,in} = f_{h,t}^{1} + f_{h,t}^{2} + f_{h,t}^{3} \quad \forall h, \forall t \tag{28}$$

$$f_{h,t}^{Gas,in} = f_{h,t}^{4} + f_{h,t}^{5} \quad \forall h, \forall t \tag{29}$$

$$\Delta HS_{h,t} = \eta_{hc}(f_{h,t}^{8} + f_{h,t}^{14}) - \frac{1}{\eta_{hd}} f_{h,t}^{15} \quad \forall h, \forall t \tag{30}$$

$$\Delta ES_{h,t} = \eta_{ec}(f_{h,t}^{2} + f_{h,t}^{6}) - \frac{1}{\eta_{ed}}(f_{h,t}^{11} + f_{h,t}^{12}) \quad \forall h, \forall t \tag{31}$$

$$\eta_{ce} f_{h,t}^{4} = f_{h,t}^{6} + f_{h,t}^{7} + f_{h,t}^{10} \quad \forall h, \forall t \tag{32}$$

$$\eta_{cg} f_{h,t}^{4} = f_{h,t}^{8} + f_{h,t}^{9} \quad \forall h, \forall t \tag{33}$$

$$\eta_{eb}(f_{h,t}^{3} + f_{h,t}^{7} + f_{h,t}^{12}) = f_{h,t}^{13} + f_{h,t}^{14} \quad \forall h, \forall t \tag{34}$$

3. Lower level: mathematical modeling of IPNGM

In this research, to simulate the IPNGM and obtain local marginal electricity price (LMEP) and local marginal gas price (LMGP) Eqs. (37)-(70) are taken into account.

3.1. The objective function of IPNGM

The objective of the IPNGM is to minimize the total cost of production, including the cost of the power production via non-gas-fired power plants (NGPPs) and their start-up and shot-down costs along with natural gas producers' costs.

$$\min \left(\sum_{t} \left(\sum_{i \in CU} (FC_{i,t} + SU_{i,t} + SD_{i,t}) + \sum_{sp} \gamma_{sp}^{Gas} V_{sp,t} \right) \right) \tag{35}$$

The first term represents the start-up, shut down, and operation costs of the NGPPs, and the second term is the cost of natural gas production, i.e., natural gas wells' cost.

3.2. Unit commitment constraints

Equations (36) and (37) illustrate start-up and shut-down costs for NGPPs, as well as start-up and shut-down fuel consumption of GFPPs are calculated by Eqs. (38)-(39).

$$SU_{i,t} \geqslant C_i^{SU} y_{i,t} \quad \forall i \in CU, \forall t \tag{36}$$

$$SD_{i,t} \geqslant C_i^{SD} z_{i,t} \quad \forall i \in CU, \forall t \tag{37}$$

$$GSU_{i,t} \geqslant C_i^{GSU} y_{i,t} \quad \forall i \in GU, \forall t \tag{38}$$

$$GSD_{i,t} \geqslant C_i^{GSD} z_{i,t} \quad \forall i \in GU, \forall t \tag{39}$$

3.3. Start-up and shut-down states of generation units

In Eq. (40), $I_{i,t}$ and $I_{i,t-1}$ show the ON state at time t and $t-1$, respectively. Also, Eq. (41) illustrates that any of the generation units cannot be at ON and OFF states at the same time.

$$y_{i,t} - z_{i,t} = I_{i,t-1} - I_{i,t} \quad \forall i, \forall t \tag{40}$$

$$y_{i,t} + z_{i,t} \leqslant 1 \quad \forall i, \forall t \tag{41}$$

3.4. Generation and ramp rate limits of generation units

Equation (42) determines the power generation limit of units. Equations (43) and (44) represent ramp-up and ramp-down limitations of power generation units.

$$P_i^{Min} I_{i,t} \leqslant P_{i,t} \leqslant P_i^{Max} I_{i,t} \quad \forall i, \forall t \tag{42}$$

$$P_{i,t} - P_{i,t-1} \leqslant (1 - y_{i,t}) R_i^{UP} + y_{i,t} P_i^{Min} \quad \forall i, \forall t \tag{43}$$

$$P_{i,t-1} - P_{i,t} \leqslant (1 - z_{i,t}) R_i^{DN} + z_{i,t} P_i^{Min} \quad \forall i, \forall t \tag{44}$$

3.5. Minimum up-time and down-time

The minimum time requirements for start-up/shutdown operations of Units are imposed by Equations (45)-(52).

$$T_i^{Ue} = \min\left\{T, T_i^{U0}\right\} \tag{45}$$

$$T_i^{De} = \min\left\{T, T_i^{D0}\right\} \tag{46}$$

$$\sum_{t=1}^{T_i^{Ue}} I_{i,t} = T_i^{Ue} \quad \forall i \tag{47}$$

$$\sum_{t=r}^{t+T_i^{Ue}-1} I_{i,r} \geqslant T_i^{U} y_{i,t} \quad \forall i, \forall t = \left[T_i^{Ue} + 1, ..., T - T_i^{U} + 1\right] \tag{48}$$

$$\sum_{t=r}^{T} (I_{i,r} - y_{i,t}) \geqslant 0 \quad \forall i, \forall t = \left[T - T_i^{U} + 2, ..., T\right] \tag{49}$$

$$\sum_{t=1}^{T_i^{De}} I_{i,t} = 0 \quad \forall i \tag{50}$$

$$\sum_{t=r}^{t+T_i^{D}-1} (1 - I_{i,r}) \geqslant T_i^{D} z_{i,t} \quad \forall i, \forall t = \left[T_i^{De} + 1, ..., T - T_i^{D} + 1\right] \tag{51}$$

$$\sum_{t=r}^{T} (1 - I_{i,r} - z_{i,t}) \geqslant 0 \quad \forall i, \forall t = \left[T - T_i^{D} + 2, ..., T\right] \tag{52}$$

3.6. Transmission system constraints

Equation (53) is the power balancing constraint. Equation (54) is the DC power flow relation, which is limited by Eqs. (55) and (56) is the wind power generation limit.

$$\sum_{j\in A_b^j} F_{b,j,t} = \sum_{i\in A_b^i} P_{i,t} + \sum_{w\in A_b^w} P_{w,t}^{Wind} - \sum_{h\in A_b^h} f_{h,t}^{Elc,in} - P_{b,t}^{D} : \lambda_{b,t}^{Elec} \quad \forall b, \forall t \tag{53}$$

$$F_{b,j,t} = (\delta_{b,t} - \delta_{j,t})/X_L \quad \forall b, \forall j, \forall t \tag{54}$$

$$-F_b^{Max} \leqslant F_{b,j,t} \leqslant F_b^{Max} \quad \forall b, \forall j, \forall t \tag{55}$$

$$0 \leqslant P_{w,t}^{Wind} \leqslant P_w^{Wind,Max} \quad \forall w, \forall t \tag{56}$$

3.7. Natural gas system model

Equation (57) shows the natural gas flow in gas network pipelines, also known as the Weymouth equation. Equations. (58) indicates the direction of natural gas flow in the pipeline, which is directly related to the pressure of the gas network nodes.

$$q_{n,m,t} = sgn(Pr_n, Pr_m) K_{n,m}^f \sqrt{Pr_{n,t}^2 - Pr_{m,t}^2} \quad \forall n, \forall m, \forall t \tag{57}$$

$$sgn(Pr_n, Pr_m) = \begin{cases} 1, & Pr_n \geqslant Pr_m \\ -1, & Pr_n \leqslant Pr_m \end{cases} \tag{58}$$

As can be seen, Eq. (57) is a nonconvex and nonlinear. This issue increases the calculation time and also makes the nodal natural gas pricing process difficult. The linearization method of Eq. (57) is shown in Appendix A.

In the following, two variables $q_{n,m,t}^{in}$, $q_{n,m,t}^{out}$ are defined in Eqs. (59) and (60) to present the flexibility of the line pack system for inflow and outflow.

$$q_{n,m,t}^{+} = \frac{q_{n,m,t}^{in} - q_{n,m,t}^{out}}{2} \quad \forall n, \forall m, \forall t \tag{59}$$

$$q_{n,m,t}^{-} = \frac{q_{m,n,t}^{in} - q_{m,n,t}^{out}}{2} \quad \forall n, \forall m, \forall t \tag{60}$$

One of the outstanding characteristics of natural gas systems is the line pack system that can act as a temporary storage system. Hence, it is an affordable solution for storing energy. The line pack system is so important to the short-term operation

of the system and represents the ability of pipelines in storing a specific amount of gas [45]. Equation (61) shows that the line pack is proportional to the mean pressure of the pipelines. Therefore, any increase in the node of a line leads to an increase in the line pack. Furthermore, Eqs. (62) and (63) determine the amount of gas that can be stored in the line pack, and Eq. (64) shows the initial amount of line pack.

$$h_{n,m,t} = K^{f}_{n,m} \frac{Pr_{n,t} + Pr_{m,t}}{2} \quad \forall n, \forall m, \forall t \tag{61}$$

$$h_{n,m,t} = h_{n,m,t-1} + q^{in}_{n,m,t} - q^{out}_{n,m,t} \quad \forall n, \forall m, \forall t \tag{62}$$

$$h_{n,m,t} = h_{n,m,0} + q^{in}_{n,m,t} - q^{out}_{n,m,t} \quad \forall n, \forall m, \forall t \tag{63}$$

$$h_{n,m,t} \geqslant h_{n,m,0} \quad \forall n, \forall m, \forall t \tag{64}$$

Supplementary constraints of the natural gas network are given in Eqs. (65)-(70). Equations (65) and (66) show the limitations in the pressure of the pipeline nodes and the amount of generated gas in the natural gas well, respectively. Equation (67) is the natural gas balancing constraint in the gas network. Equation (68) is the coupling constraint of power and natural gas networks via the Gas-Fired Power Plant (GFPP). For linearizing the Eq. (68), the introduced method in [46] is used. Equations (69) and (70) present the nodal and bus market-clearing prices that MESPs are connected to it.

$$Pr^{Min}_{n} \leqslant Pr_{n,t} \leqslant Pr^{Max}_{n} \quad \forall n, \forall t \tag{65}$$

$$\nu^{Min}_{sp} \leqslant \nu_{sp,t} \leqslant \nu^{Max}_{sp} \quad \forall sp, \forall t \tag{66}$$

$$\sum_{sp \in A^{sp}_{n}} \nu_{sp,t} - \sum_{h \in A^{h}_{n}} f^{Gas,in}_{h,t} - \sum_{l \in A^{l}_{n}} L_{l,t} = \sum_{m \in z} (q^{in}_{n,m,t} - q^{out}_{m,n,t}) : \lambda^{Gas}_{n,t} \quad \forall n, \forall t \tag{67}$$

$$L_{l,t} = a_i P^{2}_{i,t} + b_i P_{i,t} + c_i + SU_{i,t} + SD_{i,t} \quad \forall l \in A^{GU}_{l}, \forall i \in GU, \forall t \tag{68}$$

$$\lambda^{Gas}_{n,t} = \gamma^{LMGP}_{h,t} \quad \forall n \in A^{h}_{n}, \forall t, \forall h \tag{69}$$

$$\lambda^{Elec}_{b,t} = \beta^{LMEP}_{h,t} \quad \forall b = A^{h}_{b}, \forall t, \forall h \tag{70}$$

3.8. Robust optimization method

In the introduced model, LMEP values are determined by solving the market-clearing problem. However, to consider the stochastic behavior of the other participants of IPNGM (e.g., RESs), obtained LMEP from the lower level is modeled as an uncertain parameter in the upper level. In the RO method, despite stochastic approaches, there is no need for probability density functions. Therefore, in the RO method, an interval of uncertain parameter variation is utilized. Such intervals can be extracted from prediction models [47]. Indeed, these intervals can be defined as a ratio of predicted amounts. So, given that:

$$\rho_{h,t}^{LMEP\_max} = (1+\alpha)\beta_{h,t}^{LMEP} \quad \forall t, \forall h \tag{71}$$

$$\rho_{h,t}^{LMEP\_min} = (1-\alpha)\beta_{h,t}^{LMEP} \quad \forall t, \forall h \tag{72}$$

The amount can be varied from zero to one in order to adjust the uncertainty level. In the RO method, instead of objective Eq. (1), the min-max relation of Eq. (73) is replaced.

$$\min \left\{ \begin{array}{l} \sum_{t}\sum_{h} (\beta_{h,t}^{LMEP\_min}.f_{in,h,t}^{Elec} + \max_{\{S_0 | S_0| \leqslant \Gamma\}} \left[\sum_{t\in S_0}\sum_{h} \beta_{h,t}^{LMEP\_max} - \beta_{h,t}^{LMEP\_min} \right] f_{in,h,t}^{Elec} \\ + \sum_{t}\sum_{h} \gamma_{h,t}^{LMGP} f_{in,h,t}^{Gas} \end{array} \right\} \tag{73}$$

In Eq. (73), the parameter Γ determines the robustness level of the method to the conservatism level of the results. In the RO method, $\Gamma = 0$ means that the impact of the uncertain parameter on the cost deviation is totally ignored. In contrast, by adjusting $\Gamma = T$, uncertainty is considered for the whole time horizon, and the most conservative result can be obtained. Increasing the value of Γ causes an increase in the robustness level of the results against the price incrementation. Utilizing auxiliary variables of $z_{h,t}$ and $y_{h,t}$, Eq. (73) can be restated as Eq. (74) [14].

$$\min \left\{ \begin{array}{l} \sum_{t}\sum_{h} (\beta_{h,t}^{LMEP\_min}.f_{in,h,t}^{Elec} + \max_{\left\{\sum_{t}\sum_{h} z_{h,t} \leqslant \Gamma, 0 \leqslant z_{h,t} \leqslant 1, v_{in,h,t}^{e} \leqslant y_{h,t}\right\}} \\ \left[\sum_{t\in S_0}\sum_{h} \beta_{h,t}^{LMEP\_max} - \beta_{h,t}^{LMEP\_min} \right] y_{h,t} z_{h,t} + \sum_{h}\sum_{t} \gamma_{h,t}^{LMGP} f_{in,h,t}^{Gas}) \end{array} \right\} \tag{74}$$

Furthermore, employing duality theory, Eqs. (75)- (80) can be considered as the equivalent of Eq. (74). In these relations, $\zeta_{h,t}$ and ψ are dual variables associated with uncertainty intervals [48]. More details of the dual theory process in robust optimization based on MILP programming are shown in Appendix B.

$$\min \left\{ \sum_{t} \sum_{h} (\beta_{h,t}^{LMEP\_min}.f_{in,h,t}^{Elec}) + \psi\zeta_{h,t} + \sum_{h} \sum_{t} \zeta_{h,t} + \sum_{h} \sum_{t} \gamma_{h,t}^{LMGP} f_{in,h,t}^{Gas}) \right\} \tag{75}$$

$$\psi + \zeta_{h,t} \leqslant (\beta_{h,t}^{LMEP\_max} - \beta_{h,t}^{LMEP\_min}) y_{h,t} \quad \forall t, \forall h \tag{76}$$

$$\zeta_{h,t} \geqslant 0 \quad \forall t, \forall h \tag{77}$$

$$y_{h,t} \geqslant 0 \quad \forall t, \forall h \tag{78}$$

$$\nu_{in,h,t}^{e} \leqslant y_{h,t} \quad \forall t, \forall h \tag{79}$$

$$\psi \geqslant 0 \tag{80}$$

Finally, Eqs. (2)- (25) form relation of the upper level in the supplemented model.

4. Design of the MESPs participation mechanism in the IPNGM

Figure 2 indicates the introduced mechanism for MESPs in the IPNGM. This includes several participants, as follows:

1. NGPPs: These units generate power using non-gaseous fuels and sell it to the IPNGM.
2. Natural gas producers: These producers are obliged to extract the natural gas from wells and, after refining, sell it to the IPNGM.
3. Renewable energy sources: The task of RESs is to produce power using non-fossil fuels such as wind, solar, and biomass and sell them to the IPNGM.
4. IPNGM operator: The obligations that arise due to this operator are controlling and monitoring the IENGN and performing the integrated power and gas market clearing.
5. Energy consumers purchase power and natural gas from IPNGM to meet their load. Energy consumers are classified as active and passive consumers. Active

consumers are sensitive to the introduced LMPs from the wholesale market and change their scheduling depending on introduced LMPs. However, passive consumers are not sensitive to the LMPs and don't make any changes. Multi-energy entities are large-scale active consumers that can make changes in the market-clearing prices by changing their energy trading policy with the IPNGM.

The proposed market clearing mechanism is as follows:

In Figure 3, MESPs' participation in the IPNGM is illustrated as an iterative-based two-step algorithm. At first, input parameters including IENGN data, price, and values of energy producers (e.g., NGPPs, gas wells, wind turbines) and bidding/offering of consumers are submitted to the central operator. Then, the IPNGM uses the standard market-clearing tool to clear the market with the aim of maximizing social welfare, and values of LMEP and LMGP are obtained for every node and bus of the electricity and natural gas networks. By determining the values of LMEP and LMGP, the upper level of the problem, i.e., Eqs. (1)-(34) is implemented by MESPs to minimize the cost of the purchased energy. In doing so, the optimal cost of the multi-energy entities is calculated, and the load profile is updated. In the second step, IPNGM has to be cleared according to the new loads at bus b^* and node n^* (that node and bus that multi-energy entity is connected to them). Thereafter, the lower level of the problem, i.e., Eqs. (35)-(70), is solved, and new values of LMEP and LMGP are calculated. Updated new values of the LMEP, LMGP, and load profile are used to calculate the real cost of the purchased power as:

$$\text{Cost}_{\text{real}} = \sum_{t} \sum_{h} (\beta_{h,t}^{\text{LMEP}} f_{h,t}^{\text{Elc,in}} + \gamma_{h,t}^{\text{LMGP}} f_{h,t}^{\text{Gas,in}}) \tag{81}$$

Indeed, if a load shifting is required from IPNGM, the real cost of the purchased power will be equal to $\text{Cost}_{\text{real}}$. After calculating $\text{Cost}_{\text{real}}$ by Eqs. (82), the convergence of the problem is measured by Eqs. (82). If the problem-solving process does not converge, feedback is given to **step 1**. This process continues until the following criteria are reached:

$$\left| \frac{\text{Cost}_{\text{real}} - \text{Cost}}{\text{Cost}_{\text{real}}} \right| \leqslant \varepsilon \tag{82}$$

where, Cost is obtained cost from running the upper level and is its real value of it.

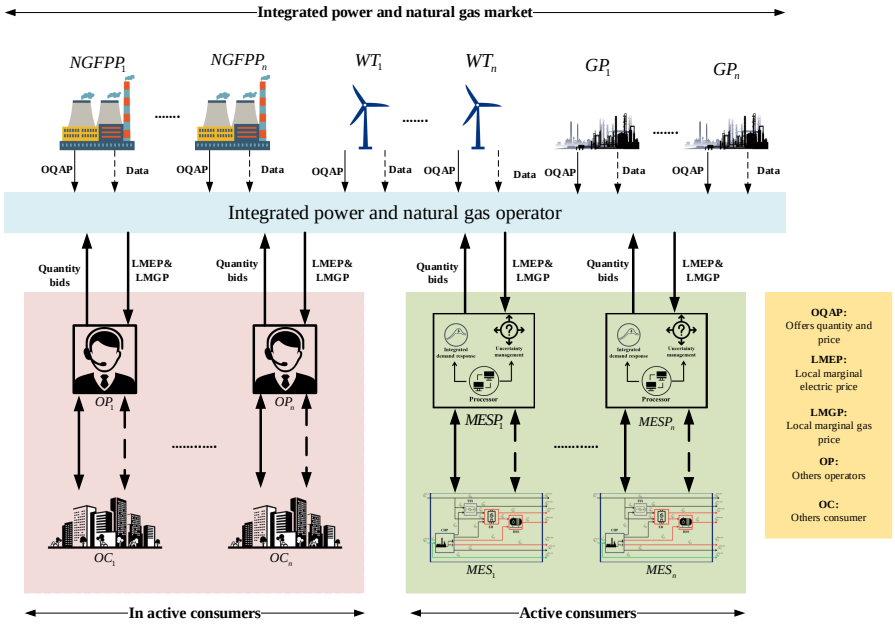

Figure 2: The introduced mechanism for MESPs participation in the IPNGM

Fig3a.pdf

Figure 3: The iterative-based two-step algorithm

In addition, $\text{Cost}_{\text{real}}$ is a stopping criterion that is considered 0.02. Obtained results verify the convergence of this mechanism.

To apply the RO method in the proposed market clearing problem, MESPs, after obtaining the final LMEP, apply the RO method. It is worth noting that electricity and natural gas network losses and the strategic behavior of other market participants are not in the main scope of the current work, and they will be taken into account in future works.

5. Simulation and numerical results

In this research, to simulate the IPNGM, a standard IEEE test system composed of a 6-bus power system integrated with a 6-node natural gas network is utilized [48, 49]. In addition, to show the robustness of the proposed model, simulations are

verified on a 118-bus power system integrated with a 10-node natural gas network [48].

6. Modified IEEE 6-bus power system integrated with 6-node natural gas network

The structure of the 6-bus power system, along with the 6-node natural gas network, is shown in Figure 4. The modified 6-bus power system includes two GFPPs, one NGPP, one wind power plant (WPP), seven transmission lines, and two loads, details of them were introduced in [48]. GFPPs are located on buses 1 and 6; NGPPs and WPP are located on buses 2 and 4, respectively. The 6-node natural gas network includes five pipelines, two natural gas producers, and six gas loads, which details can be found in [48]. Figure 5 shows the natural gas residential demand, total power demand, and predicted wind power for the 6-bus system. The introduced MES is connected to bus 5 in the power system and node 3 in the natural gas network. Power, heat, and natural gas demands of MES are indicated in Figure 6. Details of the MES's components, including the CHP unit, ESS, TSS, and boiler, are available in [50]. The proposed model is a MILP, which is implemented in the GAMS environment, and the CPLEX solver is utilized to solve the optimization problem. To provide an accurate evaluation of simulation results, four different case studies are introduced as follows:

1. Case study 1 (**CS1**): Solving the deterministic problem of MESP participation in the IPNGM in the absence of flexible sources of the MES
2. Case study 2 (**CS2**): Solving the deterministic problem of MESP participation in the IPNGM by considering flexible sources of ESS and TSS in the MES
3. Case study 3 (**CS3**): Solving the deterministic problem of MESP participation in the IPNGM by considering flexible sources of ESS, TSS, and DRP in the MES
4. Case study 4 (**CS4**): Solving the robust problem of MESP participation in the IPNGM by considering flexible sources of ESS, TSS, and DRP in the MES

CS1: Optimal scheduling of GFPPs and NGPP is depicted in Fig. 7. We can

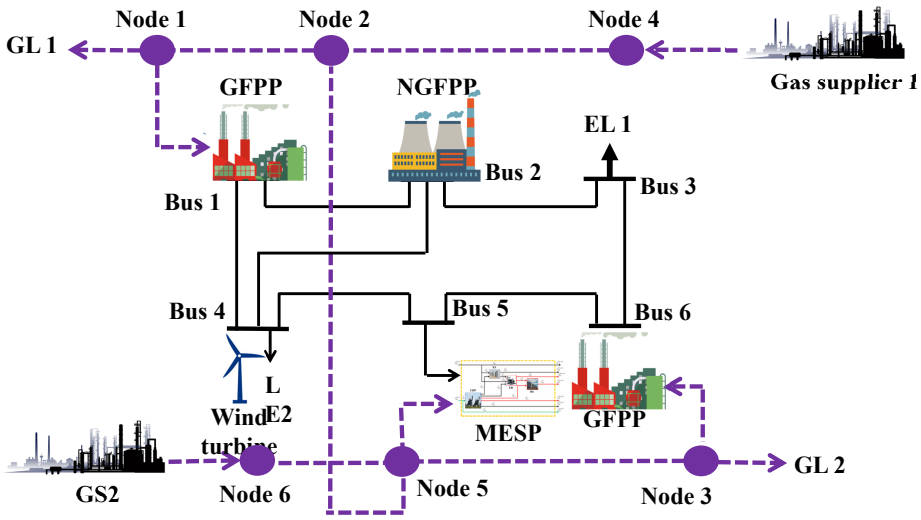

Figure 4: Structure of the 6-bus power system integrated with the 6-node natural gas network

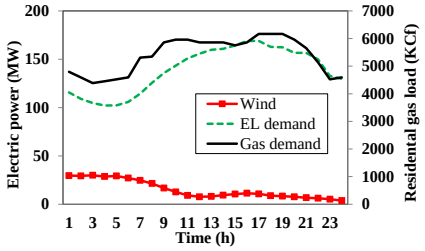

Figure 5: Load profile of power transmission system, natural gas demand and wind power

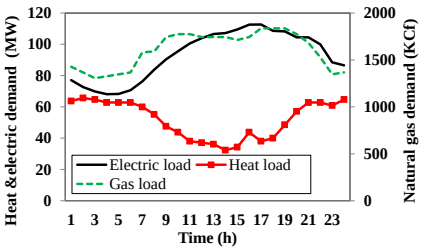

Figure 6: Power, heat, and natural gas demands of MES

see that the low-cost GFPP G1 is online during the whole scheduling time horizon. While high-cost NGPP G2 is online during hours t=10 to t=21. Since supplying local loads of the natural gas network is prior to other industrial loads, supplying natural gas during peak hours, which is occurred between hours t=15 and t=21, is limited to the GFPPs. For this reason, the G1 unit dispatch decreases at these hours, and instead, the G2 unit assumes to supply the rest of the loads. In addition, the G3 unit is online during hours t=17 and t=22. In this case study, the total operation cost of the IENGN is $405683, and the cost of the GFPPs is $389264.3 , and also the cost of the NGFPP is $16418.74.

Figure 8 indicates the natural gas dispatch of producers, in which the most dispatch of natural gas is related to the low-cost producer PG1. Dispatch of high-cost producer PG2 increases significantly during hours t=9 to t=21 due to an increase in demand for GFPPs and local loads of natural gas network. Then, after the hour t=22 decreases because of a reduction in demand for the natural gas network. The cost of the low-cost and high-cost producers are $207503.84 and $181760.42 , respectively.

Figure 9 illustrates the LMEP of the bus that MES is connected to (i.e., bus 5). According to the figure, the market-clearing price is still in the same range during hours t=1 to t=6, which is nearly $19.17/MWh. From hour t=7 to t=10 due to increasing in G1 unit production, the market clearing price increases to the value of $21.95/MWh. Between hours t=10 to t=21, the commitment of the high-cost unit G2 causes increases in the market-clearing price up to $32.63/MWh. After hour t=21, decreasing power system demand and getting out of the natural gas network peak period leads to the shutting down of the high-cost G2 unit and reduction of the G1 unit dispatch. For this reason, the market-clearing price decreases to the value of $24.37/MWh. LMGP is depicted in Fig. 9 via the noted red line. Owing to the low and uniform demand of the GFPPs and local loads of the natural gas network during hours t=1 to t=9, LMGP is $2.9 /KCfh at this period. With the increasing of high-cost unit PG2 dispatch at hours t=9 until t=16, LMGP rises to $3.36/KCfh. Considering the hours t=17 and t=18, which is the peak period for both the electricity and natural gas networks, the market-clearing price reaches $3.75/KCfh at this period. After hour t=21, with decreasing in the high-cost PG2 unit, the market-clearing price decreases to $2.9/KCfh. Note that LMEP and LMGP that is shown in Figure 9 are related to the bus and node that MES is connected to, i.e., bus 5 and node 3 of electricity and natural gas networks.

Figure 10 shows MESP's optimal scheduling for supplying MES demand in **CS1**. As illustrated, the MESP meets 55.13% of electrical demand via purchasing power from IPNGM, and 42.74% of electrical demand is supplied by the CHP unit of the MES. Moreover, optimal scheduling of MESP for supplying thermal demands of MES in **CS1** is depicted in Figure 11. Since producing thermal energy using natural gas

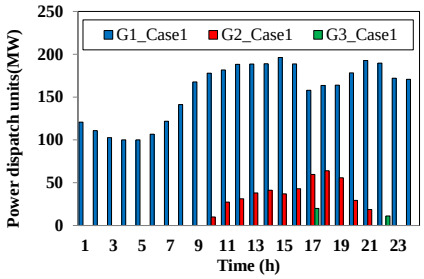

Figure 7: Hourly optimal scheduling of GFPP and NGPP in **CS1**

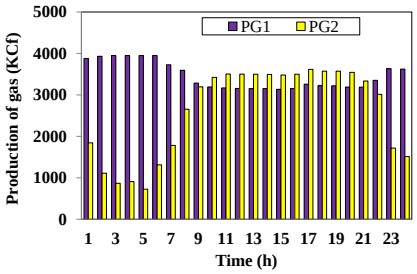

Figure 8: Hourly dispatch of the natural gas producers in **CS1**

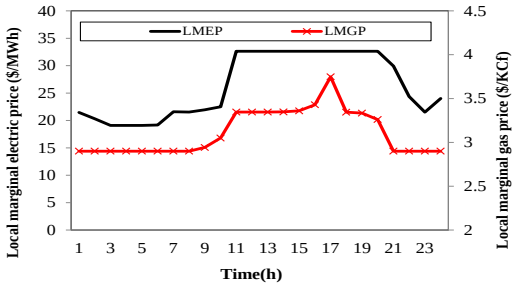

Figure 9: LMEP and LMGP of bus 5 and node 3 in the IPNGM

has a lower cost, the MESP uses the CHP unit as the first priority to supply MES thermal demands. During the peak, thermal load period of MES, which occurred at hour t=20 until t=8, MESP to balance the MES's thermal energy production and consumption is compelled to run the electrical boiler. As can be seen, 91.66% of thermal energy is met via the CHP unit, and 8.33% is met by the electrical boiler.

Figure 12 shows operation cost obtained by the iterative-based two-step algorithm, in which the convergence of the Eq. (82) is proofed. Here are how the results are obtained:

1. First step cost (Cost): At the first step, IPNGM is cleared based on basic load, then the values of LMEP and LMGP are presented to the MESP. Based on the presented prices, the MESP performs optimal scheduling and obtains the optimal operation cost (Cost).
2. Second step cost ($\text{Cost}_{\text{real}}$): After performing optimal scheduling by the MESP,

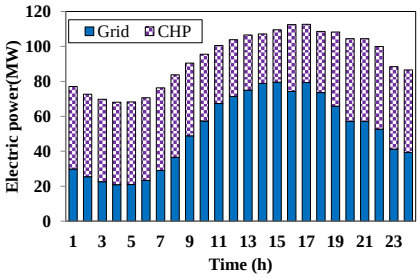

Figure 10: Hourly optimal scheduling of MESP for supplying electrical demand of MES in **CS1**

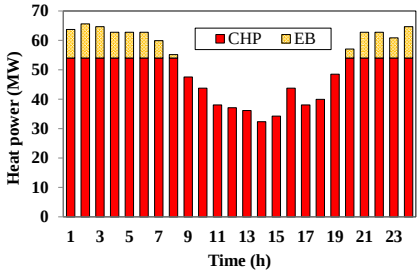

Figure 11: Hourly dispatch of the natural gas producers in **CS1**

the MES updates its load profile based on presented prices by the operator of the IPNGM, then sends the updated load profile to the operator of the IPNGM. Thereafter, the IPNGM is cleared based on the updated load profile and updated LMEP and LMGP are replaced, then real cost ($Cost_{real}$) based on Eq. (81) is calculated. The obtained costs by the first and second steps are compared with the stopping criterion of Eq. (82). If the criterion is satisfied, the procedure will be finished; else, feedback based on updated prices will be submitted to the first step.

3. The cost of the feedback 1: As illustrated, in this case study, after one feedback criterion of Eq. (82) is reached and the real cost is achieved. As depicted in Figure 12, the difference between optimal cost and the real cost is equal to zero, and the obtained results can be trustable. Note that the stopping criterion may not reach with only one feedback, and it may take several feedbacks. Moreover, it should be noted that all the results such as unit commitment, optimal scheduling of MES and etc. are provided via the iterative-based two-step algorithm for all case studies.

Figure 13 indicates the behavior of the high-cost NGPP G2 with and without the line pack. When the natural gas network is equipped with line pack, produced power by the G2 unit, especially at peak hours of the natural gas network (t= 17), decreases. As well as for the low-cost GFPP G1 in Figure 14, it can increase the produced power during the peak period of the natural gas network by considering

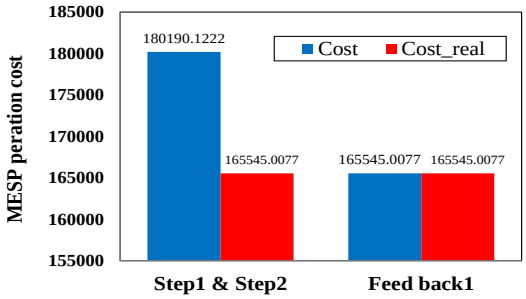

Figure 12: Obtained operation cost of the MESP via iterative-based two-step algorithm in **CS1**

Table 2: Comparison of the IENGN operation costs with and without line pack system

Cost ($)	Without line pack	With line pack
Total operation cost	405630.9371	405683.0076
NGFPP cost	16623.06428	16418.74416
GFPP cost	389007.8728	389264.2635

the line pack. In doing so, the flexibility of electricity and natural gas networks increases. According to the results, it can be concluded that the line pack system not only increases the flexibility of the natural gas network but also decreases the operation cost. In Table 2, regional operation costs are compared with and without considering the line pack. As illustrated, the operation cost of the G2 unit decreases by considering the line pack. In addition, it is obvious that G1 and G2 units' generations increase due to increases in natural gas production when the natural gas network is equipped with the line pack. Considering that line pack system flexibility is dependent on the pressure level at pipeline nodes, the storage level of pipelines can be increased by doubling the upper limit of pressure at the pipeline nodes' and consequently flexibility of the generation units and saved cost at regional area increase. Furthermore, to avoid over-displaying of figures and tables, the effect of ignoring the line pack system is evaluated in only **CS1**. Obviously, related results in other case studies are the same as in **CS1**.

CS2: In this case study, the focus is on MESP participation in IPNGM considering the energy storage systems of MES. Optimal scheduling of GFPP and NGPP are

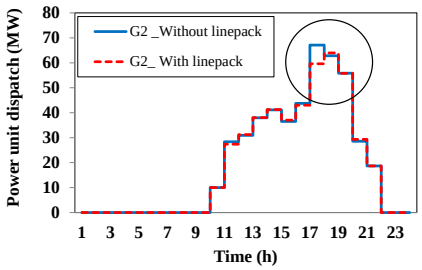

Figure 13: Comparison of the generated power of the G2 unit with and without line pack system

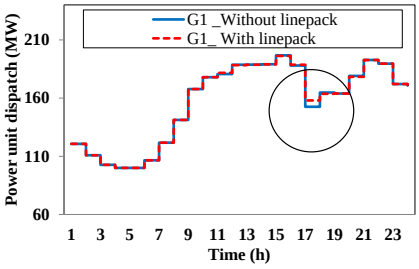

Figure 14: Comparison of the generated power of the G1 unit with and without line pack system

depicted in Figure 15. As can be seen, low-cost GFPP G1 is committed for the whole time horizon. Owing to ESS implementation by MESP, dispatch of the G1 unit is increased by 1.31% compared with **CS1**. High-cost NGPP G2 is online from hour t=10 until t=21. Hourly dispatch of unit G2 is decreased by 27.12% compared with **CS1**. Generation unit G3 is also online during hours t=16, 20, 23. In this case study, the total operation cost of the IENGN is $403205.9 , and the operation cost of the GFPP is $390834.748, as well as $12371.1 for the NGPP.

Figure 16 illustrates LMEP and LMGP in the IPNGM for **CS2**. Owing to a 27.12% reduction in the dispatch of the high-cost NGPP G2 compared with **CS1**, LMEP decreases $6.15/MWh in total. In addition, LMGP decreases at peak hours of the electricity and natural gas networks, i.e., t=17 and t= 18, due to the reduction of G2 unit dispatch.

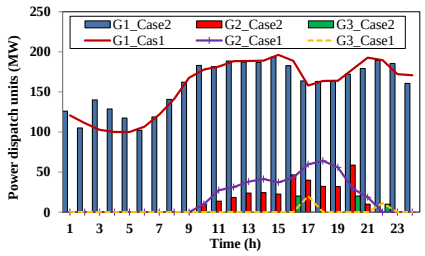

Figure 15: Hourly optimal scheduling of GFPPs and NGPP in **CS2**

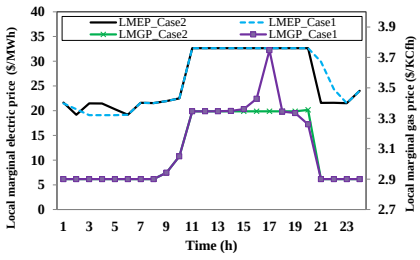

Figure 16: LMEP and LMGP at bus 5 and node 3 in the **CS2**

Figure 17 indicates the optimal hourly scheduling of the MESP for supplying

the power demand of the MES. As illustrated, ESS, with tracking of the LMEP, at low price periods starts to store power and deliver power during peak price periods. In doing so, MESP shifts some part of the purchased power from on-peak hours to off-peak hours. According to Figure 17, MESP meets 50.63% of the MES's power demand by purchasing from IPNGM, and 45.73% of the demand is met by the CHP unit of the MES. Also, 3.62% is met by ESS.

Figure 18 shows the MESP scheduling of supplying thermal demand for MES. TSS stores energy during off-peak hours and return it at on-peak hours. In doing so, 84.67% of thermal demand is met by the CHP unit, 4.22% by the boiler, and 10.24% by TSS.

Figure 19 illustrates the operation cost of the MES obtained via the iterative-based two-step algorithm. Moreover, the convergence of the Eq. (82) is proofed, in which the algorithm is converged after sending two feedback from IPNGM. According to the results, the tolerance is 0.1% at the last iteration, and it can be accepted.

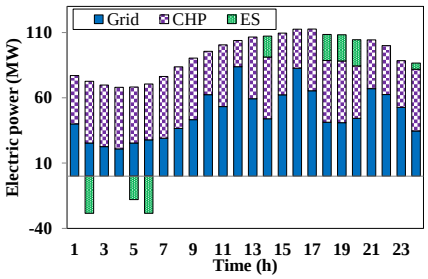

Figure 17: Hourly optimal scheduling of MESP for supplying power demand of MES in **CS2**

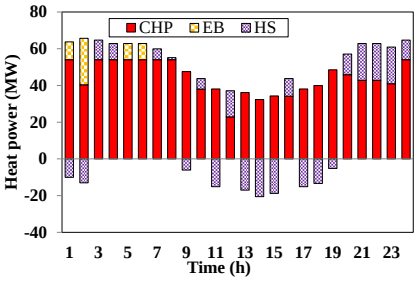

Figure 18: Hourly optimal scheduling of MESP for supplying thermal demand of MES in **CS2**

CS3: The focus of this case study is on the MESP participation in the IPNGM by considering the energy storage systems and DRP. Optimal scheduling of the GFPP and NGPP are depicted in Figure 20. Low-cost GFPP G1 is committed the whole time horizon. Due to the implementation of energy storage systems and DRP simultaneously by MES, dispatch of the G1 unit in comparison with **CS2** 2.74% is increased. High-cost NGPP G2 is online during hours t=10 until t=21. Dispatch of the G2 unit is decreased up to 19.48% compared with **CS2**. Moreover, the dispatch

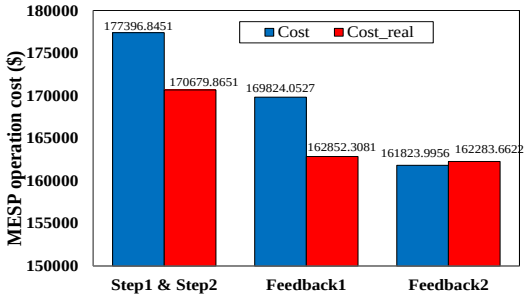

Figure 19: Obtained operation cost of the MESP via the iterative-based two-step algorithm in **CS2**

of the G3 unit is decreased by nearly 80% compared with **CS2**. The total operation cost of the IENGN is $402202.6, operation costs of the GFPP, and NGPP are $392054.8 and $10147.86, respectively.

Figure 21 indicates LMEP and LMGP in **CS3**. Owing to a 19.48% reduction in the dispatch of the high-cost NGPP G2, LMEP is reduced $20.8/MWh in comparison with **CS1** and $14.68/MWh in comparison with **CS2**. According to that, in the IPNGM electricity and natural gas networks are operated in an integrated manner, the behavior of the G2 unit affects LMGP at hours t= 14 and t= 15.

Figure 24 provides the optimal scheduling of MESP for supplying MES demands. After applying DRP on electrical loads of MES via MESP, some parts of the power demand shift from on-peak load hours to off-peak hours. The comparison of purchased power between cases 2 and 3 shows that purchased power is decreased in case 3 during on-peak hours and instead increased during off-peak hours. Applying DRP by MESP not only reduces the operation cost of the MES but also increases flexibility and reduces the operation cost of the IENGN.

Figure 23 illustrates the obtained MES's operation cost via the iterative-based two-step algorithm. In addition, the convergence of the Eq. (82) is proofed. As is seen, in this case study, with only one feedback from IPNGM, the algorithm is converged. Moreover, the tolerance is 0.013, which is acceptable.

In Table 2, the operation costs of the MES and IENGN are compared among three cases, in which implementation of flexible energy sources by the MESP leads to a 4.39% reduction in operation cost of the MES, 38.19% reduction in operation

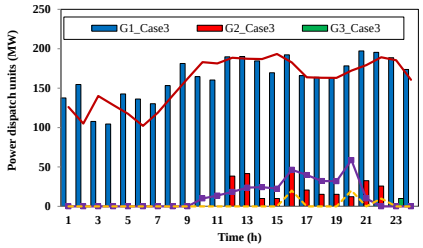

Figure 20: Hourly optimal scheduling of GFPP and NGPP in **CS3**

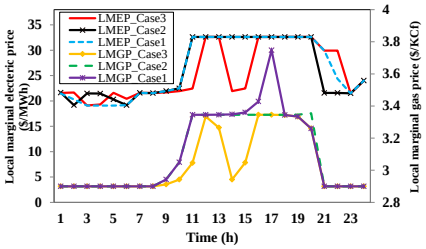

Figure 21: LMEP and LMGP at bus 5 and node 3 in **CS3**

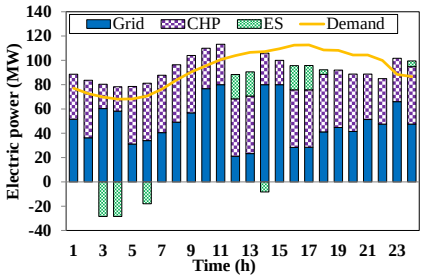

Figure 22: Hourly optimal scheduling of MESP for supplying power demand of MES in **CS3**

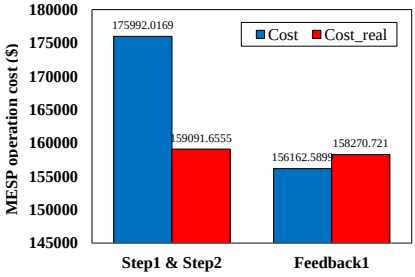

Figure 23: Obtained operation cost of the MESP via the iterative-based two-step algorithm in **CS3**

cost of the high-cost NGPP, 0.71% increasing in operation cost of the low-cost GFPP, 0.86% reduction in the total operation cost of the IENGN.

CS4: In this case study, uncertainty is also taken into account. To evaluate the results, a sensitivity analysis with the variation of the uncertainty budget from $\Gamma = 0$ to $\Gamma = T$ is conducted. Figure 24 shows the operation cost increases with increasing in the uncertainty budget. $\Gamma = 0$ means uncertainty impact is totally ignored, while $\Gamma = T$ means uncertainty impact is considered for the whole time horizon, and the most conservative result is obtained. Figures 25 and 26 indicate purchased power and total operation cost of the MES for different uncertainty budgets, respectively. As illustrated in Figure 26, the total operation cost of the MES increases with the increase of the uncertainty budget. In other words, the more risk is taken, the more cost must be paid.

Table 3: Comparison of the operation costs

Cost ($)	CS1	CS2	CS3
IENG cost	405683	403205.9	402202.6
NGFPP cost	16418.74	12371.1	10147.86
GFPP cost	389264.3	390834.7	392054.8
MESP cost	165545.01	162283.7	158270.7

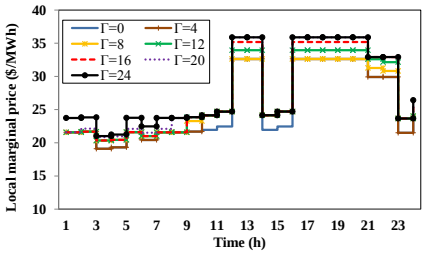

Figure 24: Price deviation of LMEP under different uncertainty budget

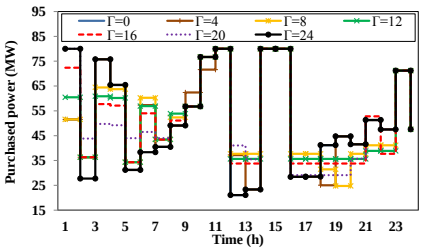

Figure 25: Purchased power under different uncertainty budgets

6.1. *Modified IEEE 118-bus system and 10-node natural gas network*

The modified IEEE 118-bus system is composed of 8 GFPPs, 46 NGPPs, 186 transmission lines, and 91 electrical loads. The total capacity of the GFPPs is 725 MW, which is 10% of the total units' capacity. Details of solution time and the number of variables are also shown in Table 5. The peak load of the power system is 5890 MW, which occurred at hour t= 17. Four wind power plants with the capacity

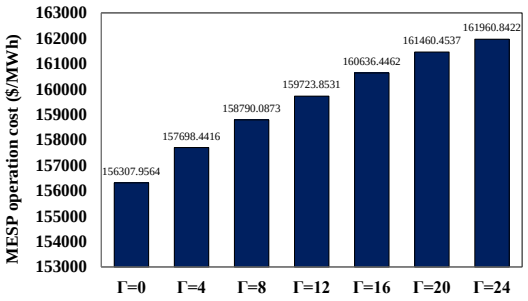

Figure 26: Impact of the uncertainty budgets on the total operation cost of the MES

of 50 MW, 50 MW, 30 MW, and 30 MW, which are located at buses 11, 30, 57, and 86, respectively. The natural gas network is composed of 10 nodes, 10 pipelines, and 12 residential loads. Furthermore, 6 MESs are located at buses 11, 28, 62, 78, 98, and 112 of the power system and nodes 4, 7, 5, 2, and 6 of the natural gas network. Details of the 118-bus system and 10-node natural gas network are available in [48]. Note that, to avoid redundancy and over-displaying figures, simulation results are provided for only MES number 2 located at bus number 28 of the power system and node number 7 of the natural gas network. Other MESs' behavior is like MES number 2.

Figure 27 shows the optimal hourly scheduling of electric power purchases by the second MESP from the IPNGM in three case studies. In the **CS2**, electric energy is charged in the ESS during off-peak and cheap hours and discharged during on-peak and expensive hours. For this reason, the purchase of electric power from the IPNGM increases in off-peak and cheap hours and decreases in on-peak and expensive hours. In **CS3** investigates the impact of implementing the DRP in MESPs. With the implementation of the DRP, part of the electric energy consumption has been shifted from on-peak and expensive hours to off-peak and cheap hours. For this reason, the purchase of electric power during cheap hours has increased compared to expensive hours. Figure 28 indicates the optimal scheduling of 8 GFPPs for three case studies. Implementation of energy storage systems and DRP via MESPs in the MES shifts power generation of units from on-peak hours to off-peak hours. In Figure 29, the optimal scheduling of all the 46 NGPPs is depicted for three case studies. Similar to the GFPPs, the power generation of NGPPs is shifted from on-peak hours to off-peak hours by applying flexible energy sources. According to Figure 30, a comparison of LMEP in **CS1**, **CS2**, and **CS3** shows the significant effect of applying energy storage systems and DRP, which lead to a reduction of LMEP. Table 4 provides the total operation costs of MESPs and IENGN for three case studies. The application of flexible sources via MESPs, not only reduces the operation costs of MES but also reduces the operation costs of the IENGN. Figure 31 shows that the increasing uncertainty budget leads to an increase in electricity prices. Moreover, Figure 32 indicates purchased power under different uncertainty budgets. In Fig-

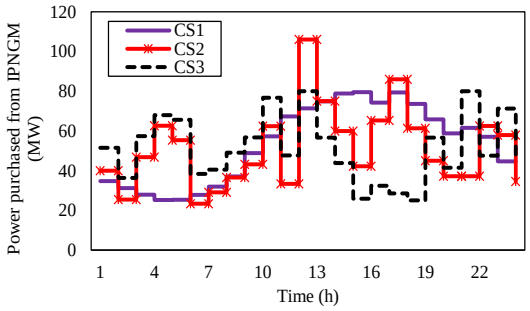

Figure 27: The optimal hourly scheduling of electric power purchases by the second MESP from the IPNGM in three case studies

ure 33, the operation costs of MESPs are shown for different uncertainty budgets. As depicted, an increase in the uncertainty budget causes increasing in the operation costs of MESPs. Figure 34 -36 also show the convergence of the iterative-based two-step algorithm (Equation (82)) respectively. In **CS1**, due to the lack of flexible energy sources (storage systems and DRP), convergence is obtained after the first feedback. In **CS2**, convergence is obtained after three times of feedback. While the convergence in the **CS3** is achieved after two feedbacks. The tolerance value in **CS1**, **CS2**, and **CS3** is 0%, 0.07%, and 0.002%, respectively.

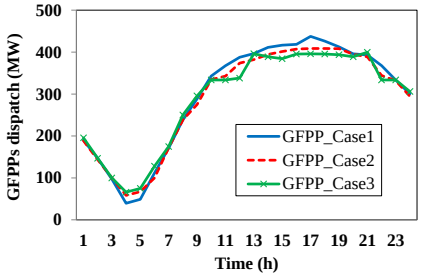

Figure 28: Generated power of 8 GFPPs in three case studies

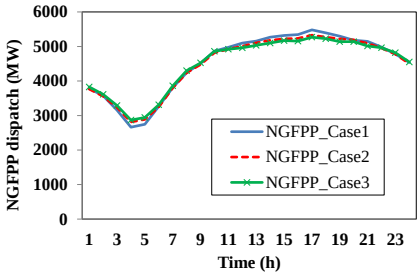

Figure 29: Total generated power of 46 NGPPs in three case studies

7. Conclusion

In this paper, a robust bilevel approach for the participation of multi-energy service providers (MESPs) in the integrated power and natural gas market (IP-

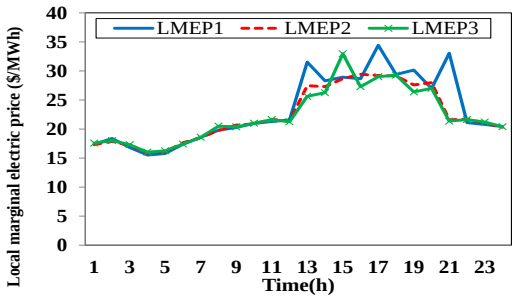

Figure 30: Comparison of LMEP at bus number 28 of the power system

Table 4: Operation costs in three case studies

Cost ($)	**CS1**	**CS2**	**CS3**
IENG cost	2758472	2737723	2733847
NGFPP cost	1167060	1162168	1160809
GFPP cost	1591411	1575556	1573037
MESP cost	162981.1	159148.2	157706.1

Table 5: Computational details in 118 bus test system for different case studies

Variables/Solution time	Case1	Case2	Case3	Case4
Single variables	47882	49752	50328	50376
Discrete variables	1722	2010	2298	2298
Solution time (min)	14.05	15.04	16.52	105

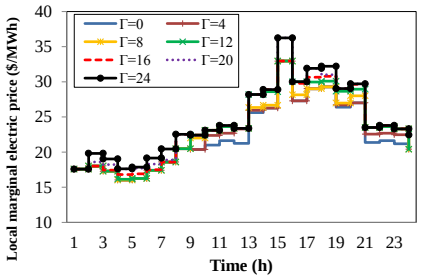

Figure 31: LMEP deviation under different uncertainty budgets in **CS4**

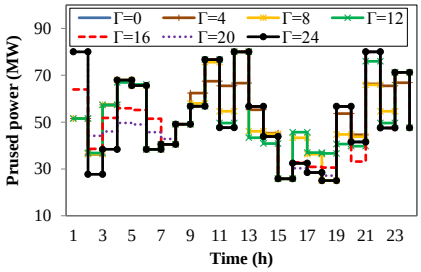

Figure 32: Purchased power under different uncertainty budgets in **CS4**

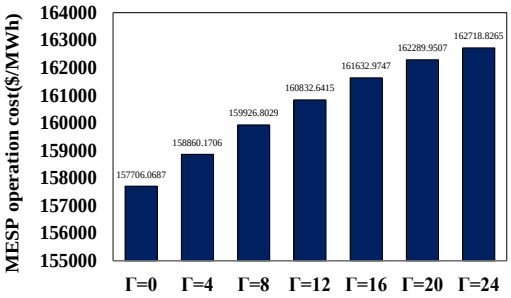

Figure 33: Impact of the uncertainty budgets on the total operation cost of the MES

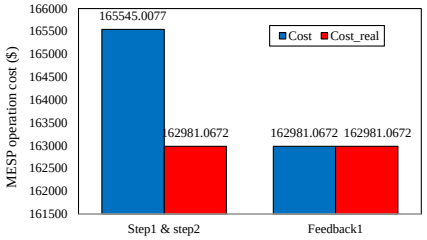

Figure 34: Obtained operation cost of the MESP via the iterative-based two-step algorithm in **CS1**

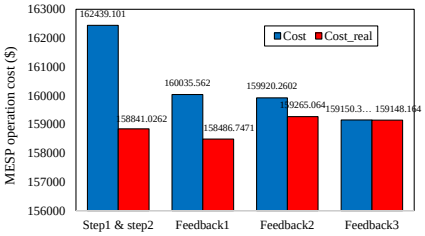

Figure 35: Obtained operation cost of the MESP via the iterative-based two-step algorithm in **CS2**

NGM) under an iterative-based two-step algorithm was proposed. At the upper level, MESPs using flexible energy sources, including energy storage systems and the demand response program (DRP) aim to minimize the purchased power and natural gas from IPNGM. At the lower level, the operator of the IPNGM aggregates bids/offers, and with the aim of social welfare maximization, clears the market. The

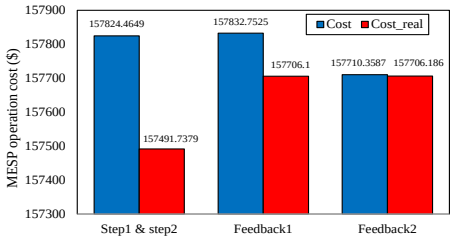

Figure 36: Obtained operation cost of the MESP via the iterative-based two-step algorithm in **CS3**

proposed study was rendered on a 6-bus power system and a 6-node natural gas system with an MES. In addition, to increase the validity of the obtained results, the proposed approach was to be carried out on a 118-bus power system and a 10-node natural gas network with six MES. The obtained results indicated that the decision-making of MESPs as responsive and large-scale consumers can affect the decisions of IPNGM's operator and vice versa. Further, it can be seen that the application of energy storage systems and DRP have positive impact on the behaviors of the multi-energy systems (MESs) and IPNGM. In addition, the following results can be summarized:

1. The operation of the natural gas network in the presence of line pack led to an increase in fuel supply to GFPP units. Considering linepack in natural gas networks while reducing 1.23% of NGFP costs increased the flexibility of the entire IPNGM.
2. The utilization of ESS and TSS, while reducing 1.97% of the total operating costs of MESP, led to a reduction of 0.61% of the IPNGM total operation costs. In addition, the presence of energy storage systems increases MESP's ability to influence the IPNGM market.
3. The implementation of the DRP while reducing 4.39% of the MESP total operating costs led to a reduction of 0.85% of IPNGM the total operating costs. Further, the coordination of energy storage systems with DRP increases the effectiveness of MESP in the IPNGM market while increasing the flexibility of the entire system.
4. By increasing the uncertainty budget in the robust optimization approach,

MESP operating costs increase. However, MESP is robust to the fluctuation behavior of LMEP.

Acknowledgments

This work was supported from DTE Network+ funded by EPSRC grant reference EP/S032053/1.

Appendix A. Natural gas network linearization

To this end, an outer approximation based on the Taylor series around constant points of pressure is employed to linearize the Weymouth equation and achieving a globally optimal solution [51]. Gas flow constraint is considered using approximated Eq. (A.1). Outer approximated values are obtained via a number of tangent lines on the surface of the Weymouth equation.

$$q_{n,m,t} \leqslant \frac{K^{f}_{n,m} PR_{n,u}}{\sqrt{PR^{2}_{n,u} - PR^{2}_{m,u}}} Pr_{n,t} - \frac{K^{f}_{n,m} PR_{m,u}}{\sqrt{PR^{2}_{n,u} - PR^{2}_{m,u}}} Pr_{m,t} \quad \forall n, \forall m, \forall u, \forall t \tag{A.1}$$

Linear constraints are generated based on selected constant points of pressure through the several values of neighbor nodes. Obtained constant pressure points are utilized to express the unidirectional gas flow in the pipelines. As pressure limitations are not equal through the neighboring nodes, they may be different from those cases obtained to express the gas flow in the reverse direction. Hence, a relation should be defined to express bidirectional gas flow in the pipelines. To this end, inequalities of Eqs. (A.2)- (A.5) are taken into account that express the bidirectional gas flow in the pipelines.

$$q_{n,m,t} = q^{+}_{n,m,t} - q^{-}_{n,m,t} \quad \forall n, \forall m, \forall t \tag{A.2}$$

$$q^{-}_{n,m,t} = M(1 - y_{n,m,t}) \quad \forall n, \forall m, \forall t \tag{A.3}$$

$$q^{+}_{n,m,t} = M y_{n,m,t} \quad \forall n, \forall m, \forall t \tag{A.4}$$

$$y_{n,m,t} \in \{1, 0\} \quad \forall n, \forall m, \forall t \tag{A.5}$$

where, $q^{+}_{n,m,t}$ represents gas flow from node n to node m and $q^{-}_{n,m,t}$ represents gas flow from node m to node n. The parameter M is a big constant. Equation (51)

has a role as same as sgn function, i.e., ensures the bidirectional gas flow in the pipelines. Equations (52)- (53) determines that only one of the $q^{+}_{n,m,t}$, $q^{-}_{n,m,t}$ can have the value inequal to zero. Moreover, to illustrate the real gas flow in the pipelines Eqs. (A.6) and (A.7) are considered.

$$q^{+}_{n,m,t} \leqslant \frac{K^{f}_{n,m} PR_{n,u}}{\sqrt{PR^{2}_{n,u} - PR^{2}_{m,u}}} Pr_{n,t} - \frac{K^{f}_{n,m} PR_{m,u}}{\sqrt{PR^{2}_{n,u} - PR^{2}_{m,u}}} Pr_{m,t} + M(1 - y_{n,m,t}) \quad \forall \langle (n,m) \in z \mid m < n \rangle, \forall u, \forall t \tag{A.6}$$

$$q^{-}_{n,m,t} \leqslant \frac{K^{f}_{n,m} PR_{m,u}}{\sqrt{PR^{2}_{m,u} - PR^{2}_{n,u}}} Pr_{m,t} - \frac{K^{f}_{n,m} PR_{n,u}}{\sqrt{PR^{2}_{m,u} - PR^{2}_{n,u}}} Pr_{n,t} + M(y_{n,m,t}) \quad \forall \langle (n,m) \in z \mid m > n \rangle, \forall u, \forall t \tag{A.7}$$

Appendix B. The duality theory process in robust optimization based on MILP programming

The duality theory can be applied to recast the min-max problem as a single level min problem. It should be noted that although the model proposed in this article is a mixed-integer linear programming (MILP), it still convex that the duality theory can be applied. In order to provide a comprehensive detail regarding the convexity of the presented model, three concepts including convex function, convex space and convex model are discussed. Firstly, the objective function is affine and as all the affine functions are convex, the objective function is definitely convex. Secondly, the search space in an optimization problem is divided into two areas, feasible and infeasible, by constraints. A constraint is convex if any linear combination of two points in its feasible area still in that area. However, in the presented constraints, there are discrete variables that make the constraints and the search area non-convex. Lastly, convex models are models that their objective functions and their relaxed constraints (viz. constraints without binary variables) are convex. In this work, as stated, the objective function is convex and since the only issue regarding non-convexity of the constraints concerns binary variables and by relaxing these variables the constraints are convex; hence, the overall model is convex [52–54]. Further, there variety of works that have applied the robust optimization on the MILP problems. For instance, in [55], the RO has been used to tackle the pernicious impact of the power market uncertainty in scheduling of industrial heat and

power consumers. With the similar aim the RO has been taken into consideration in a decentralized scheduling of microgrids in [56] to handle the power market uncertainty. Accordingly, the duality theory is taken into account and the objective function of Eq. (74) is reformulated as Eqs. (75)- (80).

References

[1] C. Zhang, L. Yang, Risk-profit analysis of regional energy service providers by regularized primal-dual interior point method, International Journal of Electrical Power & Energy Systems 135 (2022) 107542.

[2] H. Xu, H. Sun, D. Nikovski, S. Kitamura, K. Mori, H. Hashimoto, Deep reinforcement learning for joint bidding and pricing of load serving entity, IEEE Transactions on Smart Grid 10 (6) (2019) 6366–6375.

[3] M. Khorasany, A. Najafi-Ghalelou, R. Razzaghi, B. Mohammadi-Ivatloo, Transactive energy framework for optimal energy management of multi-carrier energy hubs under local electrical, thermal, and cooling market constraints, International Journal of Electrical Power & Energy Systems 129 (2021) 106803.

[4] T. Sattarpour, D. Nazarpour, S. Golshannavaz, Load serving entity interactions on residential energy management strategy: A two-level approach, Sustainable Cities and Society 40 (2018) 440–453.

[5] K. Meng, H. Yang, Z. Y. Dong, W. Guo, F. Wen, Z. Xu, Flexible operational planning framework considering multiple wind energy forecasting service providers, IEEE Transactions on Sustainable Energy 7 (2) (2015) 708–717.

[6] S. G. Q. S. A. F. H. Han, H. Cui, C. Wu, A remedial strategic scheduling model for load serving entities considering the interaction between grid-level energy storage and virtual power plants, Energies 11 (2018) 440–453.

[7] A. Halder, X. Geng, P. R. Kumar, L. Xie, Architecture and algorithms for privacy preserving thermal inertial load management by a load serving entity, in: 2017 IEEE Power Energy Society General Meeting, 2017, pp. 1–1.

[8] E. Mahboubi-Moghaddam, M. Nayeripour, J. Aghaei, Reliability constrained decision model for energy service provider incorporating demand response programs, Applied Energy 183 (2016) 552–565.

[9] H. Rashidizadeh-Kermani, M. Vahedipour-Dahraie, A. Anvari-Moghaddam, J. M. Guerrero, A stochastic bi-level decision-making framework for a load-serving entity in day-ahead and balancing markets, International Transactions on Electrical Energy Systems 29 (11) (2019) e12109.

[10] X. Fang, Q. Hu, F. Li, B. Wang, Y. Li, Coupon-based demand response considering wind power uncertainty: A strategic bidding model for load serving entities, IEEE Transactions on Power Systems 31 (2) (2016) 1025–1037.

[11] P. Sheikhahmadi, S. Bahramara, A. Mazza, G. Chicco, J. P. Catalão, Bi-level optimization model for the coordination between transmission and distribution systems interacting with local energy markets, International Journal of Electrical Power Energy Systems 124 (2021) 106392.

[12] F. H. Moghimi, T. Barforoushi, A short-term decision-making model for a price-maker distribution company in wholesale and retail electricity markets considering demand response and real-time pricing, International Journal of Electrical Power Energy Systems 117 (2020) 105701.

[13] S. Bahramara, P. Sheikhahmadi, A. Mazza, G. Chicco, M. Shafie-khah, J. P. S. Catalão, A risk-based decision framework for the distribution company in mutual interaction with the wholesale day-ahead market and microgrids, IEEE Transactions on Industrial Informatics 16 (2) (2020) 764–778.

[14] E. Mahboubi-Moghaddam, M. Nayeripour, J. Aghaei, A. Khodaei, E. Waffenschmidt, Interactive robust model for energy service providers integrating demand response programs in wholesale markets, IEEE Transactions on Smart Grid 9 (4) (2018) 2681–2690.

[15] P. Sheikhahmadi, S. Bahramara, The participation of a renewable energy-

based aggregator in real-time market: A bi-level approach, Journal of Cleaner Production 276 (2020) 123149.

[16] H. Xu, K. Zhang, J. Zhang, Optimal joint bidding and pricing of profit-seeking load serving entity, IEEE Transactions on Power Systems 33 (5) (2018) 5427–5436.

[17] Y. Jia, Z. Mi, Y. Yu, Z. Song, H. Fan, Tri-level decision-making framework for strategic trading of demand response aggregator, IET Renewable Power Generation 13 (12) (2019) 2195–2206. doi:10.1049/iet-rpg.2019.0076.

[18] M. Shafie-khah, J. P. S. Catalão, A stochastic multi-layer agent-based model to study electricity market participants behavior, IEEE Transactions on Power Systems 30 (2) (2015) 867–881. doi:10.1109/TPWRS.2014.2335992.

[19] N. Ghadimi, M. Sedaghat, K. K. Azar, B. Arandian, G. Fathi, M. Ghadamyari, An innovative technique for optimization and sensitivity analysis of a pv/dg/bess based on converged henry gas solubility optimizer: A case study, IET Generation, Transmission & Distribution (2023).

[20] G. Bo, P. Cheng, K. Dezhi, W. Xiping, L. Chaodong, G. Mingming, N. Ghadimi, Optimum structure of a combined wind/photovoltaic/fuel cell-based on amended dragon fly optimization algorithm: a case study, Energy Sources, Part A: Recovery, Utilization, and Environmental Effects 44 (3) (2022) 7109–7131.

[21] T. Zhao, X. Pan, S. Yao, C. Ju, L. Li, Strategic bidding of hybrid ac/dc microgrid embedded energy hubs: A two-stage chance constrained stochastic programming approach, IEEE Transactions on Sustainable Energy 11 (1) (2020) 116–125.

[22] V. Davatgaran, M. Saniei, S. S. Mortazavi, Optimal bidding strategy for an energy hub in energy market, Energy 148 (2018) 482 – 493.

[23] M. Zare Oskouei, M. A. Mirzaei, B. Mohammadi-Ivatloo, M. Shafiee, M. Marzband, A. Anvari-Moghaddam, A hybrid robust-stochastic approach

to evaluate the profit of a multi-energy retailer in tri-layer energy markets, Energy 214 (2021) 118948.

[24] P. Liu, T. Ding, Z. Bie, Z. Ma, Integrated demand response for multi-energy load serving entity, in: 2018 International Conference on Smart Energy Systems and Technologies (SEST), 2018, pp. 1–6.

[25] P. Liu, T. Ding, Z. Zou, Y. Yang, Integrated demand response for a load serving entity in multi-energy market considering network constraints, Applied Energy 250 (2019) 512–529.

[26] A. Najafi, H. Falaghi, J. Contreras, M. Ramezani, A stochastic bilevel model for the energy hub manager problem, IEEE Transactions on Smart Grid 8 (5) (2017) 2394–2404.

[27] M. A. Mirzaei, M. Hemmati, K. Zare, M. Abapour, B. Mohammadi-Ivatloo, M. Marzband, A. Anvari-Moghaddam, A novel hybrid two-stage framework for flexible bidding strategy of reconfigurable micro-grid in day-ahead and real-time markets, International Journal of Electrical Power & Energy Systems 123 (2020) 106293.

[28] M. Misaghian, M. Saffari, M. Kia, A. Heidari, M. Shafie-khah, J. Catalão, Tri-level optimization of industrial microgrids considering renewable energy sources, combined heat and power units, thermal and electrical storage systems, Energy 161 (2018) 396 – 411.

[29] W. Jiang, X. Wang, H. Huang, D. Zhang, N. Ghadimi, Optimal economic scheduling of microgrids considering renewable energy sources based on energy hub model using demand response and improved water wave optimization algorithm, Journal of Energy Storage 55 (2022) 105311.

[30] L. Chen, H. Huang, P. Tang, D. Yao, H. Yang, N. Ghadimi, Optimal modeling of combined cooling, heating, and power systems using developed african vulture optimization: a case study in watersport complex, Energy Sources,

Part A: Recovery, Utilization, and Environmental Effects 44 (2) (2022) 4296–4317.

[31] M. Yazdani-Damavandi, N. Neyestani, M. Shafie-khah, J. Contreras, J. P. S. Catalão, Strategic behavior of multi-energy players in electricity markets as aggregators of demand side resources using a bi-level approach, IEEE Transactions on Power Systems 33 (1) (2018) 397–411. doi:10.1109/TPWRS.2017.2688344.

[32] Z. Yang, M. Ni, H. Liu, Pricing strategy of multi-energy provider considering integrated demand response, IEEE Access 8 (2020) 149041–149051.

[33] M. Yazdani-Damavandi, N. Neyestani, G. Chicco, M. Shafie-khah, J. P. S. Catalão, Aggregation of distributed energy resources under the concept of multienergy players in local energy systems, IEEE Transactions on Sustainable Energy 8 (4) (2017) 1679–1693.

[34] M. Shafiekhani, A. Badri, M. Shafie-Khah, J. P. Catalão, Strategic bidding of virtual power plant in energy markets: A bi-level multi-objective approach, International Journal of Electrical Power & Energy Systems 113 (2019) 208–219.

[35] A. Mirzapour-Kamanaj, M. Majidi, K. Zare, R. Kazemzadeh, Optimal strategic coordination of distribution networks and interconnected energy hubs: A linear multi-follower bi-level optimization model, International Journal of Electrical Power Energy Systems 119 (2020) 105925.

[36] R. Li, W. Wei, S. Mei, Q. Hu, Q. Wu, Participation of an energy hub in electricity and heat distribution markets: An mpec approach, IEEE Transactions on Smart Grid 10 (4) (2019) 3641–3653.

[37] A. Heidari, S. S. Mortazavi, R. C. Bansal, Equilibrium state of a price-maker energy hub in a competitive market with price uncertainties, IET Renewable Power Generation 14 (6) (2020) 976–985.

[38] S. Khazeni, A. Sheikhi, M. Rayati, S. Soleymani, A. M. Ranjbar, Retail market equilibrium in multicarrier energy systems: A game theoretical approach, IEEE Systems Journal 13 (1) (2019) 738–747. doi:10.1109/JSYST.2018.2812807.

[39] X. Wang, Z. Bie, F. Liu, Y. Kou, L. Jiang, Bi-level planning for integrated electricity and natural gas systems with wind power and natural gas storage, International Journal of Electrical Power Energy Systems 118 (2020) 105738.

[40] N. Nasiri, A. Sadeghi Yazdankhah, M. A. Mirzaei, A. Loni, B. Mohammadi-Ivatloo, K. Zare, M. Marzband, A bi-level market-clearing for coordinated regional-local multi-carrier systems in presence of energy storage technologies, Sustainable Cities and Society 63 (2020) 102439.

[41] Y. Li, Z. Li, F. Wen, M. Shahidehpour, Privacy-preserving optimal dispatch for an integrated power distribution and natural gas system in networked energy hubs, IEEE Transactions on Sustainable Energy 10 (4) (2019) 2028–2038.

[42] C. Wang, W. Wei, J. Wang, L. Wu, Y. Liang, Equilibrium of interdependent gas and electricity markets with marginal price based bilateral energy trading, IEEE Transactions on Power Systems 33 (5) (2018) 4854–4867.

[43] S. Bahrami, A. Sheikhi, From demand response in smart grid toward integrated demand response in smart energy hub, IEEE Transactions on Smart Grid 7 (2) (2016) 650–658.

[44] H. Wu, M. Shahidehpour, A. Alabdulwahab, A. Abusorrah, Demand response exchange in the stochastic day-ahead scheduling with variable renewable generation, IEEE Transactions on Sustainable Energy 6 (2) (2015) 516–525.

[45] N. Nasiri, A. Sadeghi Yazdankhah, M. A. Mirzaei, A. Loni, B. Mohammadi-Ivatloo, K. Zare, M. Marzband, Interval optimization-based scheduling of interlinked power, gas, heat, and hydrogen systems, IET Renewable Power Generation 15 (6) (2021) 1214–1226.

[46] L. Wu, A tighter piecewise linear approximation of quadratic cost curves for unit commitment problems, IEEE Transactions on Power Systems 26 (4) (2011) 2581–2583.

[47] N. Nasiri, M. R. Banaei, S. Zeynali, A hybrid robust-stochastic approach for unit commitment scheduling in integrated thermal electrical systems considering high penetration of solar power, Sustainable Energy Technologies and Assessments 49 (2022) 101756.

[48] X. Zhang, M. Shahidehpour, A. Alabdulwahab, A. Abusorrah, Hourly electricity demand response in the stochastic day-ahead scheduling of coordinated electricity and natural gas networks, IEEE Transactions on Power Systems 31 (1) (2016) 592–601.

[49] N. Nasiri, S. Zeynali, S. N. Ravadanegh, M. Marzband, A hybrid robust-stochastic approach for strategic scheduling of a multi-energy system as a price-maker player in day-ahead wholesale market, Energy 235 (2021) 121398.

[50] M. Yan, N. Zhang, X. Ai, M. Shahidehpour, C. Kang, J. Wen, Robust two-stage regional-district scheduling of multi-carrier energy systems with a large penetration of wind power, IEEE Transactions on Sustainable Energy 10 (3) (2018) 1227–1239.

[51] N. Nasiri, S. Zeynali, S. N. Ravadanegh, N. Rostami, A robust decision framework for strategic behaviour of integrated energy service provider with embedded natural gas and power systems in day-ahead wholesale market, IET Generation, Transmission & Distribution (2022).

[52] S. Boyd, S. P. Boyd, L. Vandenberghe, Convex optimization, Cambridge university press, 2004.

[53] D. G. Luenberger, Y. Ye, Supplement to “linear and nonlinear programming” (2005).

[54] J. Kumar, I. U. Khalil, A. U. Haq, A. Perwaiz, K. Mehmood, Solver-based mixed integer linear programming (milp) based novel approach for hydroelectric power generation optimization, IEEE Access 8 (2020) 174880–174892.

[55] M. Alipour, K. Zare, H. Zareipour, H. Seyedi, Hedging strategies for heat and electricity consumers in the presence of real-time demand response programs, IEEE Transactions on Sustainable Energy 10 (3) (2018) 1262–1270.

[56] A. Mansour-Saatloo, Y. Pezhmani, M. A. Mirzaei, B. Mohammadi-Ivatloo, K. Zare, M. Marzband, A. Anvari-Moghaddam, Robust decentralized optimization of multi-microgrids integrated with power-to-x technologies, Applied Energy 304 (2021) 117635.

Revised Manuscript with No Changes Marked
Click here to access/download;Revised Manuscript with No Changes Marked;no_hithlight.pdf
Click here to view linked References

A Robust Bi-Level Optimization Framework for Participation of Multi-Energy Service Providers in Integrated Power and Natural Gas Markets

Nima Nasiri[a], Amin Mansour Saatloo[b], Mohammad Amin Mirzaei[b], Sajad Najafi Ravadanegh[a], Kazem Zare[b], Behnam Mohammadi-ivatloo[b], Mousa Marzband[c,d]

[a]*Electrical Engineering Department of Azarbaijan Shahid Madani University, Tabriz, Iran*
[b]*Faculty of Electrical and Computer Engineering, University of Tabriz, Tabriz, Iran*
[c]*Northumbria University, Electrical Power and Control Systems Research Group, Ellison Place NE1 8ST, Newcastle upon Tyne, United Kingdom*
[d]*Center of research excellence in renewable energy and power systems, King Abdulaziz University, Jeddah, Saudi Arabia*

Abstract

This paper presents a bi-level scheduling model for a new energy system under the concept of multi-energy service providers (MESPs) to participate in the integrated power and natural gas market (IPNGM). While the presented bi-level model takes full consideration of the unit commitment constraints of the power network and line pack constraints of the gas network into consideration at the lower level, the MESPs minimize the cost of purchasing power and natural gas by operating energy storage systems as well as the demand response program (DRP) as flexible technologies at the upper level. In order to solve the bi-level problem, an iterative-based two-step algorithm is developed. Moreover, since the MESPs cannot accurately predict other participants in the IPNGM, especially renewable energy sources (RESs), the power price determined by IPNGM is considered an uncertain parameter, and a robust optimization (RO) method is employed to capture this uncertainty. The proposal is formulated as a mixed-integer linear programming (MILP) and carried out on the IEEE 6-bus power system integrated with the 6-node natural gas network and considering one MES using the CPLEX solver in the general algebraic modeling system (GAMS) environment. Further, to show the model flexibility, simulation

Email address: s.najafi@azaruniv.ac.ir Corresponding author (Sajad Najafi Ravadanegh)

results are extended to the IEEE 118-bus power system integrated with the 10-node natural gas network by considering six MESs. The obtained results verified the effectiveness of the model by reducing the cost of the purchased power and natural gas up to 4.39% by employing flexible energy sources.

Keywords: Market-clearing, multi-energy systems, integrated electricity and natural gas networks, energy storage systems, demand response program, line pack system, robust optimization.

Nomenclature

Acronyms

CHP	Combined heat and power
IPNGM	Integrated power and natural gas market
IPNGMO	Integrated power and natural gas market operator
MESP	Multi energy service provider
MES	Multi energy system
LMEP	Local marginal electric price
LMGP	Local marginal gas price
GAMS	General algebraic modeling system
MILP	Mixed integer linear programing
IENGN	Integrated electricity and natural gas networks
GFPP	Gas fired power plant
NGFPP	Non-gas fired power plant
DRP	Demand response program
TSS	Thermal storage system

ESS	Electrical storage system
EB	Eectrical boiler
Index and sets	
i,b	Indices of power units, power system buses
n,sp,u	Indices of natural gas nods, natural gas producer, fixed pressure points
w,t,h	Indices of wind turbine, time period, multi energy system
l,Tr,z	Set of natural gas local demand, power transmission lines , natural gas network pipeline
CU,GU	Set of NGFPP, GFPP
A_b^i	Location of power units i at power system bus b
A_b^h	Location of MES h at power system bus b
A_b^w	Location of wind turbine w at power system bus b
A_n^{sp}	Location of natural gas producer sp at node n
A_n^h	Location of MES h at natural gas node n
Parameters	
γ_{sp}^{Gas}	Offer prices of natural gas producers sp ($/KCh)
P_i^{Min}, P_i^{Max}	Minimum / maximum power generation capacity of unit i (MW)
C_i^{SU}, C_i^{SD}	Startup / shutdown of NGFPP costs ($/MWh)
C_i^{GSU}, C_i^{GSD}	Start-up / shut-down of GFPPs fuel consumption (MWh)
T_i^U, T_i^D	Minimum on / off time of generation units (h)
R_i^{up}, R_i^{dn}	Ramp up/down of generation units (MW)
$\nu_{sp}^{Max}, \nu_{sp}^{Min}$	Maximum / minimum capacity of natural gas producers (Kcf)
Pr_n^{Max}, Pr_n^{Min}	Maximum / minimum pressure in natural gas network nodes (Bar)
η_{hc}, η_{hd}	Charging / discharging coefficient of the heating storage system
CHP_h^{Max}	Maximum capacity generation of the CHP unit (MW)
EB_h^{Max}	Maximum capacity heat production of the EB (MW)
HC_h^{Max}/HD_h^{Max}	Maximum charge/discharge capacity of the TSS (MW)
SC_h^{Max}/SD_h^{Max}	Maximum charge/discharge capacity of the ESS (MW)

HS_h^{Max}/ES_h^{Max}	Maximum capacity storage of the heat/electrical storage systems (MW)
y_h^K	Electric power generated from K points of CHP unit in MES h (MW)
$PR_{n,u}/PR_{m,u}$	Fixed pressure values u in the nodes of pipelines (n, m) of the NG network (Bar)
$P_w^{Wind,Max}$	Maximum output power of wind turbine (MW)
$\beta_{h,t}^{LMEP}/\gamma_{s,t}^{LMGP}$	Local marginal Electricity price/ local marginal gas price ($/MWh)
CHP_h^{Max}	Maximum natural gas input of CHP in MES h
EB_h^{Max}	Maximum input power of electric boiler in MES h
HC_h^{Max}/HD_h^{Max}	Maximum charging and discharging capacity at the heating storage system in MES h
SC_h^{Max}/SD_h^{Max}	Maximum charging and discharging capacity at the electricity storage system in MES h
ES_h^{Max}	Maximum electricity energy stored at power storage in MES h
HS_h^{Max}	Maximum heating stored in heat storage in MES h
SC_h^{Max}/SD_h^{Max}	Maximum charging and discharging capacity at the ESS in MES h
HS_h^{Max}	Maximum heating stored in TSS in MES h
$HL_{h,t}^h/EL_{h,t}^e/GL_{h,t}^g$	Heat, electric, gas demand of MES h in the period t (MW)
$L_{l,t}$	Local and industrial natural gas demand l in natural gas network at time period t (Kcf)
T_i^{Ue}, T_i^{De}	Minimum up and down time for startup and shutdown of generation unit I (h)
LPF^{Shup}, LPF^{Shdo}	Shifting-up and shifting-down load factor in DRP

Variables

$P_{i,t}$	Output power of generation unit i in time period t (MW)
$P_{w,t}^{Wind}$	Output power of wind turbine w in time period t (MW)
$F_{b,j,t}$	Electric power flow in power transmission lines (b,j) at period t (MW)
$\delta_{b,t}$	Voltage angle of power system bus b in period t (Rad)
$\lambda_{b,t}^e$	Dual variable of power system bus b in period t ($/MWh)
$\lambda_{n,t}^G$	Dual variable of natural gas network node n in period t ($/Kcfh)
$ES_{h,t}/HS_{h,t}$	The amount of electric/heat energy stored in electric and thermal storage systems at time t (MW)

$v_{sp,t}$	Gas produced from natural gas well sp in period t (Kcf)
$Pr_{n,t}$	Pressure at the nth node of the natural gas network in period t (Bar)
$\Delta HS_{h,t}, \Delta ES_{h,t}$	Changes of heating and electric stored in heat and electric storage in MES h at period t
$h_{n,m,t}$	Average mass of natural gas (line pack) in pipelines (n, m) in time period t (Kcf)
$q^{in}_{n,m,t}/q^{out}_{n,m,t}$	The amount of natural gas inlet / outlet flow in pipelines (n, m) in time period t (Kcf)
$f^{Elec,in}_{h,t}, f^{Gas,in}_{h,t}$	Electric power and natural gas inputs of MES h in the period t (MW)
$f^{Elec,out}_{h,t}, f^{Gas,out}_{h,t}$	Electric, natural gas output power of MES h in the period t (MW)
$f^{Heat,out}_{h,t}$	Heating output power of MES h in the period t (MW)
$f^{1}_{h,t}, ..., f^{15}_{h,t}$	Energy flow variables in MES h at time period t (MW)
$EL^{e}_{h,t}, EL^{g}_{h,t}$	Electric, natural gas demands of MES h in the period t (MW)
$\alpha^{K}_{h,t}$	Coefficient of CHP generation in point k of MES h at time period t
$FC_{i,t}$	Operation cost of generation unit i at time period t
$D^{Shup}_{h,t}, D^{Shdo}_{h,t}$	Shifting-up and shifting-down loads in MES h at period t
Binary Variables	
$I_{i,t}$	Commitment states of generation unit i in time period t
$y_{i,t}/z_{i,t}$	Startup and shutdown states of generation unit i in time period t
$HY_{h,t}$	Charge and discharge state of TSS in MES h at period t
$EY_{h,t}$	Charge and discharge state of ESS in MES h at period t
$y_{n,m,t}$	Binary variable to specify the direction of natural gas flow in the pipeline (n,m) at time t
$DR^{shup}_{h,t}, DR^{shdo}_{h,t}$	States of shifting-up and shifting-down loads in DRP at period t

1. Introduction

1.1. Motivation

In the modern power system, energy and load service providers aggregate end-users' power demand and participate in the wholesale power market, which is run by an independent system operator (ISO) [1]. Once the wholesale power market has been cleared, energy service providers deliver the price and power to the end-

users [2]. They may plan to minimize the cost or maximize the profit dependently. Nevertheless, the advent of multi-energy technologies such as combined heat and power (CHP) units, electrical boilers, various energy storage systems including electrical storage systems (ESS), thermal storage systems (TSS), gas storage systems (GSS) and etc. lead to an extensive interaction among multiple energy carriers in the transmission and distribution levels [3]. Thus, techno-economic interactions of the existence of multiple energy carriers, which were designed exclusively for the electricity markets, cannot respond to the requirements. Hence, researchers are looking for new and efficient mechanisms for techno-economic interactions of the multiple energy carriers. Motivated by the above discussion, this work aims to introduce a new scheduling model to involve demand-side multi-energy carrier technologies of the distribution level in the integrated power and natural gas markets (IPNGM). To do so, this work's main innovation comes in twofold. The first novelty is introducing a bilevel model to enable demand-side multi-energy technologies to participate in the wholesale electricity market by integrating them with a new energy system so-called multi-energy service provider (MESP). In the proposed bilevel model, the MESP modeling takes place in the upper level, where it participates in the IPNGM by operating its multi-energy technologies. In the lower level, where the second main novelty of this work lies, the integrated power and natural gas networks are modeled by considering unit commitment constraints for the power network and line pack constraints for the natural gas network. In the previous works, these constraints, especially unit commitment constraints of the power network, have been ignored since they make the lower problem complicated and the bilevel problem cannot be recast as a simple single-level one using KKT conditions. However, this works advances the state-of-the-art in bilevel modeling of the IPNGM by full consideration of power network constraints at the lower level and proposes a two-step algorithm to solve the bilevel problem. Moreover, this works investigates the impact of flexible technologies including electrical and thermal storage systems as well as demand response program on the IPNGM. Further, to capture the uncertainty concerns power market, a robust approach is proposed in this work to make the scheduling robust against the worst-case uncertainty realization.

1.2. Literature review

MESPs have a considerable role in different sections of the smart grids such as residential sector energy management [4], wind generation uncertainty management [5], energy storage systems and virtual power plants (VPPs) optimal management [6], ventilation systems controlling [7], and integrated DRP [8]. In addition, MESPs have a role in the energy trading procedure with the wholesale and retail energy markets. So far, many types of research have been dedicated to evaluate the energy trading mechanisms of MESPs with the wholesale and retail energy markets.

Two-stage stochastic programming for MESPs' participation in the day-ahead and real-time markets has been presented in [9]. A bidding strategy for a demand service provider has been introduced in [10], where the objective is to maximize the service provider's profit using the coupon-based DRP with a high injection of wind energy. Two bi-level approaches based on uncertainty management for the participation of distribution system service providers in the wholesale power market have been proposed in [11], in which the upper-level deals with the operation of the service provider and the lower level clears the wholesale market. Moreover, a distribution system service provider can participate in both wholesale and retail markets in [12]. To investigate the optimal decision-making aspects of a distribution system service provider in trading with microgrids (MGs) and the wholesale market simultaneously, a bilevel optimization approach has been proposed in [13]. In another study, an iterative-based two-stage framework for distribution system service provider participation in the day-ahead wholesale market with the aim of demand prediction for the distribution system has been introduced in [14], in which DRP and distribution system reliability are also considered. For participation of the distributed energy resources (DERs) aggregator in the real-time electricity market, a bilevel framework has been designed in [15], in which DERs aggregator problem is solved in the upper level, and real-time market clearing is conducted in the lower level. A bilevel problem to model a tri-layer market structure has been introduced in [16], where the upper level maximizes energy service providers' profit, and the lower level clears the market and maximizes the end-users profit. In a similar context, in [17], a tri-layer market structure has been proposed, which at

the first layer wholesale power market maximizes social welfare and at the second and third layers, respectively, demand response aggregator and energy consumers maximize their profits. In [18], a study toward electrical multi-layer market participants has been conducted, in which wholesale electricity market participants like electrical energy producers and RESs were modeled at the first layer, and responsive consumers like electrical fleets and DRP participants were modeled at the second layer. In [19], an optimization approach is presented for designing a hybrid solar/battery/diesel generator system considering the environmental effects in one of the regions of China. A photovoltaic/wind turbine/fuel cell hybrid renewable energy system in [20] is proposed to provide electricity for a Turkey region, considering reliability requirements. The Dragon fly algorithm is used in the presented approach to solving the proposed problem.

Recently, a new range of research has studied the techno-economic interactions of MESPs and other multi-energy entities with the multi-energy wholesale and retail markets. For instance, several similar pieces of research for energy trading of MESPs in the day-ahead and real-time markets have been done in [21, 22]. A hybrid stochastic/robust approach for the multi-energy retailer has been proposed in [23], in which the aims of the optimization problem are maximizing electricity, local heat, and natural gas consumers' social welfare and profit of the IPNGM. A multi-energy bidding strategy was integrated with DRP for energy trading of MESPs with IPNGM in [24] to maximize the MESPs' profit. In another study in [25], a tri-layer day-ahead multi-energy market structure for MESPs' simultaneous trading with the multi-energy wholesale and retail markets has been presented. A risk-based stochastic bilevel problem for the decision-making of MESPs to participate in the pool electricity and natural gas markets in the presence of rival MESPs has been proposed in [26]. In [27], to optimal operation of an MG in the day-ahead and real-time markets, a hybrid stochastic/IGDT scheduling model has been introduced. In order to industrial MGs' participation in the wholesale markets, a tri-level optimization framework has been presented in [28], in which at the first level, MGs try to minimize their purchased electricity costs and at the second and third levels of wholesale market-clearing and CHP units settling was performed, respectively.

In [29], an optimal scheduling model based on stochastic optimization is presented to evaluate the implementation effect of the DRP in the energy hub system considering the electricity and natural gas network constraints. This approach utilizes a water wave optimization algorithm to solve the proposed problem. An optimal approach has been investigated in [30] for the design of combined cooling, heating, and power systems in a water sports complex to reduce losses and environmental pollution.

To evaluate the trading mechanism of multi-energy players and multiple energy carriers, a bilevel model has been introduced in [31], where MESPs aggregate bids/offers of the multi-energy players and participate in the wholesale market to maximize their profits. In [32], a price-making mechanism by MESPs was presented using a bilevel model based on the Stackelberg game, in which the electricity price settlement was conducted at the upper level, and integration of the DRP was performed at the second layer. A multi-energy provider entity has been simulated in [33], which behaves as an aggregator of DERs among the wholesale market and local energy systems. Study [34] presents a bi-level scheduling model to evaluate the strategic behavior of an energy aggregator entity in the wholesale electricity market in the presence of other rivals. To study the strategic behavior of the multi-energy provider entities and power distribution system, a multi-follower bilevel optimization approach has been proposed in [35]. A mathematical programming of equilibrium constraint (MPEC) for investigating the strategic behavior of a profit-based multi-energy service provider entity in the electricity and heat markets has been proposed in [36], where the entity sends the price bids and values to the upstream markets at the upper level and market clearing was performed at the lower level. In [37], to study the strategic behavior of the MESPs in the presence of rival MESPs for participation in the day-ahead multi-energy markets, a price-making bidding strategy has been proposed. In [38], a bilevel model between a multi-energy retailer and multi-energy consumers of MESPs has been presented, in which maximizing the retailer profit and minimizing the purchased energy cost of consumers are the upper level and lower level of the problem, respectively.

Several iterative-based solution algorithms for bi- or multi-level problems have

been effectively introduced by researchers. For instance, an iterative-based bilevel planning algorithm for solving the IENGN with the consideration of wind energy intermittency has been proposed in [39]. An iterative-based two-stage stochastic framework for MESPs participation in IPNGM has been presented in [40]. In [41], a distributed algorithm based on benders decomposition to preserve the privacy of participants has been proposed to solve the optimal dispatch of the integrated electrical distribution and natural gas systems. In [42], a decomposition algorithm to achieve the best result of the recognition of electrical distribution and natural gas markets balancing with the line pack system and GSS considerations have been proposed. A distributed algorithm with DRP implementation has been presented in [43] to demonstrate a MESPs entity interaction with the electricity and natural gas corporations. In [44], a two-step sequential stochastic market clearing approach for demand response provider and ISO has been introduced.

1.3. Research gaps and contributions

To the best of the authors' knowledge, there is no focus on the robust scheduling of MESPs for participating in IPNGM in order to achieve optimal dispatch of power and natural gas for MESs under an iterative-based two-step framework. According to the reviewed literature, there exist some research gaps as follows:

1. Some literature, e.g., [4–20], have focused on the behavior of electrical energy service providers and the wholesale power market. However, the proliferation of technologies such as CHP units, electrical boilers, multi-energy storage systems and etc. require new models and management entities to interact with multiple energy carriers at the distribution and transmission levels. Hence, the mentioned research, which was designed for studying the only power market, should be restructured.
2. Many of the works like [27, 28, 30, 34–36] discussed MESPs' interactions with the wholesale power market, in which limitations of only the power network were considered, and natural gas constraints were ignored. Considering natural gas energy as one of the most important inputs of the multi-energy carrier systems, ignoring the natural gas network constraints causes unreal results.

3. In some other research such as [25, 41], the main goal is investigating the technical operation and economic interactions of MESs with multiple energy networks. However, the impact of an iterative-based two-step algorithm was not evaluated. Given the decisions of MESPs and the operator of the IPNGM have impacts on each other, so, the iterative-based two-step algorithm assists the manager of the entities to accurately evaluate the variations owing to the decisions and behaviors of the operators.

Table 1: Comparative evaluations between this study and other publications

Ref	Name of service	MESP			IPGM (Network constraints)		Linepack	Algorithm	Uncertainty
		DRP	ESS	HSS	Power	Gas			
[10]	Load serving entities	✓	×	×	✓	×	×	KKT	Stochastic
[11]	Distribution company	✓	×	×	✓	×	×	KKT	IGDT
[14]	Energy service providers	✓	×	×	✓	×	×	Two step	Robust
[15]	Renewable energy aggregator	×	✓	×	✓	×	×	KKT	Stochastic
[16]	Load serving entities	✓	×	×	✓	×	×	KKT	×
[17]	Demand response aggregator	✓	×	×	✓	×	×	KKT	×
[18]	PEV aggregators and retailers	✓	×	×	✓	×	×	KKT	Stochastic
[21]	Energy hub operators	×	✓	✓	×	×	×	×	Stochastic
[23]	Multi-energy retailer	✓	✓	✓	×	×	×	×	robust-stochastic
[24]	Multi-energy load serving entity	✓	✓	×	×	×	×	×	×
[25]	Load serving entity	✓	✓	×	×	×	×	×	CVaR
[26]	Hub manager	×	✓	×	×	×	×	KKT	CVaR
[32]	multi-energy provider	✓	×	×	×	×	×	×	×
[40]	Energy hub operator	×	✓	✓	✓	✓	✓	Two stage	Stochastic
Proposed paper	Multi energy service provider	✓	✓	✓	✓	✓	✓	Two step	Robust

To cover these research gaps and Table 1, in this paper, a bi-level approach is introduced to evaluate the MESPs impacts on the IPNGM. At the upper level, MESPs is obliged to participate in the IPNGM and dispatch the power and natural gas to MESs. The objective of the MESPs is to determine the optimal demand for flexible energy sources to minimize the total costs of the multiple energy carriers. At the lower level, the operator of the IPNGM collects bids/offers and maximizes social welfare. To simulate the IPNGM, a unit commitment problem constrained to IENGN in the presence of the flexible line pack system is used. To evaluate the counter effect of flexible energy sources and price bids introduced by IPNGM, an iterative-based two-step framework is proposed, where the first step is to determine the local marginal prices of power and natural gas via solving the unit commitment problem. Thereupon, MESPs in the presence of flexible energy sources and via introduced prices by IPNGM perform optimal scheduling at the second step. To consider the unexpected behavior of the other market participants and the stochastic nature of the RESs in the IPNGM, the introduced price by the IPNGM is considered an uncertain parameter, and the RO method is taken into account to tackle this issue. The main contribution of this paper is listed below:

1. A bi-level scheduling mechanism is proposed to evaluate the impacts of the IPNGM constrained to the IENGN on the optimal scheduling of MESPs in the presence of a flexible line pack system of the natural gas network.
2. An iterative-based two-step framework is introduced to solve the robust bi-level approach and to investigate the effect of the flexible energy sources on prices set by the IPNGM.
3. The impacts of flexible electrical and thermal storage systems employed by MESPs are investigated on the IPNGM behavior and optimal dispatch of the electrical energy sources.
4. The effect of optimal DRP implementation by MESPs on IENGN constraints is studied.

The rest of the paper is organized as follows: The next section presents the mathematical model of the introduced scheduling problem. The third section presents the iterative-based two-step algorithm and mechanism of the market-clearing. Nu-

merical results and case studies are provided in section four. Finally, the last section concludes the paper.

2. Upper level: mathematical modeling of the MESPs

In the proposed problem, MESPs aim to minimize the cost of purchased power and natural gas from IPNGM. In the objective function of Eq. (1), the first and second terms are associated with purchased power and natural gas from IPNGM, respectively.

$$\min \left\{ \sum_{t} \sum_{h} (\beta_{h,t}^{LMEP} \cdot f_{h,t}^{Elec,in} + \gamma_{h,t}^{LMGP} \cdot f_{h,t}^{Gas,in}) \right\} \tag{1}$$

2.1. MES constraints

Figure 1 shows the MES proposed in this paper. The proposed MES is equipped with a CHP unit, electric boiler, heating and electrical storage systems. In addition, it has two inputs of electricity and natural gas and three outputs of electricity, heating and natural gas. According to Figure 1, the formulation of the MES is as follows.

The positive variables in Eq. (2) represent purchased power and natural gas by MESPs from IPNGM, respectively. The proposed MESs is a directional graph with one-way energy flow at each branch. Therefore, in Eq. (3), variables are positive. Equations (4)- (7) are assigned to the CHP unit operation constraints. It should be noted that the CHP unit is modeled using the post-pressure method. Equation (8) shows the electrical boiler input limitation. Equations (9)- (11) illustrate electrical, natural gas, and thermal energy balancing of MESs, respectively. Equations (12)-(13) are related to the input and output of TSS. Further, they demonstrate that charging and discharging modes cannot be applied simultaneously. Equation (14) represents the amount of stored energy in the TSS, which is limited by Eq. (15), as well as for ESS through Eqs. (16)-(19). The initial and final SoC of ESS and TSS should be equal, as described in Eq. (20). The DRP of multi-carrier energy systems is represented via Eqs. (21)-(24), in which Eq. (21) represents that upward shift and downward shift of end-users load must be equal. Moreover, Eqs. (22)- (23) show

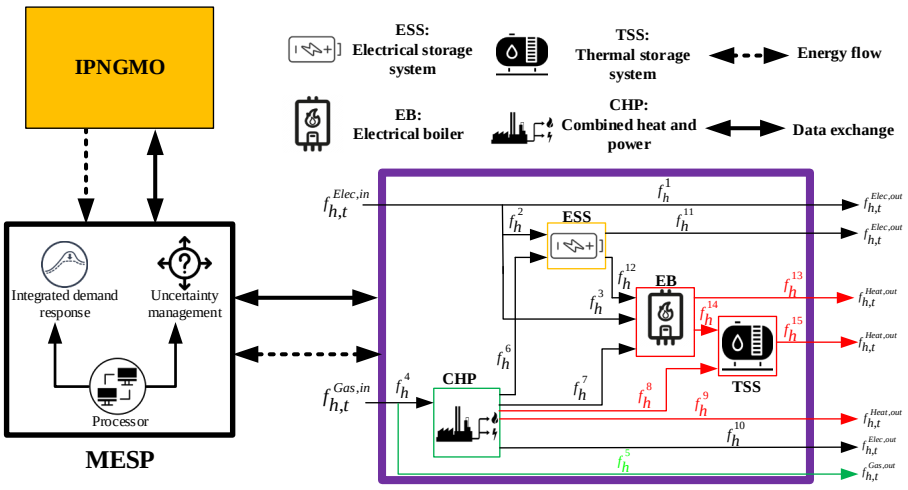

Figure 1: The proposed MESP

the amount of load that can be shifted, which is considered 15% of the total load of MES. Moreover, to prevent simultaneous upward and downward shifts, Eqs. (26)-(34) model the relationship between the input and output of equipment in MESs.

$$f_{h,t}^{Elc,in}, f_{h,t}^{Gas} \geqslant 0 \quad \forall h, \forall t \tag{2}$$

$$f_{h,t}^{1}, f_{h,t}^{2}, \ldots, f_{h,t}^{15} \geqslant 0 \quad \forall h, \forall t \tag{3}$$

$$f_{h,t}^{4} \leqslant CHP_{h}^{MAX} \quad \forall h, \forall t \tag{4}$$

$$f_{h,t}^{7} + f_{h,t}^{10} = \sum_{K} \alpha_{h,t}^{K} y_{h}^{K} \quad \forall h, \forall t \tag{5}$$

$$0 \leqslant \alpha_{h,t}^{K} \leqslant 1 \quad \forall h, \forall t, \forall k \tag{6}$$

$$\sum_{K} \alpha_{h,t}^{K} = 1 \quad \forall h, \forall t \tag{7}$$

$$f_{h,t}^{3} + f_{h,t}^{7} + f_{h,t}^{12} \leqslant EB_{h}^{Max} \quad \forall h, \forall t \tag{8}$$

$$f_{h,t}^{Elc,out} = EL_{h,t}^{e} \quad \forall h, \forall t \tag{9}$$

$$f_{h,t}^{Gas,out} = GL_{h,t}^{g} \quad \forall h, \forall t \tag{10}$$

$$f_{h,t}^{Heat,out} = HL_{h,t}^{h} \quad \forall h, \forall t \tag{11}$$

$$f_{h,t}^{8} + f_{h,t}^{14} \leqslant HY_{h,t} HC_{h}^{Max} \quad \forall h, \forall t \tag{12}$$

$$f_{h,t}^{15} \leqslant (1 - HY_{h,t}) HD_h^{Max} \quad \forall h, \forall t \tag{13}$$

$$HS_{h,t} = HS_{h,t-1} + \Delta HS_{h,t-1} \quad \forall h, \forall t \tag{14}$$

$$0 \leqslant HS_{h,t} \leqslant HS_h^{Max} \quad \forall h, \forall t \tag{15}$$

$$f_{h,t}^{2} + f_{h,t}^{6} \leqslant EY_{h,t} SC_h^{Max} \quad \forall h, \forall t \tag{16}$$

$$f_{h,t}^{11} + f_{h,t}^{12} \leqslant (1 - EY_{h,t}) SD_h^{Max} \quad \forall h, \forall t \tag{17}$$

$$ES_{h,t} = ES_{h,t-1} + \Delta ES_{h,t-1} \quad \forall h, \forall t \tag{18}$$

$$0 \leqslant ES_{h,t} \leqslant ES_h^{Max} \quad \forall h, \forall t \tag{19}$$

$$ES_{h,ini} = ES_{h,end}, HS_{h,ini} = HS_{h,end} \forall h, \forall t \tag{20}$$

$$\sum_t D_{h,t}^{Shup} = \sum_t D_{h,t}^{Shdo} \quad \forall h \tag{21}$$

$$0 \leqslant D_{h,t}^{shup} \leqslant EL_{h,t}^{e} LPF^{Shup} DR_{h,t}^{shup} \quad \forall h, \forall t \tag{22}$$

$$0 \leqslant D_{h,t}^{shdo} \leqslant EL_{h,t}^{e} LPF^{Shdo} DR_{h,t}^{shdo} \quad \forall h, \forall t \tag{23}$$

$$0 \leqslant DR_{h,t}^{shdo} + DR_{h,t}^{shup} \leqslant 1 \quad \forall h, \forall t \tag{24}$$

$$f_{h,t}^{Elec,out} = f_{h,t}^{1} + f_{h,t}^{10} + f_{h,t}^{11} + D_{h,t}^{Shedo} - D_{h,t}^{Shup} \quad \forall h, \forall t \tag{25}$$

$$f_{h,t}^{Gas,out} = f_{h,t}^{5} \quad \forall h, \forall t \tag{26}$$

$$f_{h,t}^{Heat,out} = f_{h,t}^{9} + f_{h,t}^{13} + f_{h,t}^{15} \quad \forall h, \forall t \tag{27}$$

$$f_{h,t}^{Elec,in} = f_{h,t}^{1} + f_{h,t}^{2} + f_{h,t}^{3} \quad \forall h, \forall t \tag{28}$$

$$f_{h,t}^{Gas,in} = f_{h,t}^{4} + f_{h,t}^{5} \quad \forall h, \forall t \tag{29}$$

$$\Delta HS_{h,t} = \eta_{hc}(f_{h,t}^{8} + f_{h,t}^{14}) - \frac{1}{\eta_{hd}} f_{h,t}^{15} \quad \forall h, \forall t \tag{30}$$

$$\Delta ES_{h,t} = \eta_{ec}(f_{h,t}^{2} + f_{h,t}^{6}) - \frac{1}{\eta_{ed}}(f_{h,t}^{11} + f_{h,t}^{12}) \quad \forall h, \forall t \tag{31}$$

$$\eta_{ce} f_{h,t}^{4} = f_{h,t}^{6} + f_{h,t}^{7} + f_{h,t}^{10} \quad \forall h, \forall t \tag{32}$$

$$\eta_{cg} f_{h,t}^{4} = f_{h,t}^{8} + f_{h,t}^{9} \quad \forall h, \forall t \tag{33}$$

$$\eta_{eb}(f_{h,t}^{3} + f_{h,t}^{7} + f_{h,t}^{12}) = f_{h,t}^{13} + f_{h,t}^{14} \quad \forall h, \forall t \tag{34}$$

3. Lower level: mathematical modeling of IPNGM

In this research, to simulate the IPNGM and obtain local marginal electricity price (LMEP) and local marginal gas price (LMGP) Eqs. (37)-(70) are taken into account.

3.1. The objective function of IPNGM

The objective of the IPNGM is to minimize the total cost of production, including the cost of the power production via non-gas-fired power plants (NGPPs) and their start-up and shot-down costs along with natural gas producers' costs.

$$\min \left(\sum_{t} \left(\sum_{i \in CU} (FC_{i,t} + SU_{i,t} + SD_{i,t}) + \sum_{sp} \gamma_{sp}^{Gas} V_{sp,t} \right) \right) \tag{35}$$

The first term represents the start-up, shut down, and operation costs of the NGPPs, and the second term is the cost of natural gas production, i.e., natural gas wells' cost.

3.2. Unit commitment constraints

Equations (36) and (37) illustrate start-up and shut-down costs for NGPPs, as well as start-up and shut-down fuel consumption of GFPPs are calculated by Eqs. (38)-(39).

$$SU_{i,t} \geqslant C_i^{SU} y_{i,t} \quad \forall i \in CU, \forall t \tag{36}$$

$$SD_{i,t} \geqslant C_i^{SD} z_{i,t} \quad \forall i \in CU, \forall t \tag{37}$$

$$GSU_{i,t} \geqslant C_i^{GSU} y_{i,t} \quad \forall i \in GU, \forall t \tag{38}$$

$$GSD_{i,t} \geqslant C_i^{GSD} z_{i,t} \quad \forall i \in GU, \forall t \tag{39}$$

3.3. Start-up and shut-down states of generation units

In Eq. (40), $I_{i,t}$ and $I_{i,t-1}$ show the ON state at time t and $t-1$, respectively. Also, Eq. (41) illustrates that any of the generation units cannot be at ON and OFF states at the same time.

$$y_{i,t} - z_{i,t} = I_{i,t-1} - I_{i,t} \quad \forall i, \forall t \tag{40}$$

$$y_{i,t} + z_{i,t} \leqslant 1 \quad \forall i, \forall t \tag{41}$$

3.4. Generation and ramp rate limits of generation units

Equation (42) determines the power generation limit of units. Equations (43) and (44) represent ramp-up and ramp-down limitations of power generation units.

$$P_i^{Min} I_{i,t} \leqslant P_{i,t} \leqslant P_i^{Max} I_{i,t} \quad \forall i, \forall t \tag{42}$$

$$P_{i,t} - P_{i,t-1} \leqslant (1 - y_{i,t}) R_i^{UP} + y_{i,t} P_i^{Min} \quad \forall i, \forall t \tag{43}$$

$$P_{i,t-1} - P_{i,t} \leqslant (1 - z_{i,t}) R_i^{DN} + z_{i,t} P_i^{Min} \quad \forall i, \forall t \tag{44}$$

3.5. Minimum up-time and down-time

The minimum time requirements for start-up/shutdown operations of Units are imposed by Equations (45)-(52).

$$T_i^{Ue} = \min\left\{T, T_i^{U0}\right\} \tag{45}$$

$$T_i^{De} = \min\left\{T, T_i^{D0}\right\} \tag{46}$$

$$\sum_{t=1}^{T_i^{Ue}} I_{i,t} = T_i^{Ue} \quad \forall i \tag{47}$$

$$\sum_{t=r}^{t+T_i^{Ue}-1} I_{i,r} \geqslant T_i^{U} y_{i,t} \quad \forall i, \forall t = \left[T_i^{Ue} + 1, ..., T - T_i^{U} + 1\right] \tag{48}$$

$$\sum_{t=r}^{T} (I_{i,r} - y_{i,t}) \geqslant 0 \quad \forall i, \forall t = \left[T - T_i^{U} + 2, ..., T\right] \tag{49}$$

$$\sum_{t=1}^{T_i^{De}} I_{i,t} = 0 \quad \forall i \tag{50}$$

$$\sum_{t=r}^{t+T_i^{D}-1} (1 - I_{i,r}) \geqslant T_i^{D} z_{i,t} \quad \forall i, \forall t = \left[T_i^{De} + 1, ..., T - T_i^{D} + 1\right] \tag{51}$$

$$\sum_{t=r}^{T} (1 - I_{i,r} - z_{i,t}) \geqslant 0 \quad \forall i, \forall t = \left[T - T_i^{D} + 2, ..., T\right] \tag{52}$$

3.6. Transmission system constraints

Equation (53) is the power balancing constraint. Equation (54) is the DC power flow relation, which is limited by Eqs. (55) and (56) is the wind power generation limit.

$$\sum_{j\in A_b^j} F_{b,j,t} = \sum_{i\in A_b^i} P_{i,t} + \sum_{w\in A_b^w} P_{w,t}^{Wind} - \sum_{h\in A_b^h} f_{h,t}^{Elc,in} - P_{b,t}^{D} : \lambda_{b,t}^{Elec} \quad \forall b, \forall t \tag{53}$$

$$F_{b,j,t} = (\delta_{b,t} - \delta_{j,t})/X_L \quad \forall b, \forall j, \forall t \tag{54}$$

$$-F_b^{Max} \leqslant F_{b,j,t} \leqslant F_b^{Max} \quad \forall b, \forall j, \forall t \tag{55}$$

$$0 \leqslant P_{w,t}^{Wind} \leqslant P_w^{Wind,Max} \quad \forall w, \forall t \tag{56}$$

3.7. Natural gas system model

Equation (57) shows the natural gas flow in gas network pipelines, also known as the Weymouth equation. Equations. (58) indicates the direction of natural gas flow in the pipeline, which is directly related to the pressure of the gas network nodes.

$$q_{n,m,t} = sgn(Pr_n, Pr_m) K_{n,m}^f \sqrt{Pr_{n,t}^2 - Pr_{m,t}^2} \quad \forall n, \forall m, \forall t \tag{57}$$

$$sgn(Pr_n, Pr_m) = \begin{cases} 1, & Pr_n \geqslant Pr_m \\ -1, & Pr_n \leqslant Pr_m \end{cases} \tag{58}$$

As can be seen, Eq. (57) is a nonconvex and nonlinear. This issue increases the calculation time and also makes the nodal natural gas pricing process difficult. The linearization method of Eq. (57) is shown in Appendix A.

In the following, two variables $q_{n,m,t}^{in}$, $q_{n,m,t}^{out}$ are defined in Eqs. (59) and (60) to present the flexibility of the line pack system for inflow and outflow.

$$q_{n,m,t}^{+} = \frac{q_{n,m,t}^{in} - q_{n,m,t}^{out}}{2} \quad \forall n, \forall m, \forall t \tag{59}$$

$$q_{n,m,t}^{-} = \frac{q_{m,n,t}^{in} - q_{m,n,t}^{out}}{2} \quad \forall n, \forall m, \forall t \tag{60}$$

One of the outstanding characteristics of natural gas systems is the line pack system that can act as a temporary storage system. Hence, it is an affordable solution for storing energy. The line pack system is so important to the short-term operation

of the system and represents the ability of pipelines in storing a specific amount of gas [45]. Equation (61) shows that the line pack is proportional to the mean pressure of the pipelines. Therefore, any increase in the node of a line leads to an increase in the line pack. Furthermore, Eqs. (62) and (63) determine the amount of gas that can be stored in the line pack, and Eq. (64) shows the initial amount of line pack.

$$h_{n,m,t} = K^{f}_{n,m} \frac{Pr_{n,t} + Pr_{m,t}}{2} \quad \forall n, \forall m, \forall t \tag{61}$$

$$h_{n,m,t} = h_{n,m,t-1} + q^{in}_{n,m,t} - q^{out}_{n,m,t} \quad \forall n, \forall m, \forall t \tag{62}$$

$$h_{n,m,t} = h_{n,m,0} + q^{in}_{n,m,t} - q^{out}_{n,m,t} \quad \forall n, \forall m, \forall t \tag{63}$$

$$h_{n,m,t} \geqslant h_{n,m,0} \quad \forall n, \forall m, \forall t \tag{64}$$

Supplementary constraints of the natural gas network are given in Eqs. (65)-(70). Equations (65) and (66) show the limitations in the pressure of the pipeline nodes and the amount of generated gas in the natural gas well, respectively. Equation (67) is the natural gas balancing constraint in the gas network. Equation (68) is the coupling constraint of power and natural gas networks via the Gas-Fired Power Plant (GFPP). For linearizing the Eq. (68), the introduced method in [46] is used. Equations (69) and (70) present the nodal and bus market-clearing prices that MESPs are connected to it.

$$Pr^{Min}_{n} \leqslant Pr_{n,t} \leqslant Pr^{Max}_{n} \quad \forall n, \forall t \tag{65}$$

$$\nu^{Min}_{sp} \leqslant \nu_{sp,t} \leqslant \nu^{Max}_{sp} \quad \forall sp, \forall t \tag{66}$$

$$\sum_{sp \in A^{sp}_{n}} \nu_{sp,t} - \sum_{h \in A^{h}_{n}} f^{Gas,in}_{h,t} - \sum_{l \in A^{l}_{n}} L_{l,t} = \sum_{m \in z} (q^{in}_{n,m,t} - q^{out}_{m,n,t}) : \lambda^{Gas}_{n,t} \quad \forall n, \forall t \tag{67}$$

$$L_{l,t} = a_i P^{2}_{i,t} + b_i P_{i,t} + c_i + SU_{i,t} + SD_{i,t} \quad \forall l \in A^{GU}_{l}, \forall i \in GU, \forall t \tag{68}$$

$$\lambda^{Gas}_{n,t} = \gamma^{LMGP}_{h,t} \quad \forall n \in A^{h}_{n}, \forall t, \forall h \tag{69}$$

$$\lambda^{Elec}_{b,t} = \beta^{LMEP}_{h,t} \quad \forall b = A^{h}_{b}, \forall t, \forall h \tag{70}$$

3.8. Robust optimization method

In the introduced model, LMEP values are determined by solving the market-clearing problem. However, to consider the stochastic behavior of the other participants of IPNGM (e.g., RESs), obtained LMEP from the lower level is modeled as an uncertain parameter in the upper level. In the RO method, despite stochastic approaches, there is no need for probability density functions. Therefore, in the RO method, an interval of uncertain parameter variation is utilized. Such intervals can be extracted from prediction models [47]. Indeed, these intervals can be defined as a ratio of predicted amounts. So, given that:

$$\rho_{h,t}^{LMEP\_max} = (1+\alpha)\beta_{h,t}^{LMEP} \quad \forall t, \forall h \tag{71}$$

$$\rho_{h,t}^{LMEP\_min} = (1-\alpha)\beta_{h,t}^{LMEP} \quad \forall t, \forall h \tag{72}$$

The amount can be varied from zero to one in order to adjust the uncertainty level. In the RO method, instead of objective Eq. (1), the min-max relation of Eq. (73) is replaced.

$$\min \left\{ \begin{array}{l} \sum_{t}\sum_{h}(\beta_{h,t}^{LMEP\_min}.f_{in,h,t}^{Elec} + \max_{\{S_0|S_0|\leqslant\Gamma\}} \left[\sum_{t\in S_0}\sum_{h}\beta_{h,t}^{LMEP\_max} - \beta_{h,t}^{LMEP\_min}\right] f_{in,h,t}^{Elec} \\ + \sum_{t}\sum_{h}\gamma_{h,t}^{LMGP} f_{in,h,t}^{Gas} \end{array} \right\} \tag{73}$$

In Eq. (73), the parameter Γ determines the robustness level of the method to the conservatism level of the results. In the RO method, $\Gamma = 0$ means that the impact of the uncertain parameter on the cost deviation is totally ignored. In contrast, by adjusting $\Gamma = T$, uncertainty is considered for the whole time horizon, and the most conservative result can be obtained. Increasing the value of Γ causes an increase in the robustness level of the results against the price incrementation. Utilizing auxiliary variables of $z_{h,t}$ and $y_{h,t}$, Eq. (73) can be restated as Eq. (74) [14].

$$\min \left\{ \begin{array}{l} \sum_{t}\sum_{h}(\beta_{h,t}^{LMEP\_min}.f_{in,h,t}^{Elec} + \max_{\left\{\sum_{t}\sum_{h} z_{h,t}\leqslant\Gamma, 0\leqslant z_{h,t}\leqslant 1, v_{in,h,t}^{e}\leqslant y_{h,t}\right\}} \\ \left[\sum_{t\in S_0}\sum_{h}\beta_{h,t}^{LMEP\_max} - \beta_{h,t}^{LMEP\_min}\right] y_{h,t} z_{h,t} + \sum_{h}\sum_{t}\gamma_{h,t}^{LMGP} f_{in,h,t}^{Gas}) \end{array} \right\} \tag{74}$$

Furthermore, employing duality theory, Eqs. (75)- (80) can be considered as the equivalent of Eq. (74). In these relations, $\zeta_{h,t}$ and ψ are dual variables associated with uncertainty intervals [48]. More details of the dual theory process in robust optimization based on MILP programming are shown in Appendix B.

$$\min \left\{ \sum_{t} \sum_{h} (\beta_{h,t}^{LMEP\_min}.f_{in,h,t}^{Elec}) + \psi\zeta_{h,t} + \sum_{h} \sum_{t} \zeta_{h,t} + \sum_{h} \sum_{t} \gamma_{h,t}^{LMGP} f_{in,h,t}^{Gas}) \right\} \tag{75}$$

$$\psi + \zeta_{h,t} \leqslant (\beta_{h,t}^{LMEP\_max} - \beta_{h,t}^{LMEP\_min}) y_{h,t} \quad \forall t, \forall h \tag{76}$$

$$\zeta_{h,t} \geqslant 0 \quad \forall t, \forall h \tag{77}$$

$$y_{h,t} \geqslant 0 \quad \forall t, \forall h \tag{78}$$

$$\nu_{in,h,t}^{e} \leqslant y_{h,t} \quad \forall t, \forall h \tag{79}$$

$$\psi \geqslant 0 \tag{80}$$

Finally, Eqs. (2)- (25) form relation of the upper level in the supplemented model.

4. Design of the MESPs participation mechanism in the IPNGM

Figure 2 indicates the introduced mechanism for MESPs in the IPNGM. This includes several participants, as follows:

1. NGPPs: These units generate power using non-gaseous fuels and sell it to the IPNGM.
2. Natural gas producers: These producers are obliged to extract the natural gas from wells and, after refining, sell it to the IPNGM.
3. Renewable energy sources: The task of RESs is to produce power using non-fossil fuels such as wind, solar, and biomass and sell them to the IPNGM.
4. IPNGM operator: The obligations that arise due to this operator are controlling and monitoring the IENGN and performing the integrated power and gas market clearing.
5. Energy consumers purchase power and natural gas from IPNGM to meet their load. Energy consumers are classified as active and passive consumers. Active

consumers are sensitive to the introduced LMPs from the wholesale market and change their scheduling depending on introduced LMPs. However, passive consumers are not sensitive to the LMPs and don't make any changes. Multi-energy entities are large-scale active consumers that can make changes in the market-clearing prices by changing their energy trading policy with the IPNGM.

The proposed market clearing mechanism is as follows:

In Figure 3, MESPs' participation in the IPNGM is illustrated as an iterative-based two-step algorithm. At first, input parameters including IENGN data, price, and values of energy producers (e.g., NGPPs, gas wells, wind turbines) and bidding/offering of consumers are submitted to the central operator. Then, the IPNGM uses the standard market-clearing tool to clear the market with the aim of maximizing social welfare, and values of LMEP and LMGP are obtained for every node and bus of the electricity and natural gas networks. By determining the values of LMEP and LMGP, the upper level of the problem, i.e., Eqs. (1)-(34) is implemented by MESPs to minimize the cost of the purchased energy. In doing so, the optimal cost of the multi-energy entities is calculated, and the load profile is updated. In the second step, IPNGM has to be cleared according to the new loads at bus b^* and node n^* (that node and bus that multi-energy entity is connected to them). Thereafter, the lower level of the problem, i.e., Eqs. (35)-(70), is solved, and new values of LMEP and LMGP are calculated. Updated new values of the LMEP, LMGP, and load profile are used to calculate the real cost of the purchased power as:

$$\text{Cost}_{\text{real}} = \sum_{t} \sum_{h} (\beta_{h,t}^{\text{LMEP}} f_{h,t}^{\text{Elc,in}} + \gamma_{h,t}^{\text{LMGP}} f_{h,t}^{\text{Gas,in}}) \tag{81}$$

Indeed, if a load shifting is required from IPNGM, the real cost of the purchased power will be equal to $\text{Cost}_{\text{real}}$. After calculating $\text{Cost}_{\text{real}}$ by Eqs. (82), the convergence of the problem is measured by Eqs. (82). If the problem-solving process does not converge, feedback is given to **step 1**. This process continues until the following criteria are reached:

$$\left| \frac{\text{Cost}_{\text{real}} - \text{Cost}}{\text{Cost}_{\text{real}}} \right| \leqslant \varepsilon \tag{82}$$

where, Cost is obtained cost from running the upper level and is its real value of it.

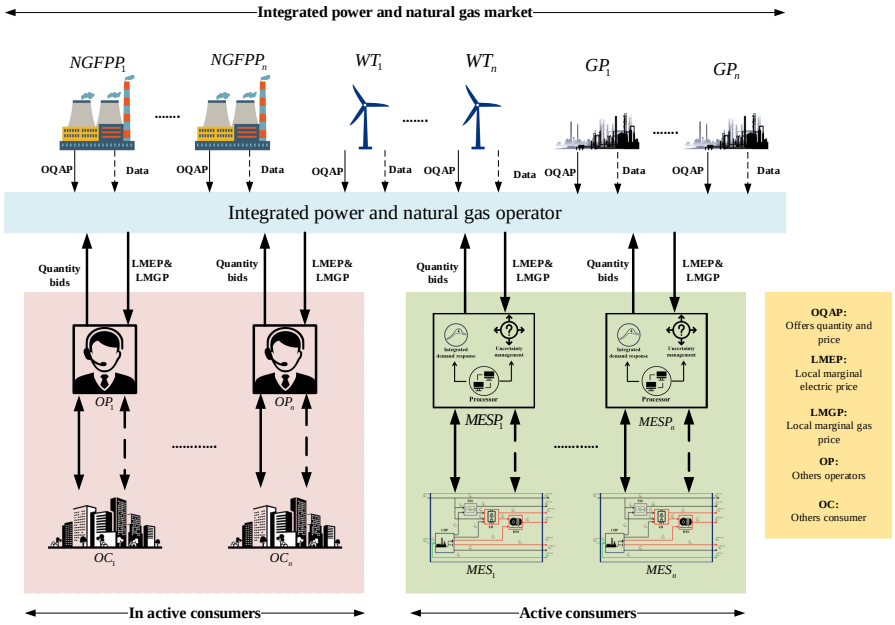

Figure 2: The introduced mechanism for MESPs participation in the IPNGM

Fig3a.pdf

Figure 3: The iterative-based two-step algorithm

In addition, $\text{Cost}_{\text{real}}$ is a stopping criterion that is considered 0.02. Obtained results verify the convergence of this mechanism.

To apply the RO method in the proposed market clearing problem, MESPs, after obtaining the final LMEP, apply the RO method. It is worth noting that electricity and natural gas network losses and the strategic behavior of other market participants are not in the main scope of the current work, and they will be taken into account in future works.

5. Simulation and numerical results

In this research, to simulate the IPNGM, a standard IEEE test system composed of a 6-bus power system integrated with a 6-node natural gas network is utilized [48, 49]. In addition, to show the robustness of the proposed model, simulations are

verified on a 118-bus power system integrated with a 10-node natural gas network [48].

6. Modified IEEE 6-bus power system integrated with 6-node natural gas network

The structure of the 6-bus power system, along with the 6-node natural gas network, is shown in Figure 4. The modified 6-bus power system includes two GFPPs, one NGPP, one wind power plant (WPP), seven transmission lines, and two loads, details of them were introduced in [48]. GFPPs are located on buses 1 and 6; NGPPs and WPP are located on buses 2 and 4, respectively. The 6-node natural gas network includes five pipelines, two natural gas producers, and six gas loads, which details can be found in [48]. Figure 5 shows the natural gas residential demand, total power demand, and predicted wind power for the 6-bus system. The introduced MES is connected to bus 5 in the power system and node 3 in the natural gas network. Power, heat, and natural gas demands of MES are indicated in Figure 6. Details of the MES's components, including the CHP unit, ESS, TSS, and boiler, are available in [50]. The proposed model is a MILP, which is implemented in the GAMS environment, and the CPLEX solver is utilized to solve the optimization problem. To provide an accurate evaluation of simulation results, four different case studies are introduced as follows:

1. Case study 1 (**CS1**): Solving the deterministic problem of MESP participation in the IPNGM in the absence of flexible sources of the MES
2. Case study 2 (**CS2**): Solving the deterministic problem of MESP participation in the IPNGM by considering flexible sources of ESS and TSS in the MES
3. Case study 3 (**CS3**): Solving the deterministic problem of MESP participation in the IPNGM by considering flexible sources of ESS, TSS, and DRP in the MES
4. Case study 4 (**CS4**): Solving the robust problem of MESP participation in the IPNGM by considering flexible sources of ESS, TSS, and DRP in the MES

CS1: Optimal scheduling of GFPPs and NGPP is depicted in Fig. 7. We can

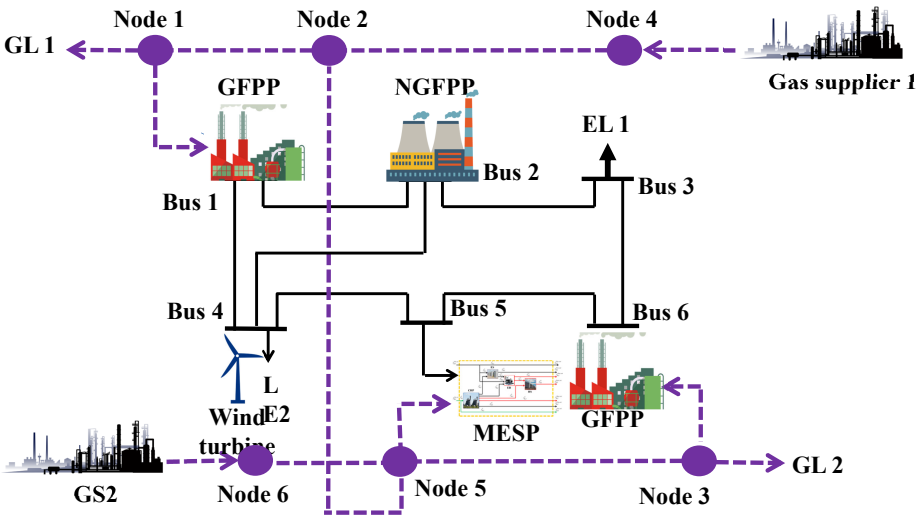

Figure 4: Structure of the 6-bus power system integrated with the 6-node natural gas network

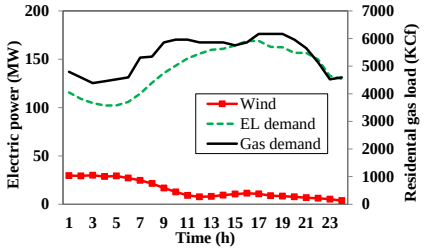

Figure 5: Load profile of power transmission system, natural gas demand and wind power

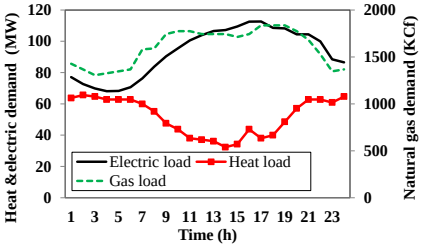

Figure 6: Power, heat, and natural gas demands of MES

see that the low-cost GFPP G1 is online during the whole scheduling time horizon. While high-cost NGPP G2 is online during hours t=10 to t=21. Since supplying local loads of the natural gas network is prior to other industrial loads, supplying natural gas during peak hours, which is occurred between hours t=15 and t=21, is limited to the GFPPs. For this reason, the G1 unit dispatch decreases at these hours, and instead, the G2 unit assumes to supply the rest of the loads. In addition, the G3 unit is online during hours t=17 and t=22. In this case study, the total operation cost of the IENGN is $405683, and the cost of the GFPPs is $389264.3 , and also the cost of the NGFPP is $16418.74.

Figure 8 indicates the natural gas dispatch of producers, in which the most dispatch of natural gas is related to the low-cost producer PG1. Dispatch of high-cost producer PG2 increases significantly during hours t=9 to t=21 due to an increase in demand for GFPPs and local loads of natural gas network. Then, after the hour t=22 decreases because of a reduction in demand for the natural gas network. The cost of the low-cost and high-cost producers are $207503.84 and $181760.42 , respectively.

Figure 9 illustrates the LMEP of the bus that MES is connected to (i.e., bus 5). According to the figure, the market-clearing price is still in the same range during hours t=1 to t=6, which is nearly $19.17/MWh. From hour t=7 to t=10 due to increasing in G1 unit production, the market clearing price increases to the value of $21.95/MWh. Between hours t=10 to t=21, the commitment of the high-cost unit G2 causes increases in the market-clearing price up to $32.63/MWh. After hour t=21, decreasing power system demand and getting out of the natural gas network peak period leads to the shutting down of the high-cost G2 unit and reduction of the G1 unit dispatch. For this reason, the market-clearing price decreases to the value of $24.37/MWh. LMGP is depicted in Fig. 9 via the noted red line. Owing to the low and uniform demand of the GFPPs and local loads of the natural gas network during hours t=1 to t=9, LMGP is $2.9 /KCfh at this period. With the increasing of high-cost unit PG2 dispatch at hours t=9 until t=16, LMGP rises to $3.36/KCfh. Considering the hours t=17 and t=18, which is the peak period for both the electricity and natural gas networks, the market-clearing price reaches $3.75/KCfh at this period. After hour t=21, with decreasing in the high-cost PG2 unit, the market-clearing price decreases to $2.9/KCfh. Note that LMEP and LMGP that is shown in Figure 9 are related to the bus and node that MES is connected to, i.e., bus 5 and node 3 of electricity and natural gas networks.

Figure 10 shows MESP's optimal scheduling for supplying MES demand in **CS1**. As illustrated, the MESP meets 55.13% of electrical demand via purchasing power from IPNGM, and 42.74% of electrical demand is supplied by the CHP unit of the MES. Moreover, optimal scheduling of MESP for supplying thermal demands of MES in **CS1** is depicted in Figure 11. Since producing thermal energy using natural gas

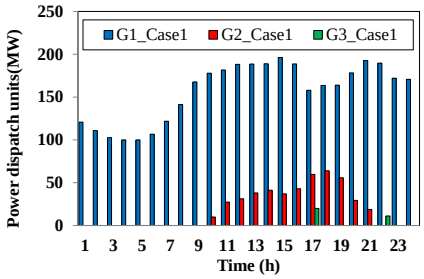

Figure 7: Hourly optimal scheduling of GFPP and NGPP in **CS1**

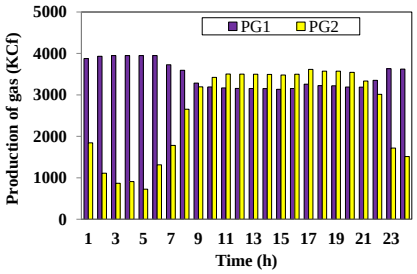

Figure 8: Hourly dispatch of the natural gas producers in **CS1**

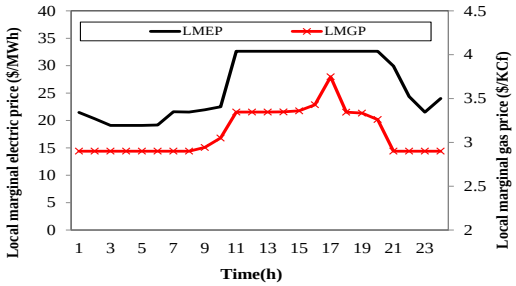

Figure 9: LMEP and LMGP of bus 5 and node 3 in the IPNGM

has a lower cost, the MESP uses the CHP unit as the first priority to supply MES thermal demands. During the peak, thermal load period of MES, which occurred at hour t=20 until t=8, MESP to balance the MES's thermal energy production and consumption is compelled to run the electrical boiler. As can be seen, 91.66% of thermal energy is met via the CHP unit, and 8.33% is met by the electrical boiler.

Figure 12 shows operation cost obtained by the iterative-based two-step algorithm, in which the convergence of the Eq. (82) is proofed. Here are how the results are obtained:

1. First step cost (Cost): At the first step, IPNGM is cleared based on basic load, then the values of LMEP and LMGP are presented to the MESP. Based on the presented prices, the MESP performs optimal scheduling and obtains the optimal operation cost (Cost).
2. Second step cost ($Cost_{real}$): After performing optimal scheduling by the MESP,

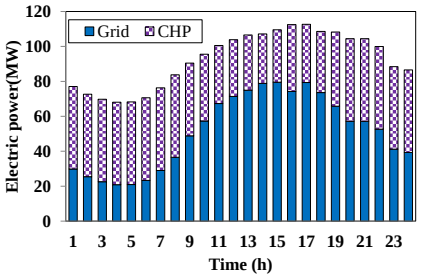

Figure 10: Hourly optimal scheduling of MESP for supplying electrical demand of MES in **CS1**

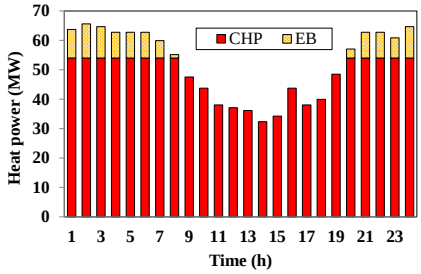

Figure 11: Hourly dispatch of the natural gas producers in **CS1**

the MES updates its load profile based on presented prices by the operator of the IPNGM, then sends the updated load profile to the operator of the IPNGM. Thereafter, the IPNGM is cleared based on the updated load profile and updated LMEP and LMGP are replaced, then real cost ($Cost_{real}$) based on Eq. (81) is calculated. The obtained costs by the first and second steps are compared with the stopping criterion of Eq. (82). If the criterion is satisfied, the procedure will be finished; else, feedback based on updated prices will be submitted to the first step.

3. The cost of the feedback 1: As illustrated, in this case study, after one feedback criterion of Eq. (82) is reached and the real cost is achieved. As depicted in Figure 12, the difference between optimal cost and the real cost is equal to zero, and the obtained results can be trustable. Note that the stopping criterion may not reach with only one feedback, and it may take several feedbacks. Moreover, it should be noted that all the results such as unit commitment, optimal scheduling of MES and etc. are provided via the iterative-based two-step algorithm for all case studies.

Figure 13 indicates the behavior of the high-cost NGPP G2 with and without the line pack. When the natural gas network is equipped with line pack, produced power by the G2 unit, especially at peak hours of the natural gas network (t= 17), decreases. As well as for the low-cost GFPP G1 in Figure 14, it can increase the produced power during the peak period of the natural gas network by considering

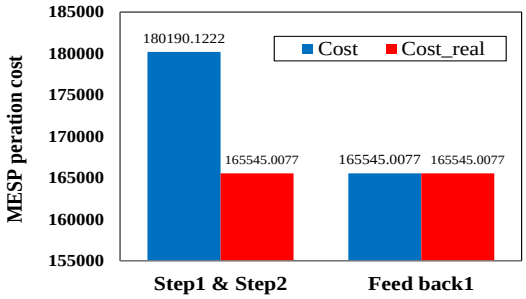

Figure 12: Obtained operation cost of the MESP via iterative-based two-step algorithm in **CS1**

Table 2: Comparison of the IENGN operation costs with and without line pack system

Cost ($)	Without line pack	With line pack
Total operation cost	405630.9371	405683.0076
NGFPP cost	16623.06428	16418.74416
GFPP cost	389007.8728	389264.2635

the line pack. In doing so, the flexibility of electricity and natural gas networks increases. According to the results, it can be concluded that the line pack system not only increases the flexibility of the natural gas network but also decreases the operation cost. In Table 2, regional operation costs are compared with and without considering the line pack. As illustrated, the operation cost of the G2 unit decreases by considering the line pack. In addition, it is obvious that G1 and G2 units' generations increase due to increases in natural gas production when the natural gas network is equipped with the line pack. Considering that line pack system flexibility is dependent on the pressure level at pipeline nodes, the storage level of pipelines can be increased by doubling the upper limit of pressure at the pipeline nodes' and consequently flexibility of the generation units and saved cost at regional area increase. Furthermore, to avoid over-displaying of figures and tables, the effect of ignoring the line pack system is evaluated in only **CS1**. Obviously, related results in other case studies are the same as in **CS1**.

CS2: In this case study, the focus is on MESP participation in IPNGM considering the energy storage systems of MES. Optimal scheduling of GFPP and NGPP are

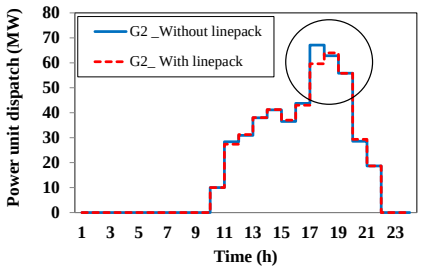

Figure 13: Comparison of the generated power of the G2 unit with and without line pack system

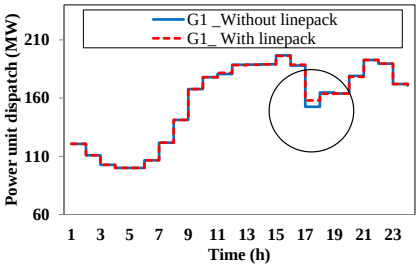

Figure 14: Comparison of the generated power of the G1 unit with and without line pack system

depicted in Figure 15. As can be seen, low-cost GFPP G1 is committed for the whole time horizon. Owing to ESS implementation by MESP, dispatch of the G1 unit is increased by 1.31% compared with **CS1**. High-cost NGPP G2 is online from hour t=10 until t=21. Hourly dispatch of unit G2 is decreased by 27.12% compared with **CS1**. Generation unit G3 is also online during hours t=16, 20, 23. In this case study, the total operation cost of the IENGN is $403205.9 , and the operation cost of the GFPP is $390834.748, as well as $12371.1 for the NGPP.

Figure 16 illustrates LMEP and LMGP in the IPNGM for **CS2**. Owing to a 27.12% reduction in the dispatch of the high-cost NGPP G2 compared with **CS1**, LMEP decreases $6.15/MWh in total. In addition, LMGP decreases at peak hours of the electricity and natural gas networks, i.e., t=17 and t= 18, due to the reduction of G2 unit dispatch.

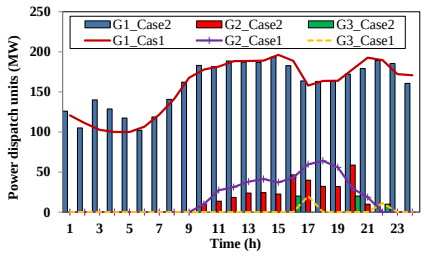

Figure 15: Hourly optimal scheduling of GFPPs and NGPP in **CS2**

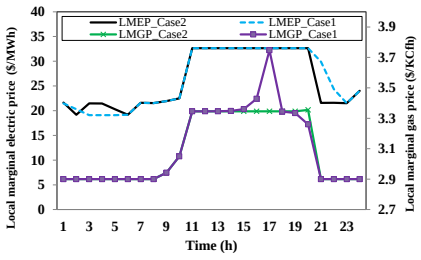

Figure 16: LMEP and LMGP at bus 5 and node 3 in the **CS2**

Figure 17 indicates the optimal hourly scheduling of the MESP for supplying

the power demand of the MES. As illustrated, ESS, with tracking of the LMEP, at low price periods starts to store power and deliver power during peak price periods. In doing so, MESP shifts some part of the purchased power from on-peak hours to off-peak hours. According to Figure 17, MESP meets 50.63% of the MES's power demand by purchasing from IPNGM, and 45.73% of the demand is met by the CHP unit of the MES. Also, 3.62% is met by ESS.

Figure 18 shows the MESP scheduling of supplying thermal demand for MES. TSS stores energy during off-peak hours and return it at on-peak hours. In doing so, 84.67% of thermal demand is met by the CHP unit, 4.22% by the boiler, and 10.24% by TSS.

Figure 19 illustrates the operation cost of the MES obtained via the iterative-based two-step algorithm. Moreover, the convergence of the Eq. (82) is proofed, in which the algorithm is converged after sending two feedback from IPNGM. According to the results, the tolerance is 0.1% at the last iteration, and it can be accepted.

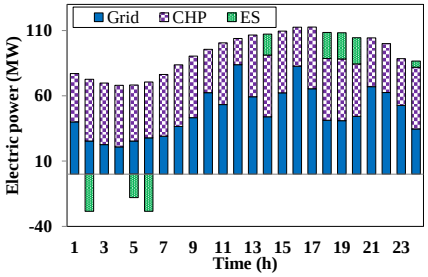

Figure 17: Hourly optimal scheduling of MESP for supplying power demand of MES in **CS2**

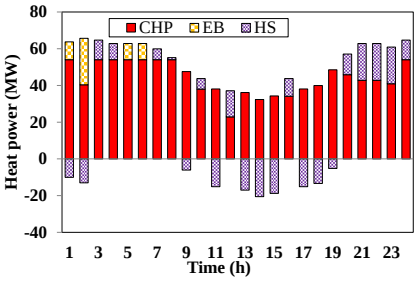

Figure 18: Hourly optimal scheduling of MESP for supplying thermal demand of MES in **CS2**

CS3: The focus of this case study is on the MESP participation in the IPNGM by considering the energy storage systems and DRP. Optimal scheduling of the GFPP and NGPP are depicted in Figure 20. Low-cost GFPP G1 is committed the whole time horizon. Due to the implementation of energy storage systems and DRP simultaneously by MES, dispatch of the G1 unit in comparison with **CS2** 2.74% is increased. High-cost NGPP G2 is online during hours t=10 until t=21. Dispatch of the G2 unit is decreased up to 19.48% compared with **CS2**. Moreover, the dispatch

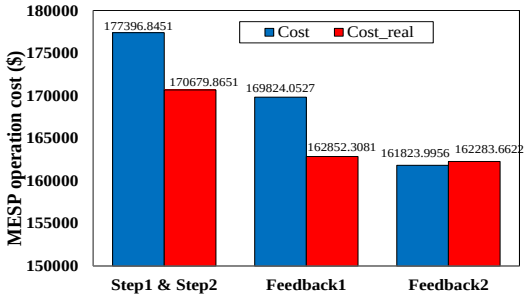

Figure 19: Obtained operation cost of the MESP via the iterative-based two-step algorithm in **CS2**

of the G3 unit is decreased by nearly 80% compared with **CS2**. The total operation cost of the IENGN is $402202.6, operation costs of the GFPP, and NGPP are $392054.8 and $10147.86, respectively.

Figure 21 indicates LMEP and LMGP in **CS3**. Owing to a 19.48% reduction in the dispatch of the high-cost NGPP G2, LMEP is reduced $20.8/MWh in comparison with **CS1** and $14.68/MWh in comparison with **CS2**. According to that, in the IPNGM electricity and natural gas networks are operated in an integrated manner, the behavior of the G2 unit affects LMGP at hours t= 14 and t= 15.

Figure 24 provides the optimal scheduling of MESP for supplying MES demands. After applying DRP on electrical loads of MES via MESP, some parts of the power demand shift from on-peak load hours to off-peak hours. The comparison of purchased power between cases 2 and 3 shows that purchased power is decreased in case 3 during on-peak hours and instead increased during off-peak hours. Applying DRP by MESP not only reduces the operation cost of the MES but also increases flexibility and reduces the operation cost of the IENGN.

Figure 23 illustrates the obtained MES's operation cost via the iterative-based two-step algorithm. In addition, the convergence of the Eq. (82) is proofed. As is seen, in this case study, with only one feedback from IPNGM, the algorithm is converged. Moreover, the tolerance is 0.013, which is acceptable.

In Table 2, the operation costs of the MES and IENGN are compared among three cases, in which implementation of flexible energy sources by the MESP leads to a 4.39% reduction in operation cost of the MES, 38.19% reduction in operation

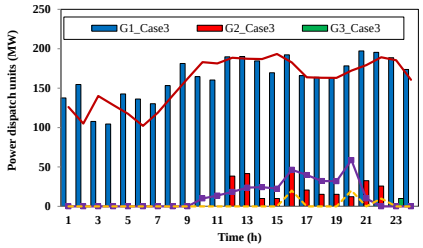

Figure 20: Hourly optimal scheduling of GFPP and NGPP in **CS3**

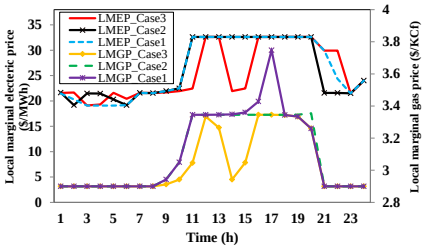

Figure 21: LMEP and LMGP at bus 5 and node 3 in **CS3**

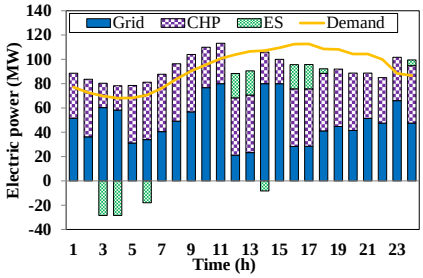

Figure 22: Hourly optimal scheduling of MESP for supplying power demand of MES in **CS3**

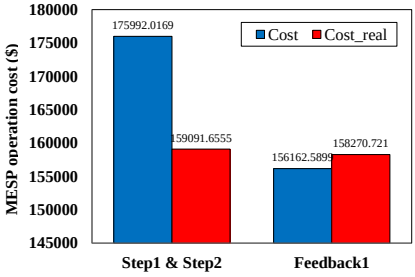

Figure 23: Obtained operation cost of the MESP via the iterative-based two-step algorithm in **CS3**

cost of the high-cost NGPP, 0.71% increasing in operation cost of the low-cost GFPP, 0.86% reduction in the total operation cost of the IENGN.

CS4: In this case study, uncertainty is also taken into account. To evaluate the results, a sensitivity analysis with the variation of the uncertainty budget from $\Gamma = 0$ to $\Gamma = T$ is conducted. Figure 24 shows the operation cost increases with increasing in the uncertainty budget. $\Gamma = 0$ means uncertainty impact is totally ignored, while $\Gamma = T$ means uncertainty impact is considered for the whole time horizon, and the most conservative result is obtained. Figures 25 and 26 indicate purchased power and total operation cost of the MES for different uncertainty budgets, respectively. As illustrated in Figure 26, the total operation cost of the MES increases with the increase of the uncertainty budget. In other words, the more risk is taken, the more cost must be paid.

Table 3: Comparison of the operation costs

Cost ($)	CS1	CS2	CS3
IENG cost	405683	403205.9	402202.6
NGFPP cost	16418.74	12371.1	10147.86
GFPP cost	389264.3	390834.7	392054.8
MESP cost	165545.01	162283.7	158270.7

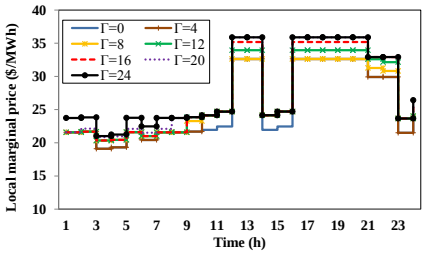

Figure 24: Price deviation of LMEP under different uncertainty budget

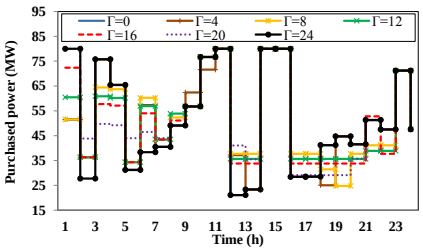

Figure 25: Purchased power under different uncertainty budgets

6.1. *Modified IEEE 118-bus system and 10-node natural gas network*

The modified IEEE 118-bus system is composed of 8 GFPPs, 46 NGPPs, 186 transmission lines, and 91 electrical loads. The total capacity of the GFPPs is 725 MW, which is 10% of the total units' capacity. Details of solution time and the number of variables are also shown in Table 5. The peak load of the power system is 5890 MW, which occurred at hour t= 17. Four wind power plants with the capacity

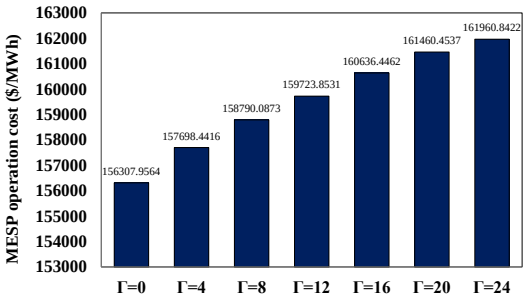

Figure 26: Impact of the uncertainty budgets on the total operation cost of the MES

of 50 MW, 50 MW, 30 MW, and 30 MW, which are located at buses 11, 30, 57, and 86, respectively. The natural gas network is composed of 10 nodes, 10 pipelines, and 12 residential loads. Furthermore, 6 MESs are located at buses 11, 28, 62, 78, 98, and 112 of the power system and nodes 4, 7, 5, 2, and 6 of the natural gas network. Details of the 118-bus system and 10-node natural gas network are available in [48]. Note that, to avoid redundancy and over-displaying figures, simulation results are provided for only MES number 2 located at bus number 28 of the power system and node number 7 of the natural gas network. Other MESs' behavior is like MES number 2.

Figure 27 shows the optimal hourly scheduling of electric power purchases by the second MESP from the IPNGM in three case studies. In the **CS2**, electric energy is charged in the ESS during off-peak and cheap hours and discharged during on-peak and expensive hours. For this reason, the purchase of electric power from the IPNGM increases in off-peak and cheap hours and decreases in on-peak and expensive hours. In **CS3** investigates the impact of implementing the DRP in MESPs. With the implementation of the DRP, part of the electric energy consumption has been shifted from on-peak and expensive hours to off-peak and cheap hours. For this reason, the purchase of electric power during cheap hours has increased compared to expensive hours. Figure 28 indicates the optimal scheduling of 8 GFPPs for three case studies. Implementation of energy storage systems and DRP via MESPs in the MES shifts power generation of units from on-peak hours to off-peak hours. In Figure 29, the optimal scheduling of all the 46 NGPPs is depicted for three case studies. Similar to the GFPPs, the power generation of NGPPs is shifted from on-peak hours to off-peak hours by applying flexible energy sources. According to Figure 30, a comparison of LMEP in **CS1**, **CS2**, and **CS3** shows the significant effect of applying energy storage systems and DRP, which lead to a reduction of LMEP. Table 4 provides the total operation costs of MESPs and IENGN for three case studies. The application of flexible sources via MESPs, not only reduces the operation costs of MES but also reduces the operation costs of the IENGN. Figure 31 shows that the increasing uncertainty budget leads to an increase in electricity prices. Moreover, Figure 32 indicates purchased power under different uncertainty budgets. In Fig-

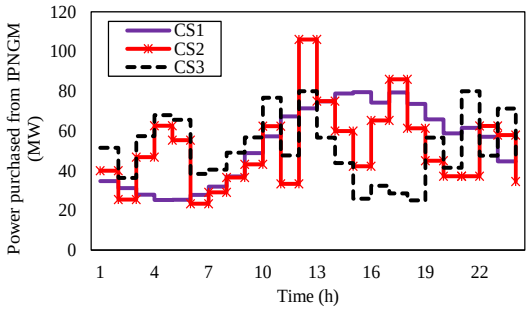

Figure 27: The optimal hourly scheduling of electric power purchases by the second MESP from the IPNGM in three case studies

ure 33, the operation costs of MESPs are shown for different uncertainty budgets. As depicted, an increase in the uncertainty budget causes increasing in the operation costs of MESPs. Figure 34 -36 also show the convergence of the iterative-based two-step algorithm (Equation (82)) respectively. In **CS1**, due to the lack of flexible energy sources (storage systems and DRP), convergence is obtained after the first feedback. In **CS2**, convergence is obtained after three times of feedback. While the convergence in the **CS3** is achieved after two feedbacks. The tolerance value in **CS1**, **CS2**, and **CS3** is 0%, 0.07%, and 0.002%, respectively.

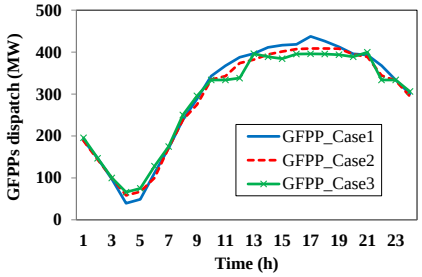

Figure 28: Generated power of 8 GFPPs in three case studies

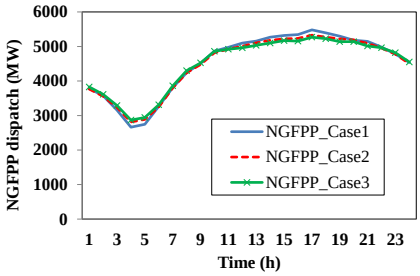

Figure 29: Total generated power of 46 NGPPs in three case studies

7. Conclusion

In this paper, a robust bilevel approach for the participation of multi-energy service providers (MESPs) in the integrated power and natural gas market (IP-

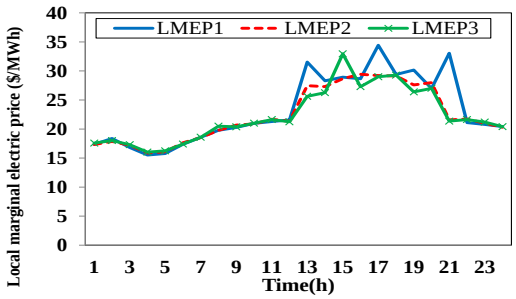

Figure 30: Comparison of LMEP at bus number 28 of the power system

Table 4: Operation costs in three case studies

Cost ($)	**CS1**	**CS2**	**CS3**
IENG cost	2758472	2737723	2733847
NGFPP cost	1167060	1162168	1160809
GFPP cost	1591411	1575556	1573037
MESP cost	162981.1	159148.2	157706.1

Table 5: Computational details in 118 bus test system for different case studies

Variables/Solution time	Case1	Case2	Case3	Case4
Single variables	47882	49752	50328	50376
Discrete variables	1722	2010	2298	2298
Solution time (min)	14.05	15.04	16.52	105

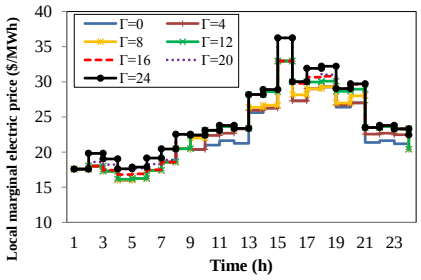

Figure 31: LMEP deviation under different uncertainty budgets in **CS4**

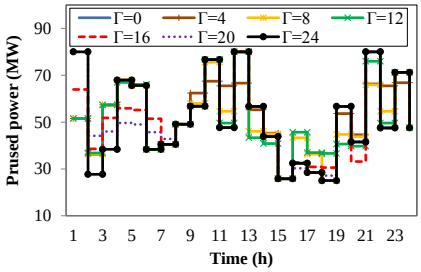

Figure 32: Purchased power under different uncertainty budgets in **CS4**

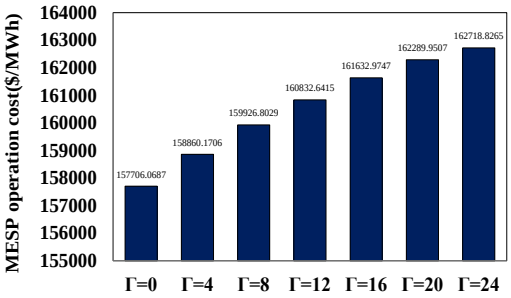

Figure 33: Impact of the uncertainty budgets on the total operation cost of the MES

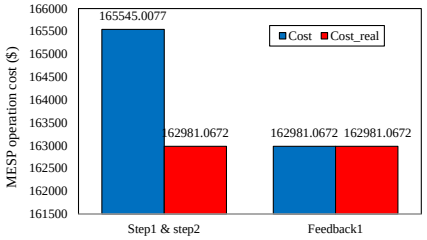

Figure 34: Obtained operation cost of the MESP via the iterative-based two-step algorithm in **CS1**

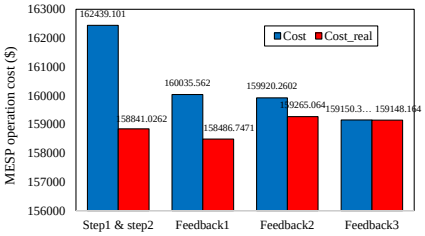

Figure 35: Obtained operation cost of the MESP via the iterative-based two-step algorithm in **CS2**

NGM) under an iterative-based two-step algorithm was proposed. At the upper level, MESPs using flexible energy sources, including energy storage systems and the demand response program (DRP) aim to minimize the purchased power and natural gas from IPNGM. At the lower level, the operator of the IPNGM aggregates bids/offers, and with the aim of social welfare maximization, clears the market. The

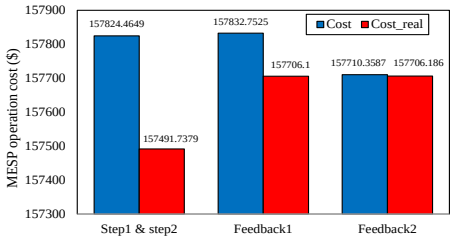

Figure 36: Obtained operation cost of the MESP via the iterative-based two-step algorithm in **CS3**

proposed study was rendered on a 6-bus power system and a 6-node natural gas system with an MES. In addition, to increase the validity of the obtained results, the proposed approach was to be carried out on a 118-bus power system and a 10-node natural gas network with six MES. The obtained results indicated that the decision-making of MESPs as responsive and large-scale consumers can affect the decisions of IPNGM's operator and vice versa. Further, it can be seen that the application of energy storage systems and DRP have positive impact on the behaviors of the multi-energy systems (MESs) and IPNGM. In addition, the following results can be summarized:

1. The operation of the natural gas network in the presence of line pack led to an increase in fuel supply to GFPP units. Considering linepack in natural gas networks while reducing 1.23% of NGFP costs increased the flexibility of the entire IPNGM.
2. The utilization of ESS and TSS, while reducing 1.97% of the total operating costs of MESP, led to a reduction of 0.61% of the IPNGM total operation costs. In addition, the presence of energy storage systems increases MESP's ability to influence the IPNGM market.
3. The implementation of the DRP while reducing 4.39% of the MESP total operating costs led to a reduction of 0.85% of IPNGM the total operating costs. Further, the coordination of energy storage systems with DRP increases the effectiveness of MESP in the IPNGM market while increasing the flexibility of the entire system.
4. By increasing the uncertainty budget in the robust optimization approach,

MESP operating costs increase. However, MESP is robust to the fluctuation behavior of LMEP.

Acknowledgments

This work was supported from DTE Network+ funded by EPSRC grant reference EP/S032053/1.

Appendix A. Natural gas network linearization

To this end, an outer approximation based on the Taylor series around constant points of pressure is employed to linearize the Weymouth equation and achieving a globally optimal solution [51]. Gas flow constraint is considered using approximated Eq. (A.1). Outer approximated values are obtained via a number of tangent lines on the surface of the Weymouth equation.

$$q_{n,m,t} \leqslant \frac{K^f_{n,m} PR_{n,u}}{\sqrt{PR^2_{n,u} - PR^2_{m,u}}}\, Pr_{n,t} - \frac{K^f_{n,m} PR_{m,u}}{\sqrt{PR^2_{n,u} - PR^2_{m,u}}}\, Pr_{m,t} \quad \forall n, \forall m, \forall u, \forall t \tag{A.1}$$

Linear constraints are generated based on selected constant points of pressure through the several values of neighbor nodes. Obtained constant pressure points are utilized to express the unidirectional gas flow in the pipelines. As pressure limitations are not equal through the neighboring nodes, they may be different from those cases obtained to express the gas flow in the reverse direction. Hence, a relation should be defined to express bidirectional gas flow in the pipelines. To this end, inequalities of Eqs. (A.2)- (A.5) are taken into account that express the bidirectional gas flow in the pipelines.

$$q_{n,m,t} = q^+_{n,m,t} - q^-_{n,m,t} \quad \forall n, \forall m, \forall t \tag{A.2}$$

$$q^-_{n,m,t} = M(1 - y_{n,m,t}) \quad \forall n, \forall m, \forall t \tag{A.3}$$

$$q^+_{n,m,t} = M y_{n,m,t} \quad \forall n, \forall m, \forall t \tag{A.4}$$

$$y_{n,m,t} \in \{1, 0\} \quad \forall n, \forall m, \forall t \tag{A.5}$$

where, $q^+_{n,m,t}$ represents gas flow from node n to node m and $q^-_{n,m,t}$ represents gas flow from node m to node n. The parameter M is a big constant. Equation (51)

has a role as same as sgn function, i.e., ensures the bidirectional gas flow in the pipelines. Equations (52)- (53) determines that only one of the $q^{+}_{n,m,t}$, $q^{-}_{n,m,t}$ can have the value inequal to zero. Moreover, to illustrate the real gas flow in the pipelines Eqs. (A.6) and (A.7) are considered.

$$q^{+}_{n,m,t} \leqslant \frac{K^{f}_{n,m} PR_{n,u}}{\sqrt{PR^{2}_{n,u} - PR^{2}_{m,u}}} Pr_{n,t} - \frac{K^{f}_{n,m} PR_{m,u}}{\sqrt{PR^{2}_{n,u} - PR^{2}_{m,u}}} Pr_{m,t} + M(1 - y_{n,m,t}) \quad \forall \langle (n,m) \in z \mid m < n \rangle, \forall u, \forall t \tag{A.6}$$

$$q^{-}_{n,m,t} \leqslant \frac{K^{f}_{n,m} PR_{m,u}}{\sqrt{PR^{2}_{m,u} - PR^{2}_{n,u}}} Pr_{m,t} - \frac{K^{f}_{n,m} PR_{n,u}}{\sqrt{PR^{2}_{m,u} - PR^{2}_{n,u}}} Pr_{n,t} + M(y_{n,m,t}) \quad \forall \langle (n,m) \in z \mid m > n \rangle, \forall u, \forall t \tag{A.7}$$

Appendix B. The duality theory process in robust optimization based on MILP programming

The duality theory can be applied to recast the min-max problem as a single level min problem. It should be noted that although the model proposed in this article is a mixed-integer linear programming (MILP), it still convex that the duality theory can be applied. In order to provide a comprehensive detail regarding the convexity of the presented model, three concepts including convex function, convex space and convex model are discussed. Firstly, the objective function is affine and as all the affine functions are convex, the objective function is definitely convex. Secondly, the search space in an optimization problem is divided into two areas, feasible and infeasible, by constraints. A constraint is convex if any linear combination of two points in its feasible area still in that area. However, in the presented constraints, there are discrete variables that make the constraints and the search area non-convex. Lastly, convex models are models that their objective functions and their relaxed constraints (viz. constraints without binary variables) are convex. In this work, as stated, the objective function is convex and since the only issue regarding non-convexity of the constraints concerns binary variables and by relaxing these variables the constraints are convex; hence, the overall model is convex [52–54]. Further, there variety of works that have applied the robust optimization on the MILP problems. For instance, in [55], the RO has been used to tackle the pernicious impact of the power market uncertainty in scheduling of industrial heat and

power consumers. With the similar aim the RO has been taken into consideration in a decentralized scheduling of microgrids in [56] to handle the power market uncertainty. Accordingly, the duality theory is taken into account and the objective function of Eq. (74) is reformulated as Eqs. (75)- (80).

References

[1] C. Zhang, L. Yang, Risk-profit analysis of regional energy service providers by regularized primal-dual interior point method, International Journal of Electrical Power & Energy Systems 135 (2022) 107542.

[2] H. Xu, H. Sun, D. Nikovski, S. Kitamura, K. Mori, H. Hashimoto, Deep reinforcement learning for joint bidding and pricing of load serving entity, IEEE Transactions on Smart Grid 10 (6) (2019) 6366–6375.

[3] M. Khorasany, A. Najafi-Ghalelou, R. Razzaghi, B. Mohammadi-Ivatloo, Transactive energy framework for optimal energy management of multi-carrier energy hubs under local electrical, thermal, and cooling market constraints, International Journal of Electrical Power & Energy Systems 129 (2021) 106803.

[4] T. Sattarpour, D. Nazarpour, S. Golshannavaz, Load serving entity interactions on residential energy management strategy: A two-level approach, Sustainable Cities and Society 40 (2018) 440–453.

[5] K. Meng, H. Yang, Z. Y. Dong, W. Guo, F. Wen, Z. Xu, Flexible operational planning framework considering multiple wind energy forecasting service providers, IEEE Transactions on Sustainable Energy 7 (2) (2015) 708–717.

[6] S. G. Q. S. A. F. H. Han, H. Cui, C. Wu, A remedial strategic scheduling model for load serving entities considering the interaction between grid-level energy storage and virtual power plants, Energies 11 (2018) 440–453.

[7] A. Halder, X. Geng, P. R. Kumar, L. Xie, Architecture and algorithms for privacy preserving thermal inertial load management by a load serving entity, in: 2017 IEEE Power Energy Society General Meeting, 2017, pp. 1–1.

[8] E. Mahboubi-Moghaddam, M. Nayeripour, J. Aghaei, Reliability constrained decision model for energy service provider incorporating demand response programs, Applied Energy 183 (2016) 552–565.

[9] H. Rashidizadeh-Kermani, M. Vahedipour-Dahraie, A. Anvari-Moghaddam, J. M. Guerrero, A stochastic bi-level decision-making framework for a load-serving entity in day-ahead and balancing markets, International Transactions on Electrical Energy Systems 29 (11) (2019) e12109.

[10] X. Fang, Q. Hu, F. Li, B. Wang, Y. Li, Coupon-based demand response considering wind power uncertainty: A strategic bidding model for load serving entities, IEEE Transactions on Power Systems 31 (2) (2016) 1025–1037.

[11] P. Sheikhahmadi, S. Bahramara, A. Mazza, G. Chicco, J. P. Catalão, Bi-level optimization model for the coordination between transmission and distribution systems interacting with local energy markets, International Journal of Electrical Power Energy Systems 124 (2021) 106392.

[12] F. H. Moghimi, T. Barforoushi, A short-term decision-making model for a price-maker distribution company in wholesale and retail electricity markets considering demand response and real-time pricing, International Journal of Electrical Power Energy Systems 117 (2020) 105701.

[13] S. Bahramara, P. Sheikhahmadi, A. Mazza, G. Chicco, M. Shafie-khah, J. P. S. Catalão, A risk-based decision framework for the distribution company in mutual interaction with the wholesale day-ahead market and microgrids, IEEE Transactions on Industrial Informatics 16 (2) (2020) 764–778.

[14] E. Mahboubi-Moghaddam, M. Nayeripour, J. Aghaei, A. Khodaei, E. Waffenschmidt, Interactive robust model for energy service providers integrating demand response programs in wholesale markets, IEEE Transactions on Smart Grid 9 (4) (2018) 2681–2690.

[15] P. Sheikhahmadi, S. Bahramara, The participation of a renewable energy-

based aggregator in real-time market: A bi-level approach, Journal of Cleaner Production 276 (2020) 123149.

[16] H. Xu, K. Zhang, J. Zhang, Optimal joint bidding and pricing of profit-seeking load serving entity, IEEE Transactions on Power Systems 33 (5) (2018) 5427–5436.

[17] Y. Jia, Z. Mi, Y. Yu, Z. Song, H. Fan, Tri-level decision-making framework for strategic trading of demand response aggregator, IET Renewable Power Generation 13 (12) (2019) 2195–2206. doi:10.1049/iet-rpg.2019.0076.

[18] M. Shafie-khah, J. P. S. Catalão, A stochastic multi-layer agent-based model to study electricity market participants behavior, IEEE Transactions on Power Systems 30 (2) (2015) 867–881. doi:10.1109/TPWRS.2014.2335992.

[19] N. Ghadimi, M. Sedaghat, K. K. Azar, B. Arandian, G. Fathi, M. Ghadamyari, An innovative technique for optimization and sensitivity analysis of a pv/dg/bess based on converged henry gas solubility optimizer: A case study, IET Generation, Transmission & Distribution (2023).

[20] G. Bo, P. Cheng, K. Dezhi, W. Xiping, L. Chaodong, G. Mingming, N. Ghadimi, Optimum structure of a combined wind/photovoltaic/fuel cell-based on amended dragon fly optimization algorithm: a case study, Energy Sources, Part A: Recovery, Utilization, and Environmental Effects 44 (3) (2022) 7109–7131.

[21] T. Zhao, X. Pan, S. Yao, C. Ju, L. Li, Strategic bidding of hybrid ac/dc microgrid embedded energy hubs: A two-stage chance constrained stochastic programming approach, IEEE Transactions on Sustainable Energy 11 (1) (2020) 116–125.

[22] V. Davatgaran, M. Saniei, S. S. Mortazavi, Optimal bidding strategy for an energy hub in energy market, Energy 148 (2018) 482 – 493.

[23] M. Zare Oskouei, M. A. Mirzaei, B. Mohammadi-Ivatloo, M. Shafiee, M. Marzband, A. Anvari-Moghaddam, A hybrid robust-stochastic approach

to evaluate the profit of a multi-energy retailer in tri-layer energy markets, Energy 214 (2021) 118948.

[24] P. Liu, T. Ding, Z. Bie, Z. Ma, Integrated demand response for multi-energy load serving entity, in: 2018 International Conference on Smart Energy Systems and Technologies (SEST), 2018, pp. 1–6.

[25] P. Liu, T. Ding, Z. Zou, Y. Yang, Integrated demand response for a load serving entity in multi-energy market considering network constraints, Applied Energy 250 (2019) 512–529.

[26] A. Najafi, H. Falaghi, J. Contreras, M. Ramezani, A stochastic bilevel model for the energy hub manager problem, IEEE Transactions on Smart Grid 8 (5) (2017) 2394–2404.

[27] M. A. Mirzaei, M. Hemmati, K. Zare, M. Abapour, B. Mohammadi-Ivatloo, M. Marzband, A. Anvari-Moghaddam, A novel hybrid two-stage framework for flexible bidding strategy of reconfigurable micro-grid in day-ahead and real-time markets, International Journal of Electrical Power & Energy Systems 123 (2020) 106293.

[28] M. Misaghian, M. Saffari, M. Kia, A. Heidari, M. Shafie-khah, J. Catalão, Tri-level optimization of industrial microgrids considering renewable energy sources, combined heat and power units, thermal and electrical storage systems, Energy 161 (2018) 396 – 411.

[29] W. Jiang, X. Wang, H. Huang, D. Zhang, N. Ghadimi, Optimal economic scheduling of microgrids considering renewable energy sources based on energy hub model using demand response and improved water wave optimization algorithm, Journal of Energy Storage 55 (2022) 105311.

[30] L. Chen, H. Huang, P. Tang, D. Yao, H. Yang, N. Ghadimi, Optimal modeling of combined cooling, heating, and power systems using developed african vulture optimization: a case study in watersport complex, Energy Sources,

Part A: Recovery, Utilization, and Environmental Effects 44 (2) (2022) 4296–4317.

[31] M. Yazdani-Damavandi, N. Neyestani, M. Shafie-khah, J. Contreras, J. P. S. Catalão, Strategic behavior of multi-energy players in electricity markets as aggregators of demand side resources using a bi-level approach, IEEE Transactions on Power Systems 33 (1) (2018) 397–411. doi:10.1109/TPWRS.2017.2688344.

[32] Z. Yang, M. Ni, H. Liu, Pricing strategy of multi-energy provider considering integrated demand response, IEEE Access 8 (2020) 149041–149051.

[33] M. Yazdani-Damavandi, N. Neyestani, G. Chicco, M. Shafie-khah, J. P. S. Catalão, Aggregation of distributed energy resources under the concept of multienergy players in local energy systems, IEEE Transactions on Sustainable Energy 8 (4) (2017) 1679–1693.

[34] M. Shafiekhani, A. Badri, M. Shafie-Khah, J. P. Catalão, Strategic bidding of virtual power plant in energy markets: A bi-level multi-objective approach, International Journal of Electrical Power & Energy Systems 113 (2019) 208–219.

[35] A. Mirzapour-Kamanaj, M. Majidi, K. Zare, R. Kazemzadeh, Optimal strategic coordination of distribution networks and interconnected energy hubs: A linear multi-follower bi-level optimization model, International Journal of Electrical Power Energy Systems 119 (2020) 105925.

[36] R. Li, W. Wei, S. Mei, Q. Hu, Q. Wu, Participation of an energy hub in electricity and heat distribution markets: An mpec approach, IEEE Transactions on Smart Grid 10 (4) (2019) 3641–3653.

[37] A. Heidari, S. S. Mortazavi, R. C. Bansal, Equilibrium state of a price-maker energy hub in a competitive market with price uncertainties, IET Renewable Power Generation 14 (6) (2020) 976–985.

[38] S. Khazeni, A. Sheikhi, M. Rayati, S. Soleymani, A. M. Ranjbar, Retail market equilibrium in multicarrier energy systems: A game theoretical approach, IEEE Systems Journal 13 (1) (2019) 738–747. doi:10.1109/JSYST.2018.2812807.

[39] X. Wang, Z. Bie, F. Liu, Y. Kou, L. Jiang, Bi-level planning for integrated electricity and natural gas systems with wind power and natural gas storage, International Journal of Electrical Power Energy Systems 118 (2020) 105738.

[40] N. Nasiri, A. Sadeghi Yazdankhah, M. A. Mirzaei, A. Loni, B. Mohammadi-Ivatloo, K. Zare, M. Marzband, A bi-level market-clearing for coordinated regional-local multi-carrier systems in presence of energy storage technologies, Sustainable Cities and Society 63 (2020) 102439.

[41] Y. Li, Z. Li, F. Wen, M. Shahidehpour, Privacy-preserving optimal dispatch for an integrated power distribution and natural gas system in networked energy hubs, IEEE Transactions on Sustainable Energy 10 (4) (2019) 2028–2038.

[42] C. Wang, W. Wei, J. Wang, L. Wu, Y. Liang, Equilibrium of interdependent gas and electricity markets with marginal price based bilateral energy trading, IEEE Transactions on Power Systems 33 (5) (2018) 4854–4867.

[43] S. Bahrami, A. Sheikhi, From demand response in smart grid toward integrated demand response in smart energy hub, IEEE Transactions on Smart Grid 7 (2) (2016) 650–658.

[44] H. Wu, M. Shahidehpour, A. Alabdulwahab, A. Abusorrah, Demand response exchange in the stochastic day-ahead scheduling with variable renewable generation, IEEE Transactions on Sustainable Energy 6 (2) (2015) 516–525.

[45] N. Nasiri, A. Sadeghi Yazdankhah, M. A. Mirzaei, A. Loni, B. Mohammadi-Ivatloo, K. Zare, M. Marzband, Interval optimization-based scheduling of interlinked power, gas, heat, and hydrogen systems, IET Renewable Power Generation 15 (6) (2021) 1214–1226.

[46] L. Wu, A tighter piecewise linear approximation of quadratic cost curves for unit commitment problems, IEEE Transactions on Power Systems 26 (4) (2011) 2581–2583.

[47] N. Nasiri, M. R. Banaei, S. Zeynali, A hybrid robust-stochastic approach for unit commitment scheduling in integrated thermal electrical systems considering high penetration of solar power, Sustainable Energy Technologies and Assessments 49 (2022) 101756.

[48] X. Zhang, M. Shahidehpour, A. Alabdulwahab, A. Abusorrah, Hourly electricity demand response in the stochastic day-ahead scheduling of coordinated electricity and natural gas networks, IEEE Transactions on Power Systems 31 (1) (2016) 592–601.

[49] N. Nasiri, S. Zeynali, S. N. Ravadanegh, M. Marzband, A hybrid robust-stochastic approach for strategic scheduling of a multi-energy system as a price-maker player in day-ahead wholesale market, Energy 235 (2021) 121398.

[50] M. Yan, N. Zhang, X. Ai, M. Shahidehpour, C. Kang, J. Wen, Robust two-stage regional-district scheduling of multi-carrier energy systems with a large penetration of wind power, IEEE Transactions on Sustainable Energy 10 (3) (2018) 1227–1239.

[51] N. Nasiri, S. Zeynali, S. N. Ravadanegh, N. Rostami, A robust decision framework for strategic behaviour of integrated energy service provider with embedded natural gas and power systems in day-ahead wholesale market, IET Generation, Transmission & Distribution (2022).

[52] S. Boyd, S. P. Boyd, L. Vandenberghe, Convex optimization, Cambridge university press, 2004.

[53] D. G. Luenberger, Y. Ye, Supplement to “linear and nonlinear programming” (2005).

[54] J. Kumar, I. U. Khalil, A. U. Haq, A. Perwaiz, K. Mehmood, Solver-based mixed integer linear programming (milp) based novel approach for hydroelectric power generation optimization, IEEE Access 8 (2020) 174880–174892.

[55] M. Alipour, K. Zare, H. Zareipour, H. Seyedi, Hedging strategies for heat and electricity consumers in the presence of real-time demand response programs, IEEE Transactions on Sustainable Energy 10 (3) (2018) 1262–1270.

[56] A. Mansour-Saatloo, Y. Pezhmani, M. A. Mirzaei, B. Mohammadi-Ivatloo, K. Zare, M. Marzband, A. Anvari-Moghaddam, Robust decentralized optimization of multi-microgrids integrated with power-to-x technologies, Applied Energy 304 (2021) 117635.